

Insulin-Like Growth Factor-Binding Protein 2 Supports Hematopoietic Stem Cell

Expansion: From In Vitro to In Vivo

APPROVED BY SUPERVISORY COMMITTEE

Philip Thorpe, Ph.D.

Rolf Brekken, Ph.D.

Felix Yarovinsky, M.D.

Lily Huang, Ph.D.

Cheng Cheng (Alec) Zhang, Ph.D.

Special Acknowledgements

I would like to thank Mrs. Betty Ward, high school teacher, for teaching English and introducing me to the American's culture.

I would like to thank Gary Rhodes, Ph.D., undergraduate mentor, for his guidance and introducing me to science.

I also would like to thank Cheng Cheng (Alec) Zhang, Ph.D., graduate school mentor, for his supports and guidance.

Thank you for enabled!

Dedication

In loving memory of my mother, Huong Thi Nguyen, 1947-1990.

Insulin-Like Growth Factor-Binding Protein 2 Supports Hematopoietic Stem Cell

Expansion: From In Vitro to In Vivo

Hoang Huynh

Hoang Dinh Huynh

DISSERTATION

Presented to the Faculty of the Graduate School of Biomedical Sciences

The University of Texas Southwestern Medical Center at Dallas

In Partial Fulfillment of the Requirements

For the Degree of

DOCTOR OF PHILOSOPHY

The University of Texas Southwestern Medical Center at Dallas

Dallas, Texas

April, 2011

Insulin-Like Growth Factor-Binding Protein 2 Supports Hematopoietic Stem Cell
Expansion: From In Vitro to In Vivo

Hoang Dinh Huynh

The University of Texas Southwestern Medical Center at Dallas, 2011

Cheng Cheng (Alec) Zhang, Ph.D.

Successful hematopoietic stem cell (HSC) transplantation is often limited by the numbers of HSCs, and robust methods to expand HSCs *ex vivo* are needed. We previously showed that angiopoietin-like proteins (Angptls), a group of growth factors isolated from a fetal liver HSC supportive cell population, improved *ex vivo* expansion of HSCs. Here we demonstrate that insulin-like growth factor binding protein 2 (IGFBP2), secreted by a tumorigenic cell line, also enhanced *ex vivo* expansion of mouse HSCs. As measured by competitive repopulation analyses, there was a 48-fold increase in numbers of long-term repopulating mouse HSCs after 21 days of culture. This is the first demonstration that IGFBP2 stimulates expansion or proliferation of murine stem cells. Our finding also suggests that certain cancer cells synthesize proteins that can stimulate HSC expansion.

To further study the function of IGFBP2 *in vivo*, we showed that IGFBP2-null mice have fewer HSCs than wild-type mice. While IGFBP2 has little cell-autonomous effect on HSC function, we found decreased *in vivo* repopulation of HSCs in primary and secondary transplanted IGFBP2-null recipients. Importantly, bone marrow stromal cells that are deficient for IGFBP2 have significantly decreased ability to support the expansion of repopulating HSCs. To investigate the mechanism by which IGFBP2 supports HSC activity, we demonstrated that HSCs in IGFBP2-null mice had decreased survival and cycling, downregulated expression of anti-apoptotic factor Bcl-2, and upregulated expression of cell cycle inhibitors p21, p16, p19, p57, and PTEN. Moreover, we found that the C-terminus, but not the RGD domain, of extrinsic IGFBP2 was essential for support of HSC activity. Defective signaling of the IGF type I receptor did not rescue the decreased repopulation of HSCs in IGFBP2-null recipients, suggesting that the environmental effect of IGFBP2 on HSCs is independent of IGF-IR mediated signaling. Therefore, as an environmental factor, IGFBP2 supports the survival and cycling of HSCs.

Table of Contents

Chapter One: Insulin-Like Growth Factor-Bonding Protein 2 Secreted by a Tumorigenic Cell Line Supports <i>Ex Vivo</i> Expansion of Mouse Hematopoietic Stem Cells		1
1.1: Abstract		2
1.2: Introduction		3
1.3: Materials and Methods		6
1.4: Results		10
1.5: Discussion		21
1.6: References		24
 Chapter Two: IGF Binding Protein 2 Supports the Survival and Cycling of Hematopoietic Stem Cells		 29
2.1: Abstract		30
2.2: Introduction		31
2.3: Materials and Methods		33
2.4: Results		38
2.5: Discussion		60
2.6: References		65
 Chapter Three: Components of the Hematopoietic Compartments in Tumor Stroma and Tumor-bearing Mice		 72
3.1: Abstract		73
3.2: Introduction		74
3.3: Materials and Methods		76
3.4: Results		80
3.5: Discussion		96
3.6: References		100
 Acknowledgements		 103

List of Figures and Tables

Chapter One: Insulin-Like Growth Factor-Binding Protein 2 Secreted by a Tumorigenic Cell Line Supports *Ex Vivo* Expansion of Mouse Hematopoietic Stem Cells

Figure 1. Serum-free conditioned medium collected from 293T cells stimulates <i>ex vivo</i> expansion of HSCs	11
Figure 2. IGFBP2 is the factor in serum-free 293T conditioned medium that stimulates <i>ex vivo</i> expansion of HSCs	13
Figure 3. Purified IGFBP2 stimulates <i>ex vivo</i> expansion of HSCs	16
Figure 4. Limiting dilution analysis of the repopulating ability of HSCs before and after culture	18
Figure 5. IGFBP2 induced rapid p42/44 MAPK activation and several Hox gene expression	20
Table 1. Partial list of peptides identified from mass spectrometry analysis of the fraction of serum-free conditioned medium of 293T cells	13
Table 2. Peripheral blood analysis of mice fully reconstituted by cultured hematopoietic stem cells	17

Chapter Two: IGF Binding Protein 2 Supports the Survival and Cycling of Hematopoietic Stem Cells

Figure 1. IGFBP2-null mice have fewer HSCs than wild-type mice	39
Figure 2. IGFBP2 has little cell-autonomous effect on HSCs	42
Figure 3. IGFBP2 supports the repopulation of HSCs in the BM environment	45
Figure 4. IGFBP2 supports the survival and cycling of HSCs in the BM	49
Figure 5. The C-terminus of IGFBP2 is essential for IGFBP2's HSC supportive activity	53
Figure 6. IGFBP2 modulates Wnt activities in hematopoietic stem cells	57
Figure 7. IGFBP2 induces the TOPFLASH activities through Frizzled 8	

receptor and LDL receptor-related protein 6	58-59
Supplementary Figure 1. Characterization of the IGFBP2 null mice	40
Supplementary Figure 2. The expression pattern of IGFBP2 in BM stroma	43
Supplementary Figure 3. IGFBP2 supports the increase of the number of HSCs in the BM environment	46
Supplementary Figure 4. Characterization of cell fates of HSCs in IGFBP2-null mice	50
Supplementary Figure 5. The HSC supportive effect of IGFBP2 is independent of IGF-IR mediated signaling	54

Chapter Three: Components of the Hematopoietic Compartments in Tumor Stroma and Tumor-bearing Mice

Figure 1. Analysis of the hematopoietic compartment of LL2 tumor stroma	83-84
Figure 2. Analysis of the hematopoietic compartment of the LL2 tumor-bearing mice	87-88
Figure 3. Tumor stromal hematopoietic cells stimulate LL2 tumor development	91
Figure 4. Mice with the IGF-IR ^{-/-} tumor stromal HSCs had slower tumor development in the LL2 implantation model than mice reconstituted with wild-type HSCs	94
Table 1. Repopulating hematopoietic stem cells and differentiated hematopoietic cells exist in LL2 tumor stroma	82

Abbreviations

IGFBP2: Insulin-Like Growth Factor-Binding Protein 2

HSC: Hematopoietic Stem Cell

Angptls: Angiopoietin-like proteins

SCF: Stem Cell Factor

TPO: Thrombopoietin

FGF-1: Fibroblast Growth Factor-1

IGF-1: Insulin-Like Growth Factor-1

IGF-2: Insulin-Like Growth Factor-2

LT-HSC: Long-term Hematopoietic Stem Cell

ST-HSC: Short-term Hematopoietic Stem Cell

MPP: Multipotent Progenitor

SP: Side Population

FACS: Fluorescence-Activated Cell Sorting

RT-PCR: Reverse Transcriptase Polymerase Chain Reaction

STF: SCF, TPO, and FGF-1

STIF: SCF, TPO, IGF-2, FGF-1

LSK: Lin⁻Sca-1⁺Kit⁺

LSKFC: Lin⁻Sca-1⁺Kit⁺Flk2⁻CD34⁻

CRU: Competitive Repopulating Units

TGF- β : Transformed Growth Factor- β

IL-1: Interleukin-1

Hox: homeodomain

IGF-IR: Insulin-Like Growth Factor-Type I Receptor

Frz8: Frizzled 8

LRP6: LDL Receptor-related Protein 6

WT: Wildtype

KO: Knock-out

CFU: Colony Forming Unit

CFU-GEMM: Granulocyte, Erythrocyte, Monocyte, and Megakaryocyte

CFU-GM: Granulocyte and Macrophage

BFU-E: Erythroid Burst-Forming Unit

CFU-E: Erythroid

CFU-pre-B: pre B-lymphoid

AML: Acute Myeloid Leukemia

ALL: Acute Lymphoblastic Leukemia

LL2: Lewis Lung type-2

**Insulin-Like Growth Factor-Binding Protein 2 Secreted by a Tumorigenic Cell Line
Supports *Ex Vivo* Expansion of Mouse Hematopoietic Stem Cells**

ABSTRACT

Successful hematopoietic stem cell (HSC) transplantation is often limited by the numbers of HSCs, and robust methods to expand HSCs *ex vivo* are needed. We previously showed that angiopoietin-like proteins (Angptls), a group of growth factors isolated from a fetal liver HSC supportive cell population, improved *ex vivo* expansion of HSCs. Here we demonstrate that insulin-like growth factor binding protein 2 (IGFBP2), secreted by a tumorigenic cell line, also enhanced *ex vivo* expansion of mouse HSCs. Based on these findings, we established a completely defined, serum-free culture system for mouse HSCs, containing SCF, TPO, FGF-1, Angptl3, and IGFBP2. As measured by competitive repopulation analyses, there was a 48-fold increase in numbers of long-term repopulating mouse HSCs after 21 days of culture. This is the first demonstration that IGFBP2 stimulates expansion or proliferation of murine stem cells. Our finding also suggests that certain cancer cells synthesize proteins that can stimulate HSC expansion.

INTRODUCTION

Over the past 50 years, hematopoietic cells serve as a major source of cellular therapy for bone marrow transplantation. Advance understanding of hematopoietic stem cell biology offers the promising treatments for a range of blood diseases. An ideal hematopoietic graft contains a mixture of cells including committed progenitor cells that provide immediate recovery of differentiated lymphoid and myeloid cells, and hematopoietic stem cells (HSCs) that provide long-term durable engraftment. In fact, hematopoietic stem cells were used as therapies to treat patients with leukemia, lymphoma, other cancers, and genetic defects such as sickle cell anemia and thalassemia¹. In clinical setting, one major limitation to the application of bone marrow transplantation has been the absolute number of stem cells available due to its unique low frequency in the bone marrow. HSCs are also a promising cell target for gene therapies². One of the most important parameters for successful HSC transplantation is the dose of transplanted HSCs. Expansion of HSCs in culture will improve the survival rates of cancer patients who receive HSC transplantation and will also allow amplification of umbilical cord blood HSCs for use by adult patients. Furthermore, methods that facilitate *ex vivo* expansion of HSCs will greatly boost the development of gene therapy by allowing selection of transduced HSCs in which the desired genes are introduced into the appropriate DNA location.

Numerous attempts have been made to increase the number of long-term (LT)-HSCs in culture^{3,4}. Some such systems involve unknown factors that allow the stem cells to survive and multiply in number. The unknown factors can be supplied by co-culturing the stem cells with feeder cells, which secrete an undefined panel of factors, or

can be supplied by adding undefined serum products to the growth medium. In the mouse model system, the use of stromal cell lines or combinations of cytokines resulted in significant self-renewal of HSCs assayed 4-6 weeks post-transplant and have led to as much as a 6-fold expansion of murine LT-HSC activity in culture⁵⁻⁹. The introduction of exogenous transcription factors can expand HSCs more dramatically¹⁰⁻¹³, though gene transduction of HSCs may cause undesired outcome for patients in clinical settings due to random integration of viral vectors². There remains a need for methods and compositions that allow the *in vitro* and/or *ex vivo* propagation of HSCs in a chemically defined medium, while maintaining the potency of the propagated cells.

The fates of HSCs – self renewal, differentiation, apoptosis, or quiescence - are regulated by components of their *in vivo* niche or microenvironment^{14, 15}. We previously showed that IGF-2 as well as several angiopoietin-like proteins (Angptls), a group of growth factors secreted by a fetal liver HSC - supportive cell population, supported *ex vivo* expansion of murine HSCs¹⁶⁻¹⁸. Here we demonstrate that insulin-like growth factor binding protein 2 (IGFBP2), secreted by a cultured tumorigenic cell line, stimulated *ex vivo* expansion of mouse HSCs.

Based on these findings, we established a completely defined serum- free culture system for murine HSCs, which includes growth factors SCF, TPO, FGF-1, Angptl3, and IGFBP2. As measured by competitive repopulation analyses, there was a 48-fold increase in numbers of long-term repopulating mouse HSCs after 3 weeks of culture. To our knowledge, this is the highest level of *ex vivo* expansion of HSCs yet achieved in a defined culture. This is also the first demonstration that IGFBP2 stimulates the expansion

of murine stem cells. Our findings suggest that other cancer cells may secrete IGFBP2 or other HSC –stimulating proteins.

MATERIALS AND METHODS

Mice

C57 BL/6 CD45.2 and CD45.1 mice were purchased from the Jackson Laboratory or the National Cancer Institute, and were maintained at the Whitehead Institute or the University of Texas Southwestern Medical Center animal facility. All animal experiments were performed with the approval of Massachusetts Institute of Technology or the University of Texas Southwestern Committee on Animal Care.

Culture medium

STIF medium is defined as StemSpan serum-free medium (StemCell Technologies) supplemented with 10 µg/ml heparin (Sigma), 10 ng/ml mouse SCF (R&D Systems), 20 ng/ml mouse TPO (R&D Systems), 20 ng/ml mouse IGF-2 (R&D Systems), and 10 ng/ml human FGF-1 (Invitrogen). STF medium was the same medium but without IGF-2. The indicated amounts of purified mouse Angptl3 (a gift from R&D Systems), or human IGFBP2 (R&D Systems) was added. Conditioned medium was collected from confluent 293T or 3T3 cells after overnight culture.

Mouse HSC culture

Twenty BM SP Sca-1⁺ CD45⁺ cells isolated from 8-10 week old C57BL/6 CD45.2 mice were plated in one well of a U-bottom 96-well plate (3799; Corning) with 160 µl of the indicated medium. Cells were cultured at 37°C in 5% CO₂ and indicated levels of O₂. For the purpose of competitive transplantation, we pooled cells from 12

culture wells and mixed them with competitor/supportive cells before the indicated numbers of cells were transplanted into each mouse. For Western blotting, bone marrow Lin⁻ cells isolated by AutoMacs (Miltenyi Biotechnology Inc.) or by fluorescence-activated cell sorting (FACS) were cultured overnight in STF medium, followed by starvation for 4 h in serum-free medium (containing 0.5% bovine serum albumin), and treatment with 500 ng/ml IGFBP2. For quantitative RT-PCR, Lin⁻Sca-1⁺Kit⁺Flk-2⁻ cells were cultured in STF medium for 3 days, followed by replacement with fresh STF medium. One hour later, 500 ng/ml IGFBP2 was added as indicated.

Flow cytometry

Donor bone marrow cells were isolated from 8-10 week old C57BL/6 CD45.2 mice. SP Sca-1⁺ CD45⁺ cells were isolated as described¹⁸. Lin⁻Sca-1⁺Kit⁺Flk-2⁻ cells were isolated by staining with a Biotinylated lineage cocktail (anti-CD3, anti-CD5, anti-B220, anti-Mac-1, anti-Gr-1, anti-Ter119, and anti-7-4; StemCell Technologies) followed by streptavidin-PE/Cy5.5, anti-Sca-1-FITC, anti-Kit-APC, and anti-Flk-2-PE. For analyzing repopulation of mouse HSCs, peripheral blood cells of recipient CD45.1 mice were collected by retro-orbital bleeding, followed by lysis of red blood cells and staining with anti-CD45.2-FITC, and anti-CD45.1-PE, and anti-Thy1.2-PE (for T-lymphoid lineage), anti-B220-PE (for B-lymphoid lineage), anti-Mac-1-PE, anti-Gr-1-PE (cells costaining with anti-Mac-1 and anti-Gr-1 were deemed to be of the myeloid lineage), or anti-Ter119-PE (for erythroid lineage) monoclonal antibodies (BD Pharmingen). The “percent repopulation” shown in all Figures was based on the staining results of anti-

CD45.2-FITC and anti-CD45.1-PE. In all cases FACS analysis of the above listed lineages was also performed to confirm multilineage reconstitution.

Competitive reconstitution analysis

The indicated numbers of mouse CD45.2 donor cells were mixed with 1×10^5 freshly isolated CD45.1 competitor bone marrow cells, and the mixture injected intravenously *via* the retro-orbital route into each of a group of 6-9 week old CD45.1 mice previously irradiated with a total dose of 10 Gy. 10^6 bone marrow cells collected from primary recipients were used for secondary transplantation. To measure reconstitution of transplanted mice, peripheral blood was collected at the indicated times post-transplant and the presence of CD45.1⁺ and CD45.2⁺ cells in lymphoid and myeloid compartments were measured as described¹⁶⁻¹⁹. Calculation of CRUs in limiting dilution experiments was conducted using L-Calc software (StemCell Technologies)¹⁹.

Western blots

Purified proteins or crude proteins in conditioned medium were analyzed by electrophoresis on 4-12% NuPage Bis-Tris polyacrylamide gels (Invitrogen), and proteins were electroblotted onto nitrocellulose membranes. To detect IGFBP2, the membranes were probed with anti-IGFBP2 polyclonal antibody (AF674, R&D Systems) at 0.1 $\mu\text{g/ml}$, followed with the horseradish peroxidase-conjugated donkey-anti-goat antibody and detected by a chemiluminescence kit (Pierce Inc.). Total MAPK p42/44 and their phosphorylated forms were detected using rabbit anti-mouse p42/44 or pp42/44 antibodies (Cell Signaling Technology).

Mass Spectrometry

The conditioned medium was resolved by SDS-PAGE. Protein “bands” ranging from 10 –70 kD were excised and samples analyzed by the MIT mass spectrometry core facility. Trypsin digestion was performed, and peptide mixtures were loaded onto a triphasic liquid chromatography LC/LC column and tandem mass spectra were analyzed.

Quantitative RT-PCR

Total RNA was isolated from bone marrow Lin⁻Sca-1⁺Kit⁺Flk-2⁻ cells. First-strand cDNA was synthesized using SuperScript II RT (Invitrogen). Samples were analyzed in triplicate 25 µl reactions (300 nM of primers, 12.5 µl of Master mix), which was adapted from the standard protocol provided in SyBR Green PCR Master Mix and RT-PCR Protocols provided by Applied Biosystems. Primers were purchased from Qiagen or Sigma. The default PCR protocol was used on an Applied Biosystems Prism 7000 Sequence Detection System. The mRNA level in each population was normalized to the level of beta-actin RNA transcripts present in the same sample as described^{18, 20}.

RESULTS

Conditioned medium collected from non-transfected 293T cells stimulates *ex vivo* expansion of HSCs

Recently, we identified Angptls as a group of new growth factors for HSCs¹⁸. We found that recombinant Angptls, present in the serum-free medium of transiently transfected 293T cells, supported *ex vivo* expansion of mouse bone marrow HSCs¹⁸. In the course of several control experiments, we found, surprisingly, that serum-free conditioned medium collected from non-transfected 293T cells also supported expansion of HSCs, albeit much less well than the medium from cells transduced with Angptl genes. In the experiment shown in Figure 1A, twenty freshly isolated CD45.2 bone marrow side population (SP) Sca-1⁺ CD45⁺ cells, a highly enriched HSC population, were cultured for 10 days in fresh serum-free medium supplemented with SCF, TPO, IGF-2, and FGF-1 (STIF medium); these had an average of 10.4% engraftment in recipients, as measured by competitive reconstitution analysis at 5 months post-transplant (Figure 1A, bar 1). By contrast, the same HSCs cultured in conditioned medium collected from 293T cells that was later supplemented with SCF, TPO, IGF-2, and FGF-1, had a much higher engraftment of 50.5% (Fig. 1A, bar 2). This suggests that an HSC-stimulating activity resides in 293T-conditioned medium. This activity, however, was depleted after freeze/thaw of the conditioned medium (Fig. 1A, bar 3). The expanded cells were able to repopulate both lymphoid and myeloid lineages (Figure 1B), demonstrating expansion of repopulating HSCs. In another experiment, the conditioned medium collected from nontransfected 293T cells was supplemented with SCF, TPO, and FGF-1 (without IGF-

2); this medium also stimulated HSC expansion, whereas the conditioned medium from another cell line, 3T3 cells, did not support HSC expansion (data not shown).

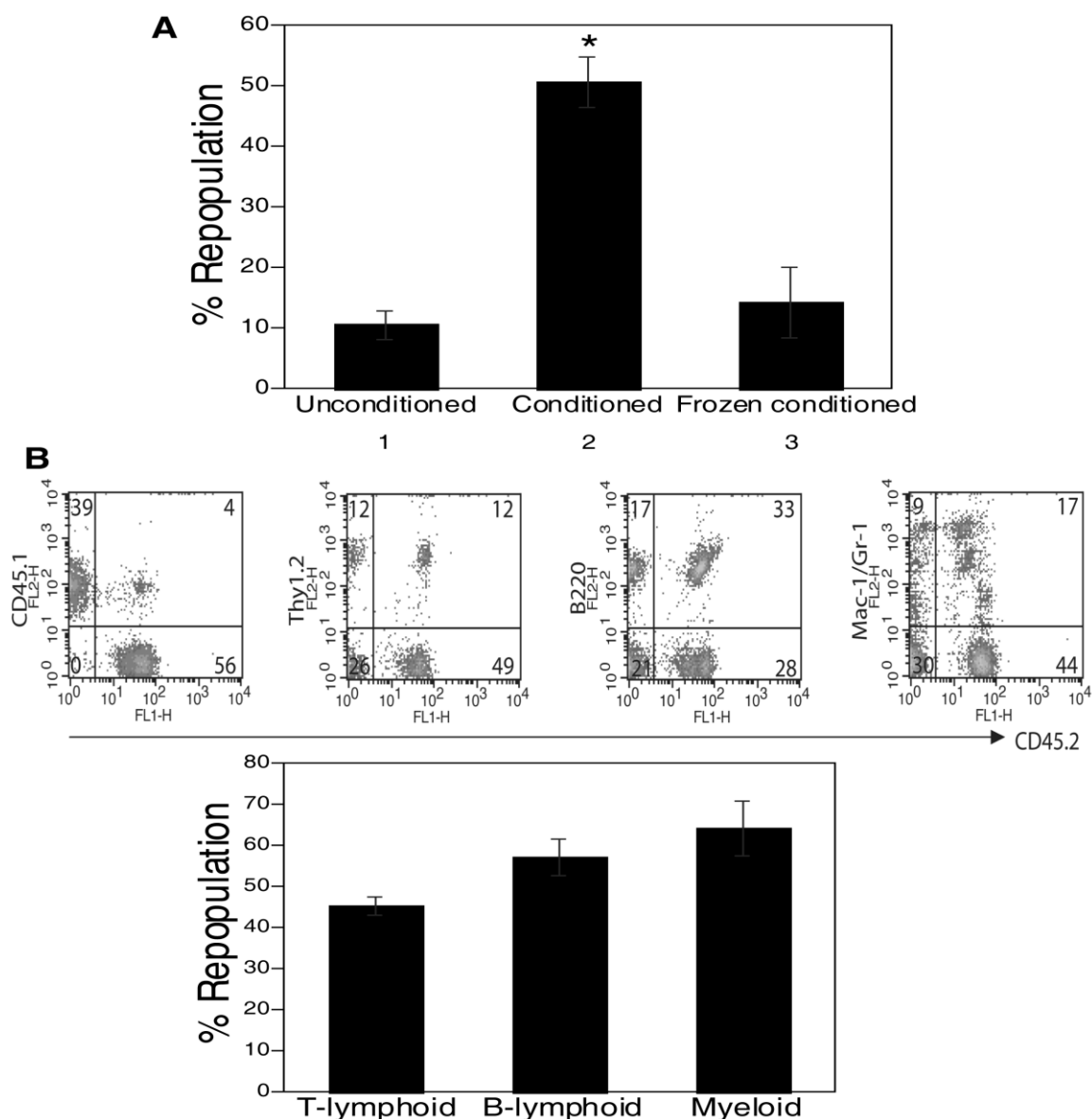


Figure 1. Serum-free conditioned medium collected from 293T cells stimulates *ex vivo* expansion of HSCs. (A) Twenty freshly isolated CD45.2 bone marrow SP Sca-1⁺ CD45⁺ cells were cultured for 10 days in serum-free IMDM medium supplemented with 10 ng/ml SCF, 20 ng/ml TPO, 20 ng/ml IGF-2, and 10 ng/ml FGF-1 (STIF medium; bar 1), in freshly collected serum-free conditioned medium from 293T cells that was supplemented with the same growth factors (conditioned STIF medium) (bar 2), or in the same conditioned medium which had undergone freeze/thaw (bar 3). Then the entirety of the cultures was co-transplanted with 1×10^5 CD45.1 total bone marrow cells into CD45.1 recipients (n = 5-6). Engraftment at 5 months post-transplant is shown. * Significantly different from bars 1 and 3 values. Student's t-test, p < 0.005. (B) Multilineage contribution of cultured cells at conditions represented by bar 2 at 5 months

post-transplant (n = 6). Data shown in the top panel are representative FACS plots of peripheral blood mononuclear cells from one mouse at 5 months post-transplant (bar 2 of Fig. 1A.) Percentages of cells in each quadrant are listed. The summary of data from mice in bar 2 of Fig. 1A is plotted in the bottom panel (B).

IGFBP-2 is the factor expressed by 293T cells that supports HSC expansion

To identify the HSC supportive activity, we used several sizing columns to fractionate serum-free 293T conditioned medium and evaluated the ability of each fraction to support HSC growth. The analysis showed that the HSC supportive activity resided in protein fractions with molecular weights between 10 and 70 kD (data not shown). This result, together with the fact that the HSC stimulating activity was abolished by freeze/thaw, suggested that a protein, secreted by 293T cells, was responsible for stimulating *ex vivo* expansion of HSCs. To this end, we resolved the serum-free 293T conditioned medium using SDS-PAGE and analyzed the protein contents by mass spectrometry. By excluding non-secreted proteins and peptides found in both control serum-free IMDM and 3T3-conditioned medium samples, we focused on a small set of proteins that are present in 293T cell conditioned medium with a molecular weight less than 70 kD (Table 1). One of the candidate proteins was IGFBP2. We confirmed by western blotting that IGFBP2 was expressed in the conditioned medium of 293T cells, but not in that of 3T3 cells (Figure 2A).

We performed a preliminary analysis of the effectiveness of IGFBP2 in supporting the culture of HSCs. In serum-free STIF medium, doses of recombinant IGFBP2 that were equal to or higher than 100 ng/mL supported HSC expansion; Timp-1 did not support expansion at any of the tested concentrations (data not shown). Addition of neutralizing anti-IGFBP2 antibody to HSC cultures completely blocked expansion of

HSCs (compare bars 2 and 4 with bars 1 and 3 in Figure 2B; $p < 0.05$). Thus IGFBP2 is the major factor produced by 293T cells that supports HSC expansion. Considering that 100 ng/mL of IGFBP2 is approximately 3 nM, IGFBP2 stimulated HSC expansion at the nanomolar level.

Characteristic	Accession no.				
	P18065	PO1033	POCOP6	P35555	P36955
Gene	<i>IGFBP2</i>	<i>Timp-1</i>	Neuropeptide S	<i>Fibrillin-1</i>	Pigment epithelium-derived factor
No. of peptides	37	20	12	13	15
Total peptides	46	22	24	22	22
Percentage of coverage	8.45%	5.32%	15.01%	5.70%	2.99%
Molecular weight	35,114	23,156	10,096	26,129	46,313

Proteins also found in the control serum-free samples are not shown.
Abbreviation: IGFBP2, insulin-like growth factor-binding protein 2.

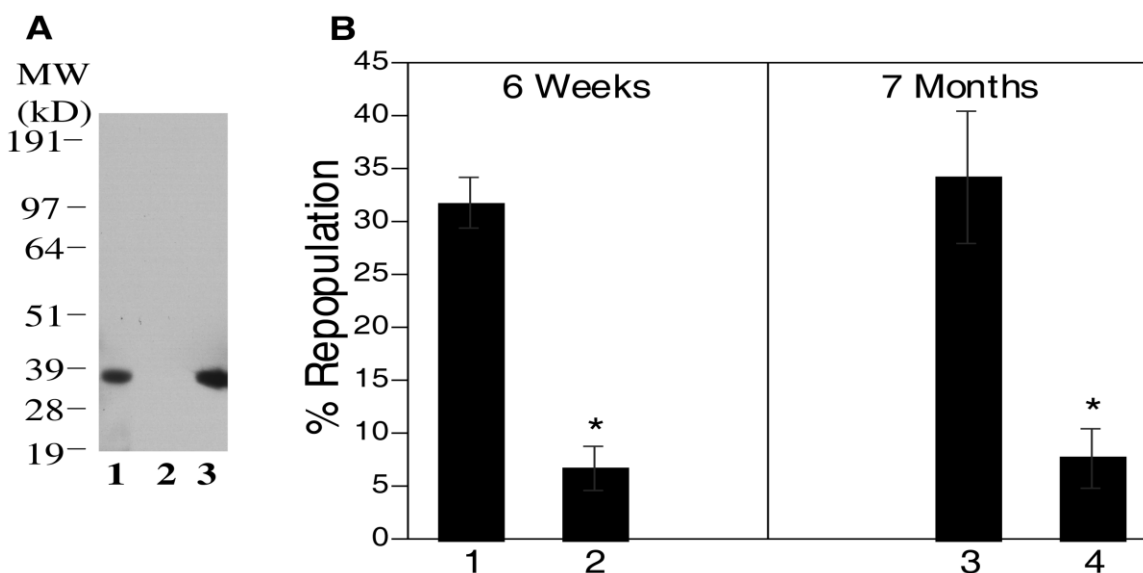


Figure 2. IGFBP2 is the factor in serum-free 293T conditioned medium that stimulates *ex vivo* expansion of HSCs. (A) Western blot analysis of purified human IGFBP2 (positive control; bar 1), serum-free 3T3 cell- conditioned medium (negative control; bar 2), and serum-free 293T cell -conditioned medium (bar 3) detected by an anti-IGFBP2 polyclonal antibody. (B) Twenty freshly isolated CD45.2 bone marrow SP Sca-1⁺ CD45⁺ cells were cultured 10 days in 160 µl serum-free conditioned medium of 293T cells (bars 1 and 3) supplemented with SCF, TPO and FGF-1, or in the same medium containing 10 µg/ml anti-IGFBP2 antibody (bars 2 and 4), respectively. Together with 1 x 10⁵ competitor CD45.1 bone marrow cells, the total culture was injected into CD45.1 recipients (n = 4 - 5). Peripheral blood cells from transplanted mice were analyzed for the presence of CD45.2⁺ cells in lymphoid and myeloid compartments at 6 weeks (bars 1, 2) or 7 months (bars 3, 4) after transplant. *, Significantly different from the value of bar 1 or 3; $p < 0.05$. Abbreviations: kD, kilodalton; MW, molecular weight.

Purified recombinant IGFBP-2 stimulates *ex vivo* expansion of HSCs

We tried to add purified IGFBP2 to the HSC culture medium, in the absence or presence of other factors. As with other known HSC growth factors, IGFBP2 alone could not support HSC expansion; the inclusion of IGFBP2 in our serum-free medium supplemented with SCF, TPO, FGF-1, and IGF-2 supported expansion of HSCs (data not shown). Because IGFBP2 can bind and modulate the biological effects of IGFs²¹, we next tested whether IGFBP2 stimulated HSC expansion if we did not add IGF-2 to the culture. Figure 3 shows that culture of HSCs in the presence of SCF, TPO, and FGF-1 (STF medium) supplemented with IGFBP2 results in dramatically increased repopulating activities compared to freshly isolated HSCs. In one experiment (Figure 3A), twenty freshly isolated SP Sca-1⁺ CD45⁺ cells supported an average of 1.0% engraftment (bar 1). The cultured progenies of the same number of cells after 10 days in STF medium had an increased engraftment of 9.8% (bar 2). Again, culture of the same number of purified HSCs in 293T conditioned medium supplemented with SCF, TPO, and FGF-1 (293T conditioned STF medium) resulted in a dramatic increase of repopulating HSC activity, to 39.3% (bar 3). The addition of 100 ng/ml recombinant IGFBP2 to STF medium also resulted in a large increase in HSC expansion (bar 4) relative to freshly isolated cells or cells cultured in STF medium (bars 1 and 2). Consistent with the results of Figure 2B, treatment of 293T conditioned STF medium with 10 µg/ml anti-IGFBP2 neutralizing antibody again abrogated the HSC stimulating effect of IGFBP2 (bar 5); the control isotype antibody did not show any inhibitory effect (bar 6).

We next tested whether IGFBP2 had HSC stimulatory effects that were additive to those of Angptl3, an HSC growth factor we recently identified¹⁸. When 20 CD45.2 bone marrow SP Sca-1⁺ CD45⁺ cells were cultured for 10 days in STF medium, a modest engraftment of $7.9 \pm 3.6\%$ at 4 month post-transplant was observed (Figure 3B, bar 4). The inclusion of IGFBP2 in the culture significantly increased the engraftment to $24.4 \pm 7.3\%$ (bar 5). The addition of Angptl3 further increased the engraftment to $49.2 \pm 11.3\%$ (bar 6). The numbers of total cells after 10 days of culture were on average 5000 and did not differ significantly among the different conditions. In particular the numbers of Lin⁻ Sca-1⁺Kit⁺ cells or Lin⁻Sca-1⁺IGF2-hFc⁺PrP⁻CD62L⁻ cells, populations enriched for cultured mouse hematopoietic HSCs and progenitors¹⁷, were also not significantly different. This attests to the notion that bone marrow transplantation is still the only reliable method to measure HSC activity; surface phenotypes are unreliable metrics of actual numbers of HSCs. Thus, in the absence of IGF-2, both IGFBP2 and Angptl3 stimulate the expansion of long- term repopulating murine HSCs.

To ensure that the LT-HSCs indeed were expanded during culture, we pooled the bone marrow from primary recipients and transplanted them into secondary recipients. The originally cultured donor cells repopulated lymphoid and myeloid lineages at 1.5, 4, and 7 months after the secondary transplant (Figures 3C and 3D).

In an additional experiment that demonstrated multilineage reconstitution, we cultured one hundred CD45.1 bone marrow SP Sca-1⁺ CD45⁺ cells for 10 days in serum-free STF medium supplemented with 100 ng/ml IGFBP2. The cells were then cotransplanted with 1×10^6 CD45.2 bone marrow Sca-1⁻ cells into CD45.2 recipients. At 6 months post-transplant, those recipient mice fully reconstituted with CD45.1 cultured

donor cells were selected for peripheral blood analysis (n= 3). A comparison of the peripheral blood cell counts with normal non-reconstituted mice showed normal numbers of erythrocytes and platelets and normal hematocrits and hemoglobin levels (Table 2). These experiments reinforce our conclusion that IGFBP2 supports *ex vivo* expansion of HSCs with an effect independent of that of other known HSC growth factors, including Angptls.

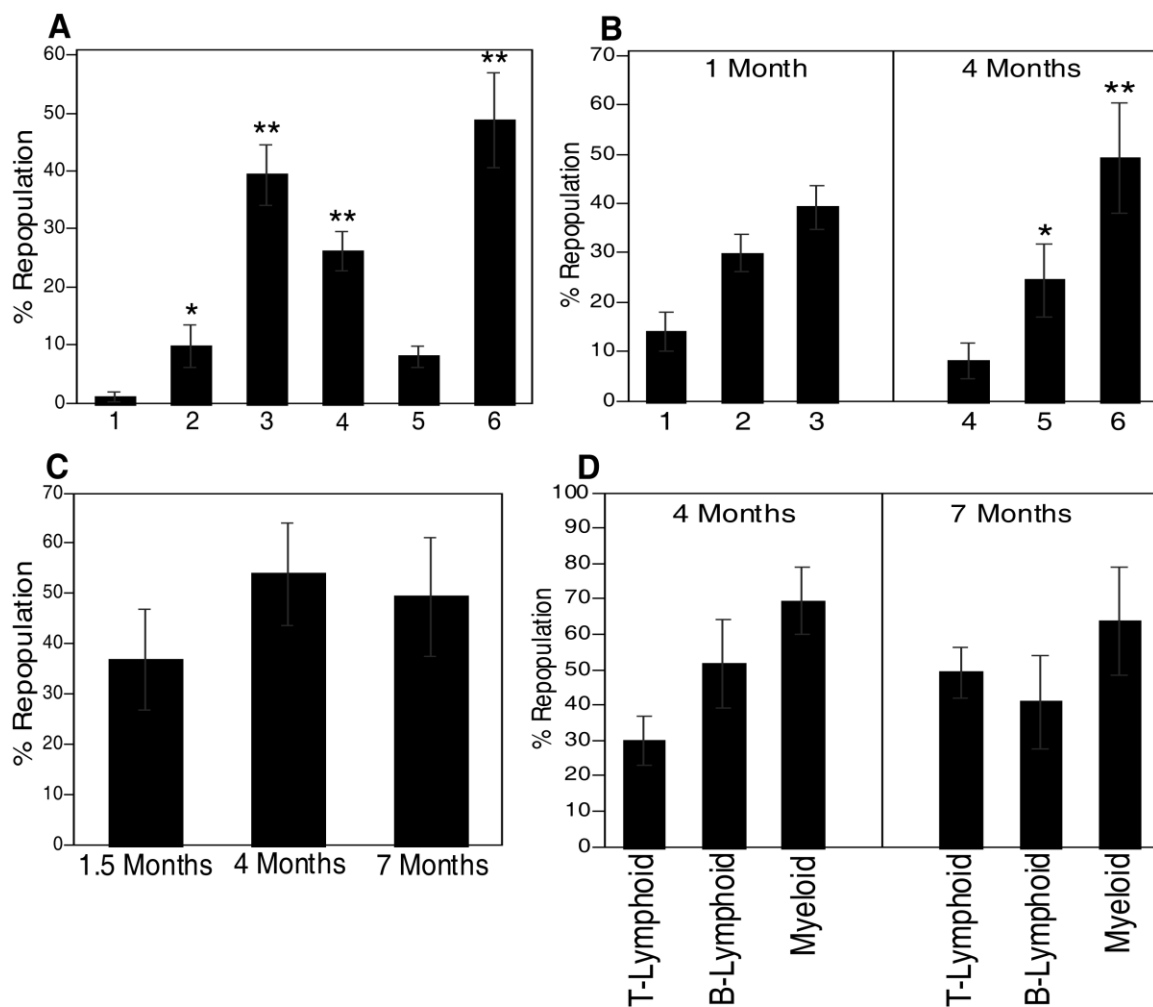


Figure 3. Purified IGFBP2 stimulates *ex vivo* expansion of HSCs. (A) Shown are competitive repopulation at 4 months post-transplant from 20 freshly isolated SP Sca-1⁺ CD45⁺ cells (bar 1), the progenies of the same number of cells cultured for 10 days in STF medium (bar 2), in 293T conditioned medium supplemented with SCF, TPO and FGF-1 (293T conditioned STF medium) (bar 3), in STF medium with 100 ng/ml IGFBP2 (bar 4), in 293T conditioned STF medium pretreated with 10 µg/ml anti-IGFBP2 antibody (bar 5), and in 293T conditioned STF medium pretreated with 10 µg/ml control

antibody (bar 6), respectively ($n = 5$). * or ** Significantly different from the value of bar 1 or bars 2 and 5 respectively, $p < 0.05$. **(B)** Twenty CD45.2 bone marrow SP Sca-1⁺ CD45⁺ cells were cultured for 10 days in serum-free medium with 10 ng/ml SCF, 20 ng/ml TPO, 10 ng/ml FGF-1 (STF medium) (bars 1 and 4); in STF medium containing 500 ng/ml IGFBP2 (bars 2 and 5); and in STF medium containing both 500 ng/ml IGFBP2 and 100 ng/ml Angptl3 (bars 3 and 6). The cells were then cotransplanted with 1×10^5 CD45.1 total bone marrow cells into CD45.1 recipients ($n = 6 - 7$). Engraftments at 1 month or 4 months post-transplant are shown. * or ** Significantly different from bar 4 or bar 5 value respectively. Student's t-test, $p < 0.05$. **(C-D)** Bone marrow of 3 mice at conditions represented by bar 6 of Fig. 3C were pooled at 4 months post-transplant and transplanted into secondary recipients. Total hematopoietic and multilineage engraftments of secondary transplanted mice ($n = 5$) are shown.

Table 2. Peripheral blood analysis of mice fully reconstituted by cultured hematopoietic stem cells

Hematologic parameter	Reconstituted mice	Normal mice
WBC count, per mm ³	8.1 ± 1.3	7.4 ± 1.9
RBC count, × 10 ⁶ per mm ³	7.0 ± 0.8	8.8 ± 1.2
RBC morphology	Normal	Normal
Hematocrit, %	37.3 ± 3.9	43.0 ± 5.6
Hemoglobin, g/dl	10.7 ± 1.3	14.1 ± 0.7
Platelet count, per mm ³	888.7 ± 150.0	840.7 ± 103.5

One hundred CD45.1 bone marrow side population Sca-1⁺CD45⁺ cells were cultured for 10 days in serum-free SCF, thrombopoietin, and fibroblast growth factor-1 medium also containing 100 ng/ml IGFBP2. The cells were then cotransplanted with 1×10^6 CD45.2 bone marrow Sca-1⁻ cells into CD45.2 recipients. At 6 months post-transplant, those recipient mice fully reconstituted with CD45.1 cultured donor cells (with no CD45.2 cells) were selected for peripheral blood analysis ($n = 3$). Normal nonreconstituted CD45.2 mice were also analyzed ($n = 3$). Abbreviations: IGFBP2, insulin-like growth factor-binding protein 2; RBC, red blood cell; WBC, white blood cell.

A cocktail including IGFBP2 supports an approximately 48-fold increase in numbers of repopulating HSCs

We then developed a defined culture condition that included IGFBP2 for expansion of HSCs. Figure 4 shows that a cocktail containing IGFBP2 dramatically increased the numbers of HSCs in culture after 21 days of culture. Freshly isolated BM SP CD45⁺Sca-1⁺ cells were either directly transplanted or cultured for 21 days at normal O₂ in serum-free STF medium supplemented with Angptl3 and IGFBP2. The frequency of repopulating cells (competitive repopulating units or CRU frequency) for freshly isolated SP CD45⁺Sca-1⁺ cells was 1 per 34 (95% confidence interval for mean: 1/17 to 1/68, n = 24). After culture, the number of cells was too few to be counted accurately. Therefore we normalized the CRU frequency to the number of cells added to the culture. After culture the CRU frequency increased to 1/0.7 input equivalent cells (95% confidence interval for mean: 1/0.3 to 1/1.4, n = 26). This represents a more than 48-fold increase in the number of functional LT-HSCs (increase = 34 / 0.7; P < 0.05, Student's *t* test). To our knowledge, this is the highest level of *ex vivo* expansion of HSCs yet achieved in a defined culture.

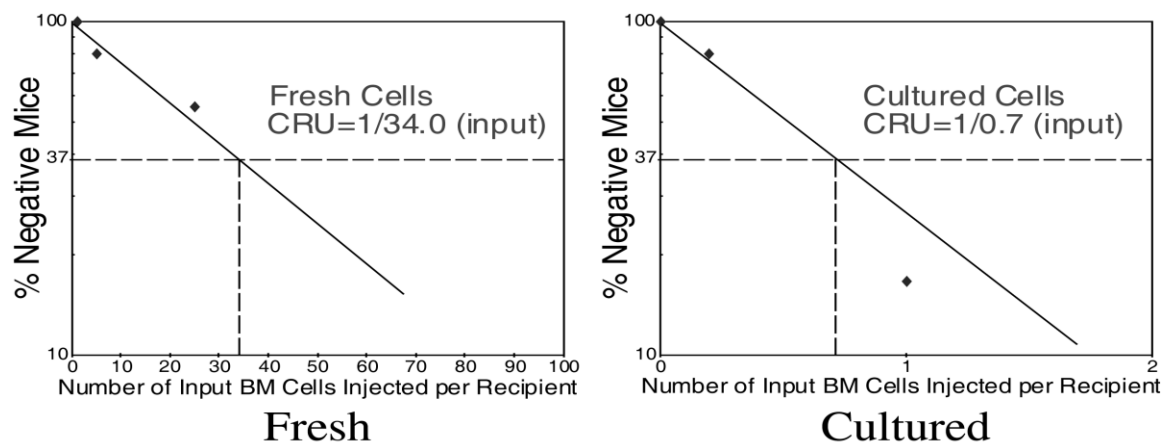


Figure 4. Limiting dilution analysis of the repopulating ability of HSCs before and after culture. Adult BM SP Sca-1⁺ CD45⁺ cells were directly transplanted or cultured for

21 days in serum-free conditioned STF medium containing 100 ng/ml of purified Angptl3 and 500 ng/ml IGFBP2. Irradiated CD45.1 congenic mice were injected with 1×10^5 CD45.1 BM competitor cells and 1, 5, 25, or 100 freshly isolated SP CD45+Sca-1+ cells (left; $n = 24$) or the cultured progenies of 0.2, 1, 5, or 10 SP CD45+Sca-1+ cells (right; $n = 26$). One hundred freshly isolated SP Sca-1⁺ CD45⁺ cells and the cultured progeny of 5 or 10 input cells repopulated all recipients and these data points are not plotted. Plotted is the percentage of recipient mice containing more than 1% CD45.2 myeloid and lymphoid cells in nucleated peripheral blood cells 4 months after transplant, versus the number of input- equivalent cells injected.

IGFBP2 rapidly activates MAP kinase and upregulates HoxB4 expression.

To gain insight into the mechanisms by which IGFBP2 supports HSC expansion, we performed western blotting of bone marrow Lin⁻ cells treated with IGFBP2. As Figure 5A shows, IGFBP2 induced a time-dependent phosphorylation of the MAPK p42/44 pathway in this mixed population of hematopoietic progenitors. The activation of this pathway initiated at 5 min and increased over time. This result was reproduced in at least four additional experiments, and suggests that IGFBP2 directly bind to hematopoietic progenitors.

To identify the intracellular factors that are induced by IGFBP2 in HSCs, a set of transcripts important for HSC function was assessed by quantitative RT-PCR. Treatment by IGFBP2 led to induction in the levels of several Hox mRNAs in bone marrow Lin⁻ Sca-1⁺Kit⁺Flk-2⁻ cells²², including HoxA3, HoxB3, HoxB4, and HoxC6 (Figure 5B).

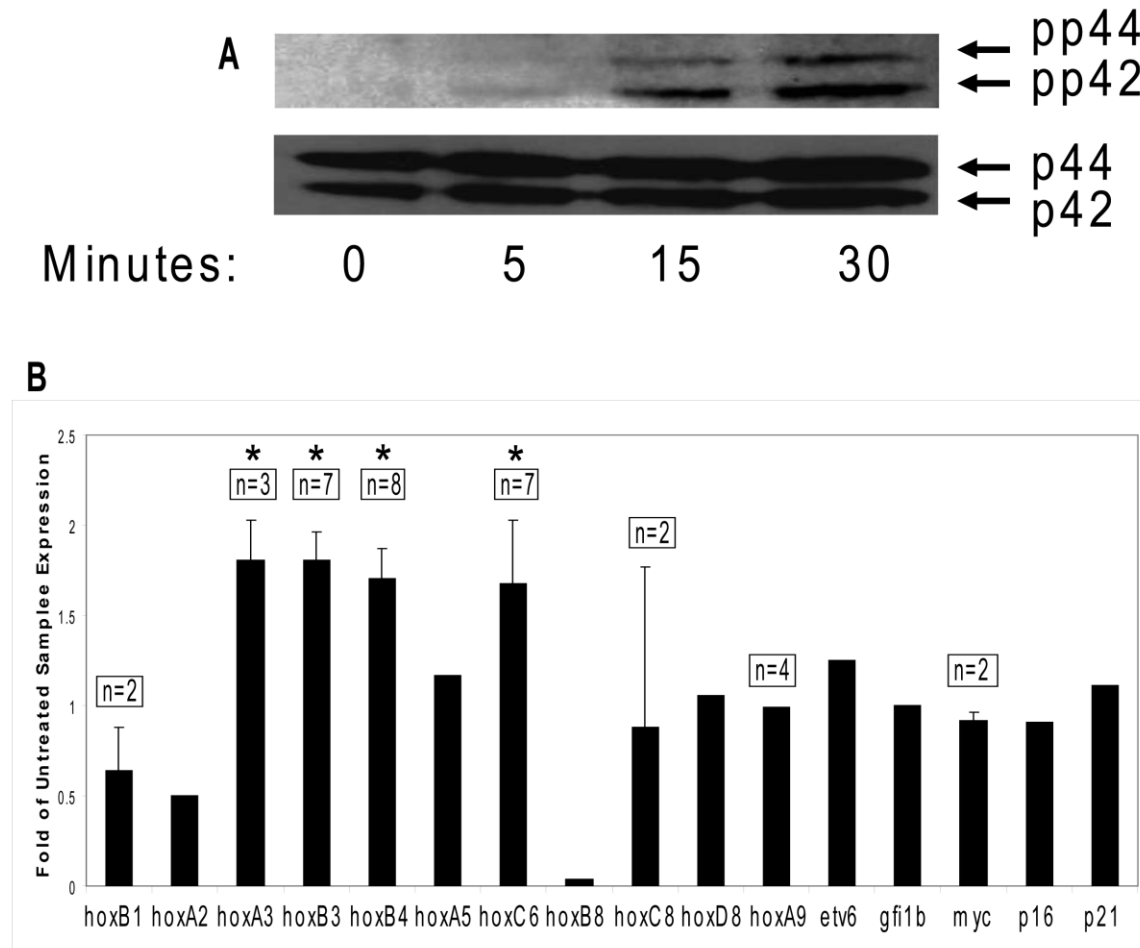


Figure 5. IGFBP2 induced rapid p42/44 MAPK activation and several Hox gene expression. (A) Bone marrow Lin⁻ cells were starved for 4 h in serum-free IMDM containing 0.5% BSA, and then subjected to treatment with 500 ng/ml recombinant IGFBP2 for 0, 5, 15, and 30 min. Cells were directly lysed in RIPA buffer. Protein lysates from equal numbers of cells (30 μ l lysate equivalent to 2×10^5 cells /lane) were subjected to Western blotting analysis. Levels of phosphorylated and total p42/44MAPK proteins are shown. (B) Bone marrow Lin⁻Sca-1⁺Kit⁺Flk-2⁻ cells were cultured in STF medium, treated with or without 100 ng/ml IGFBP2 for 3 h before being collected for analysis. The gene expression in samples untreated by IGFBP2 was normalized to 1. The numbers of replicated experiments are shown. Each experiment contained three real-time PCR reactions. Shown are the results of averages of all real-time PCR reactions. *Significantly different from the values of untreated samples, $p < 0.05$.

DISCUSSION

Previously we showed that IGF-2 and Angptls independently stimulated expansion *ex vivo* of hematopoietic stem cells¹⁶⁻¹⁸. Here we establish that IGFBP2 is an additional HSC supportive factor secreted by tumorigenic 293T cells. IGFBPs are a family of six circulating proteins that bind IGF-1 and IGF-2 with an affinity equal or greater than that of the three IGF receptors. IGFBPs modulate the biological effects of IGFs by controlling IGF distribution, function, and activity²¹. IGFBP2 preferentially binds IGF-2 over IGF-1. IGFBP2 is expressed in the fetus and in a number of adult tissues and biological fluids²³. It is overexpressed in many tumors and in some cases its expression level correlates with the grade of malignancy²⁴⁻²⁶. The expression of IGFBP2 is controlled by a number of hormones, growth factors, transcription factors, including growth hormone, insulin, IGF-1, IGF-2, TGF- β , IL-1, chorionic gonadotropin, follicle-stimulating hormone, estrogen, glucocorticoids, SP1, activating enhancer binding protein 4, and NF κ B (reviewed in reference²⁶), as well as p53²⁷.

Our finding that IGFBP2 promotes the expansion of HSCs was unexpected in light of the IGF-dependent inhibitory effects that IGFBP2 has on normal somatic growth²⁸. Nevertheless, consistent with our result, IGFBP2 deficient mice showed decreased spleen weight and total splenic lymphocyte numbers²⁹. Recently, several studies suggested that, in addition to modulating IGF activities, IGFBP2 also has intrinsic bioactivities that are independent of IGF1 or IGF2. For example, IGFBP2 binds to the cell surface^{24,30} and its binding to integrin alpha 5^{24,31,32}, or alpha v³³ influences cell mobility^{24,31,32} and proliferation^{25,26}. IGFBP2 was shown to stimulate telomerase activity²⁵, modulate MAPK and PI3K activities²⁵, and activate MMP-2³⁴ and the Akt

pathway³¹. In addition, it was shown that oxidative stress lead to the uptake of IGFBP2 into the cell cytosol after 12-24 hours^{26,35}.

Here we showed that IGFBP2 stimulated *ex vivo* expansion of HSCs even when IGF-2 was not included in the culture medium. It also has additive or synergistic effects with Angptl3 and other HSC cytokines including SCF, TPO, FGF-1. Consistently, in bone marrow Lin⁻ cells, a population enriched in HSCs and hematopoietic progenitors, IGFBP2 stimulated activation of MAPK within five minutes, suggesting that IGFBP2 binds to an as yet unidentified receptor on the cell surface and induces a signal transduction pathway that is important for HSC proliferation³⁶. Future studies will be conducted to clarify whether IGFBP2 directly stimulates signal transduction pathways in purified HSCs and whether IGF- initiated signaling is involved.

We also showed that, within 3 h of treatment, IGFBP2 induced expression of several Hox genes in bone marrow Lin⁻Sca-1⁺Kit⁺Flk2⁻ cells, a cell population highly enriched in HSCs. Hox proteins are an evolutionary preserved family characterized by a 60-amino acid DNA-binding homeodomain. Hox genes of the A, B, and C, but not the D, clusters are transcribed during normal hematopoiesis³⁷. Importantly, ectopic expression of HoxB4 supports HSC self-renewal in culture¹². These results support our preliminary hypothesis that IGFBP2 supports HSC expansion partially through upregulation of the expression of several Hox genes. Further studies are needed to investigate the detailed mechanism for IGFBP2's function on HSCs.

It is surprising that IGFBP2 was identified as a protein secreted by a tumorigenic cell line that supports stem cells. It is known that bone marrow hematopoietic progenitors can be recruited to solid tumor sites *in vivo*³⁸. We plan to test whether other cancer cells

are enriched in HSC stimulating activities such as IGFBP2. This may open a new avenue for the study of stem cell niches in pathological conditions. It will also be interesting to determine whether the role of IGFBP2 in solid cancer development has any connection with its ability to expand HSCs in the tumor microenvironment. Our finding that IGFBP2 stimulates the expansion of HSCs suggests that IGFBP2 may be a growth promoter for certain normal and cancer stem cells.

In summary, we isolated IGFBP2 as an HSC-supportive secreted factor from the conditioned medium of tumorigenic 293T cells. The ability of IGFBP2 to support HSC expansion is independent of the addition of previously identified factors, including IGF-2 and Angptls. Added together to a serum- free defined medium, IGFBP2, Angptl3, SCF, TPO, and FGF-1 supported a ~48 fold increase of repopulating HSCs in culture. This is the first demonstration that IGFBP2 stimulates expansion or proliferation of murine stem cells. The culture conditions that we have defined for expansion of HSCs will be useful for a variety of applications, including HSC transplantation, gene delivery, and drug discovery. Though the work described in this paper is confined to mouse HSCs, we recently showed that a serum-free culture containing SCF, TPO, FGF-1, Angiopoietin-like 5, and IGFBP2 supports a ~14-20 fold net expansion of repopulating human cord blood HSCs ³⁹.

REFERENCES

1. Bryder D, Rossi DJ, Weissman IL. Hematopoietic stem cells: the paradigmatic tissue-specific stem cell. *Am J Pathol.* 2006;169:338-346.
2. Verma IM, Weitzman MD. Gene therapy: twenty-first century medicine. *Annu Rev Biochem.* 2005;74:711-738.
3. Sauvageau G, Iscove NN, Humphries RK. In vitro and in vivo expansion of hematopoietic stem cells. *Oncogene.* 2004;23:7223-7232.
4. Sorrentino BP. Clinical strategies for expansion of haematopoietic stem cells. *Nat Rev Immunol.* 2004;4:878-888.
5. Kros J, Austin P, Beslu N, et al. In vitro expansion of hematopoietic stem cells by recombinant TAT-HOXB4 protein. *Nat Med.* 2003;9:1428-1432.
6. Willert K, Brown JD, Danenberg E, et al. Wnt proteins are lipid-modified and can act as stem cell growth factors. *Nature.* 2003;423:448-452.
7. Moore KA, Ema H, Lemischka IR. In vitro maintenance of highly purified, transplantable hematopoietic stem cells. *Blood.* 1997;89:4337-4347.
8. Fraser CC, Eaves CJ, Szilvassy SJ, et al. Expansion in vitro of retrovirally marked totipotent hematopoietic stem cells. *Blood.* 1990;76:1071-1076.
9. Miller CL, Eaves CJ. Expansion in vitro of adult murine hematopoietic stem cells with transplantable lympho-myeloid reconstituting ability. *Proc Natl Acad Sci U S A.* 1997;94:13648-13653.
10. Bunting KD, Galipeau J, Topham D, et al. Effects of retroviral-mediated MDR1 expression on hematopoietic stem cell self-renewal and differentiation in culture. *Ann N Y Acad Sci.* 1999;872:125-140; discussion 140-121.

11. Varnum-Finney B, Xu L, Brashem-Stein C, et al. Pluripotent, cytokine-dependent, hematopoietic stem cells are immortalized by constitutive Notch1 signaling. *Nat Med.* 2000;6:1278-1281.
12. Antonchuk J, Sauvageau G, Humphries RK. HOXB4-induced expansion of adult hematopoietic stem cells ex vivo. *Cell.* 2002;109:39-45.
13. Reya T, Duncan AW, Ailles L, et al. A role for Wnt signalling in self-renewal of haematopoietic stem cells. *Nature.* 2003;423:409-414.
14. Domen J, Weissman IL. Self-renewal, differentiation or death: regulation and manipulation of hematopoietic stem cell fate. *Mol Med Today.* 1999;5:201-208.
15. Wineman J, Moore K, Lemischka I, et al. Functional heterogeneity of the hematopoietic microenvironment: rare stromal elements maintain long-term repopulating stem cells. *Blood.* 1996;87:4082-4090.
16. Zhang CC, Lodish HF. Insulin-like growth factor 2 expressed in a novel fetal liver cell population is a growth factor for hematopoietic stem cells. *Blood.* 2004;103:2513-2521.
17. Zhang CC, Lodish HF. Murine hematopoietic stem cells change their surface phenotype during ex vivo expansion. *Blood.* 2005;105:4314-4320.
18. Zhang CC, Kaba M, Ge G, et al. Angiopoietin-like proteins stimulate ex vivo expansion of hematopoietic stem cells. *Nat Med.* 2006;12:240-245.
19. Zhang CC, Steele AD, Lindquist S, et al. Prion protein is expressed on long-term repopulating hematopoietic stem cells and is important for their self-renewal. *Proc Natl Acad Sci U S A.* 2006;103:2184-2189.

20. Liao MJ, Zhang CC, Zhou B, et al. Enrichment of a population of mammary gland cells that form mammospheres and have in vivo repopulating activity. *Cancer Res.* 2007;67:8131-8138.
21. Ranke MB, Elmlinger M. Functional role of insulin-like growth factor binding proteins. *Horm Res.* 1997;48 Suppl 4:9-15.
22. Christensen JL, Weissman IL. Flk-2 is a marker in hematopoietic stem cell differentiation: a simple method to isolate long-term stem cells. *Proc Natl Acad Sci U S A.* 2001;98:14541-14546.
23. Rajaram S, Baylink DJ, Mohan S. Insulin-like growth factor-binding proteins in serum and other biological fluids: regulation and functions. *Endocr Rev.* 1997;18:801-831.
24. Schutt BS, Langkamp M, Rauschnabel U, et al. Integrin-mediated action of insulin-like growth factor binding protein-2 in tumor cells. *J Mol Endocrinol.* 2004;32:859-868.
25. Moore MG, Wetterau LA, Francis MJ, et al. Novel stimulatory role for insulin-like growth factor binding protein-2 in prostate cancer cells. *Int J Cancer.* 2003;105:14-19.
26. Hoeflich A, Reisinger R, Lahm H, et al. Insulin-like growth factor-binding protein 2 in tumorigenesis: protector or promoter? *Cancer Res.* 2001;61:8601-8610.
27. Grimberg A, Coleman CM, Shi Z, et al. Insulin-like growth factor binding protein-2 is a novel mediator of p53 inhibition of insulin-like growth factor signaling. *Cancer Biol Ther.* 2006;5:1408-1414.

28. Hoeflich A, Wu M, Mohan S, et al. Overexpression of insulin-like growth factor-binding protein-2 in transgenic mice reduces postnatal body weight gain. *Endocrinology*. 1999;140:5488-5496.
29. Wood TL, Rogler LE, Czick ME, et al. Selective alterations in organ sizes in mice with a targeted disruption of the insulin-like growth factor binding protein-2 gene. *Mol Endocrinol*. 2000;14:1472-1482.
30. Russo VC, Bach LA, Werther GA. Cell membrane association of insulin-like growth factor binding protein-2 (IGFBP-2) in the rat brain olfactory bulb. *Prog Growth Factor Res*. 1995;6:329-336.
31. Dunlap SM, Celestino J, Wang H, et al. Insulin-like growth factor binding protein 2 promotes glioma development and progression. *Proc Natl Acad Sci U S A*. 2007;104:11736-11741.
32. Wang GK, Hu L, Fuller GN, et al. An interaction between insulin-like growth factor-binding protein 2 (IGFBP2) and integrin alpha5 is essential for IGFBP2-induced cell mobility. *J Biol Chem*. 2006;281:14085-14091.
33. Pereira JJ, Meyer T, Docherty SE, et al. Bimolecular interaction of insulin-like growth factor (IGF) binding protein-2 with alphavbeta3 negatively modulates IGF-I-mediated migration and tumor growth. *Cancer Res*. 2004;64:977-984.
34. Wang H, Shen W, Huang H, et al. Insulin-like growth factor binding protein 2 enhances glioblastoma invasion by activating invasion-enhancing genes. *Cancer Res*. 2003;63:4315-4321.

35. Besnard V, Corroyer S, Trugnan G, et al. Distinct patterns of insulin-like growth factor binding protein (IGFBP)-2 and IGFBP-3 expression in oxidant exposed lung epithelial cells. *Biochim Biophys Acta*. 2001;1538:47-58.
36. Zhao S, Zoller K, Masuko M, et al. JAK2, complemented by a second signal from c-kit or flt-3, triggers extensive self-renewal of primary multipotential hemopoietic cells. *EMBO J*. 2002;21:2159-2167.
37. Abramovich C, Pineault N, Ohta H, et al. Hox genes: from leukemia to hematopoietic stem cell expansion. *Ann N Y Acad Sci*. 2005;1044:109-116.
38. Kaplan RN, Psaila B, Lyden D. Niche-to-niche migration of bone-marrow-derived cells. *Trends Mol Med*. 2007;13:72-81.
39. Zhang CC, Kaba M, Iizuka S, et al. Angiopoietin-like 5 and IGFBP2 stimulate ex vivo expansion of human cord blood hematopoietic stem cells as assayed by NOD/SCID transplantation. *Blood*. 2008; 111:3415-3423.

**IGF Binding Protein 2 Supports the Survival and Cycling of Hematopoietic Stem
Cells**

ABSTRACT

The role of IGF binding protein 2 (IGFBP2) in cell growth is intriguing and largely undefined. Previously we identified IGFBP2 as an extrinsic factor that supports *ex vivo* expansion of hematopoietic stem cells (HSCs). Here we showed that IGFBP2-null mice have fewer HSCs than wild-type mice. While IGFBP2 has little cell-autonomous effect on HSC function, we found decreased *in vivo* repopulation of HSCs in primary and secondary transplanted IGFBP2-null recipients. Importantly, bone marrow stromal cells that are deficient for IGFBP2 have significantly decreased ability to support the expansion of repopulating HSCs. To investigate the mechanism by which IGFBP2 supports HSC activity, we demonstrated that HSCs in IGFBP2-null mice had decreased survival and cycling, downregulated expression of anti-apoptotic factor Bcl-2, and upregulated expression of cell cycle inhibitors p21, p16, p19, p57, and PTEN. Moreover, we found that the C-terminus, but not the RGD domain, of extrinsic IGFBP2 was essential for support of HSC activity. Defective signaling of the IGF type I receptor did not rescue the decreased repopulation of HSCs in IGFBP2-null recipients, suggesting that the environmental effect of IGFBP2 on HSCs is independent of IGF-IR mediated signaling. Therefore, as an environmental factor, IGFBP2 supports the survival and cycling of HSCs.

INTRODUCTION

The number of hematopoietic stem cells (HSCs) is determined by the balance among different cell fates – self-renewal, differentiation, apoptosis, and migration – which are regulated by the intrinsic factors and environmental cues *in vivo* or *in vitro*^{1,2}. We have identified a number of growth factors and secreted proteins that support the repopulation of HSCs and have developed an efficient serum-free system to support *ex vivo* expansion of mouse and human HSCs³⁻⁵. Insulin-like growth factor binding protein 2 (IGFBP2) is one of these secreted proteins; we isolated IGFBP2 from a cancer line that supports *ex vivo* expansion of HSCs^{6,7}.

IGFBP2 is a member of the IGFBP family that is found in all vertebrates; it modulates the biological effects of IGFs by controlling the distribution, function, and activity of IGF-1 and IGF-2⁸. IGFBP2 is expressed in the fetus and in a number of adult tissues and biological fluids. It is also overexpressed in many tumors and in some cases its expression level correlates with grade of malignancy⁹⁻¹¹. The level of IGFBP2 appears to be low in well-differentiated tumors but high in poorly differentiated tumors¹². The known functions of IGFBP2 are very interesting. IGFBP2 displays IGF-dependent inhibitory effects on normal somatic cell growth. However, several studies demonstrated that IGFBP2 has intrinsic bioactivities that are independent of IGF-1 or IGF-2. IGFBP2 stimulates proliferation, survival, differentiation, and motility of various types of cells^{9, 13-20}. Multiple mechanisms for these IGF-independent actions of IGFBP2 have been proposed. One line of studies supported the concept that intracellular IGFBP2 binds integrin and supports cell survival¹³. A second line of studies suggested that IGFBP2 acts as secreted proteins and binds to cell surface receptors. For example, when bound to the

cell surface integrin, extrinsic IGFBP2 influences cell mobility and proliferation^{9-11, 21}. IGFBP2 also binds to Frizzled 8 and LDL receptor-related protein 6 and is proposed to antagonize Wnt signaling in heart cells²². Moreover, another line of research showed that extrinsic IGFBP2 can be taken up by cells upon oxidative stress; it enters the cytosol after 12-24 hours^{11, 23}.

The roles of IGFBP2 in the hematopoietic system are largely undefined. IGFBP2 supports *ex vivo* expansion of both mouse and human HSCs and is essential for the HSC-supportive activity of activated endothelium^{6, 7, 24}. IGFBP2-null mice have lower spleen weights and total splenic lymphocyte numbers and decreased number and function of mouse osteoblasts in a gender-specific manner^{25, 26}. The IGFBP2 level is negatively associated with the progress of acute leukemia^{27, 28} and the expression of IGFBP2 is a factor for the prediction of relapse of these blood cancer^{27, 29-31}. To gain mechanistic insights into the action of IGFBP2, we tried to address several questions: 1) Does IGFBP2 regulate HSC activity *in vivo*? 2) What cell fate(s) of HSCs does IGFBP2 regulate? 3) Which part of IGFBP2 is essential to its HSC supportive activity? In this study, we found that IGFBP2 had little cell-autonomous effect but environmental IGFBP2 positively supported HSC activity in the mouse bone marrow (BM). In IGFBP2 null mice, HSCs showed decreased survival and cycling, downregulated expression of anti-apoptotic factor Bcl-2, and upregulated expression of cell cycle inhibitors. We further demonstrated that the C-terminus, but not the RGD domain, of secreted IGFBP2 is essential for support of HSC activity, and the environmental effect of IGFBP2 on HSCs is independent of IGF-IR mediated signaling.

MATERIALS AND METHODS

Mice

C57BL/6 CD45.2 and CD45.1 mice were purchased from the National Cancer Institute and the University of Texas Southwestern Medical Center animal breeding core facility. The IGFBP2^{+/-} mice originally obtained from Lexicon Genetics, Inc. were backcrossed to C57BL/6 CD45.2 mice 10 times to obtain IGFBP2-null and wild-type (WT) control littermates. IGF-IR^{+/-} mice as previously described³² were in a pure C57BL/6 background. Mice were maintained at the University of Texas Southwestern Medical Center animal facility. All animal experiments were performed with the approval of UT Southwestern Committee on Animal Care. To genotype mice, DNA was extracted from tail tips and a DNAeasy kit was used according to the manufacturer's instructions (Sigma). The IGFBP2 and/or LacZ-neomycin (neo) insert was amplified in a 3-primer PCR using primers 5'GGGTTCTCCTGGCTGGTGACTC3' and 5'GAGTCTCCCTGGATCTGATTAAGG3' for IGFBP2 and 5'GGGTTCTCCTGGCTGGTGACTC3' and 5'ATAAACCCCTCTTG CAGTTGCATC3' for the lacZ-neomycin insert. The cycling conditions were 94° C for 2 minutes, followed by 35 cycles of 94° C for 45 seconds, 60° C for 45 seconds, and 72° C for 60 seconds, followed by a final extension of 72° C for 5 minutes. To perform RT-PCR to detect IGFBP2 expression in Supplementary Fig. 1, primers 5'GGAGGGCGAAGCATGCGGCGTCTAC3' and 5'GCCCATCTGCCGGTGCTGTTTCATTGACCTT3' were used. To perform real-time RT-PCR to detect IGFBP2 expression in other figures, a primer set purchased from

Qiagen (cat #: QT00269542) was used. Western blots were performed to detect the IGFBP2 protein using the goat anti-IGFBP2 antibody (SC-6002; Santa Cruz Biotechnology).

Mouse HSC culture

Indicated numbers of BM Lin⁻Sca-1⁺Kit⁺Flk-2⁻CD34⁻ cells were isolated from 8-12 week old C57BL/6 mice and were plated into wells of a U-bottom 96-well plate (3799; Corning). StemSpan serum-free medium (StemCell Technologies) was used as the basal medium. The basal medium supplemented with 10 µg/ml heparin (Sigma), 10 ng/ml mouse SCF (R&D Systems), 20 ng/ml mouse TPO (R&D Systems), and 10 ng/ml human FGF-1 (Invitrogen) was used as STF medium. FBS was included in the STF medium in the co-culture experiment as described³³. Cells were cultured at 37°C in 5% CO₂ and the normal level of O₂. For the purpose of competitive transplantation, cells from 12 culture wells were pooled and mixed with competitor/supportive cells before the indicated numbers of cells were transplanted into each mouse as we have done previously³⁻⁷.

Flow cytometry

Donor BM cells were isolated from 8-12 week old C57BL/6 CD45.2 (or CD45.1 as indicated) mice. Lin⁻Sca-1⁺Kit⁺Flk2⁻CD34⁻ cells were isolated by staining with a biotinylated lineage cocktail (anti-CD3, anti-CD5, anti-B220, anti-Mac-1, anti-Gr-1, anti-Ter119; StemCell Technologies) followed by streptavidin-PE/Cy5.5, anti-Sca-1-FITC, anti-Kit-APC, anti-Flk-2-PE, and anti-CD34-PE. For repopulation analysis of mouse

HSCs, peripheral blood cells of recipient mice were collected by retro-orbital bleeding. Red blood cells were lysed, and samples were stained with anti-CD45.2-FITC, anti-CD45.1-PE, anti-Thy1.2-PE (for T-lymphoid lineage), anti-B220-PE (for B-lymphoid lineage), anti-Mac-1-PE or anti-Gr-1-PE (cells co-staining with anti-Mac-1 and anti-Gr-1 were deemed to be of the myeloid lineage) monoclonal antibodies (BD Pharmingen). The “percent repopulation” shown in all figures was based on the staining results of anti-CD45.2-FITC and anti-CD45.1-PE. In all cases FACS analysis of the above listed lineages was also performed to confirm multi-lineage reconstitution as previously described^{3-7, 34}.

Cell cycle and apoptosis analysis

The cell cycle analysis with Hoechst and pyronin Y staining was performed as described³³. Briefly, the Lin⁻Sca-1⁺Kit⁺Flk2⁻CD34⁻ cells were collected in Hank's buffered salt solution medium containing 10% FBS, 1 g/L glucose, and 20 mM HEPES (pH 7.2). Cells were washed, Hoechst 33342 (Invitrogen) was added to 20 µg/ml, and cells were incubated at 37 °C for 45 min after which pyronin Y (1 µg/ml, Sigma) was added. Cells were incubated for another 15 min at 37 °C, washed, and resuspended in cold PBS. Samples were immediately analyzed by flow cytometry (BD Biosciences, FACSAria).

To examine the BrdU incorporation, mice were given three intraperitoneal injections of BrdU (Sigma) (3 mg every 24 hr) in PBS and maintained on 0.2 mg/ml BrdU in the drinking water for 72 hr. After 72 hr, the BM was harvested and stained with antibodies against lineage markers, c-Kit, and Sca-1. Cells were fixed, permeablized, and

denatured, and anti-BrdU-PE (BD Pharmingen) was used to examine the BrdU incorporation as described³³. To examine the apoptosis, Lin⁻Sca-1⁺Kit⁺ cells were stained with PE-conjugated anti-annexin V and 7-AAD according to manufacturer's manual (BD Pharmingen).

Competitive reconstitution analysis

The indicated numbers of mouse CD45.2 or CD45.1 donor cells were mixed with 1×10^5 freshly isolated CD45.1 or CD45.2 competitor BM cells and the mixture was injected intravenously *via* the retro-orbital route into each of a group of 6-9 week old CD45.1 or CD45.2 mice previously irradiated with a total dose of 10 Gy. One million BM cells collected from primary recipients were used for the secondary transplantation as described³³.

Quantitative RT-PCR

Total RNA was isolated from FACS-collected BM Lin⁻Sca-1⁺Kit⁺Flk2⁻CD34⁻ cells, differentiated lineage cells, or non-hematopoietic cells. First-strand cDNA was synthesized using SuperScript II RT (Invitrogen). Samples were analyzed in triplicate 25- μ l reactions (300 nM each primer, 12.5 μ l of Master mix) as adapted from the standard protocol provided in SYBR Green PCR Master Mix and RT-PCR Protocols provided by Applied Biosystems. Primers were purchased from Qiagen or Sigma. The default PCR protocol was used on an Applied Biosystems Prism 7000 Sequence Detection System. The mRNA level in each population was normalized to the level of β -actin RNA transcripts present in the same sample as described⁶.

Colony assays

IGFBP2-null or WT BM cells were resuspended in IMDM with 2% FBS and then seeded into methylcellulose medium M3334 (StemCell Technologies) for CFU-E, M3434 (StemCell Technologies) for CFU-GEMM, CFU-GM, and BFU-E, M3630 (StemCell Technologies) for CFU-Pre-B assays, according to the manufacturer's protocols and as described previously³³.

RESULTS

IGFBP2-null mice have fewer stem cells

To determine the effect of IGFBP2 on HSCs *in vivo*, we evaluated IGFBP2-null mice in C57BL/6 background. The lack of IGFBP2 was confirmed in BM and serum of these mice by RT-PCR and western blotting, respectively (Supplementary Figures 1a and 1b). As reported before²⁵, the IGFBP2-null mice did not show an overt phenotype. The total BM cellularity was normal in both male (Supplementary Fig. 1c) and female mice (Supplementary Fig. 1d). Importantly, however, IGFBP2-null mice had significantly fewer BM HSCs (measured as Lin⁻Sca-1⁺Kit⁺Fli2⁻CD34⁻ (LSKFC) cells) than did WT mice of either gender (Figs. 1a and 1b). The colony forming unit (CFU) assay was performed to evaluate the levels of certain hematopoietic progenitors. This assay indicated that the null mice had more CFU-E and CFU-GM than did the WT mice; however, BFU-E, CFU-Pre-B, and CFU-GEMM did not differ significantly (Fig. 1c). The differences in numbers of HSCs and certain hematopoietic progenitors in IGFBP2-null BM compared to those in WT BM may be due to one of two effects: 1) IGFBP2 may have different effects on HSCs and differentiated cells or 2) the increased numbers of CFU-E and CFU-GM in null mice may counterbalance the lower number of HSCs and maintain homeostasis.

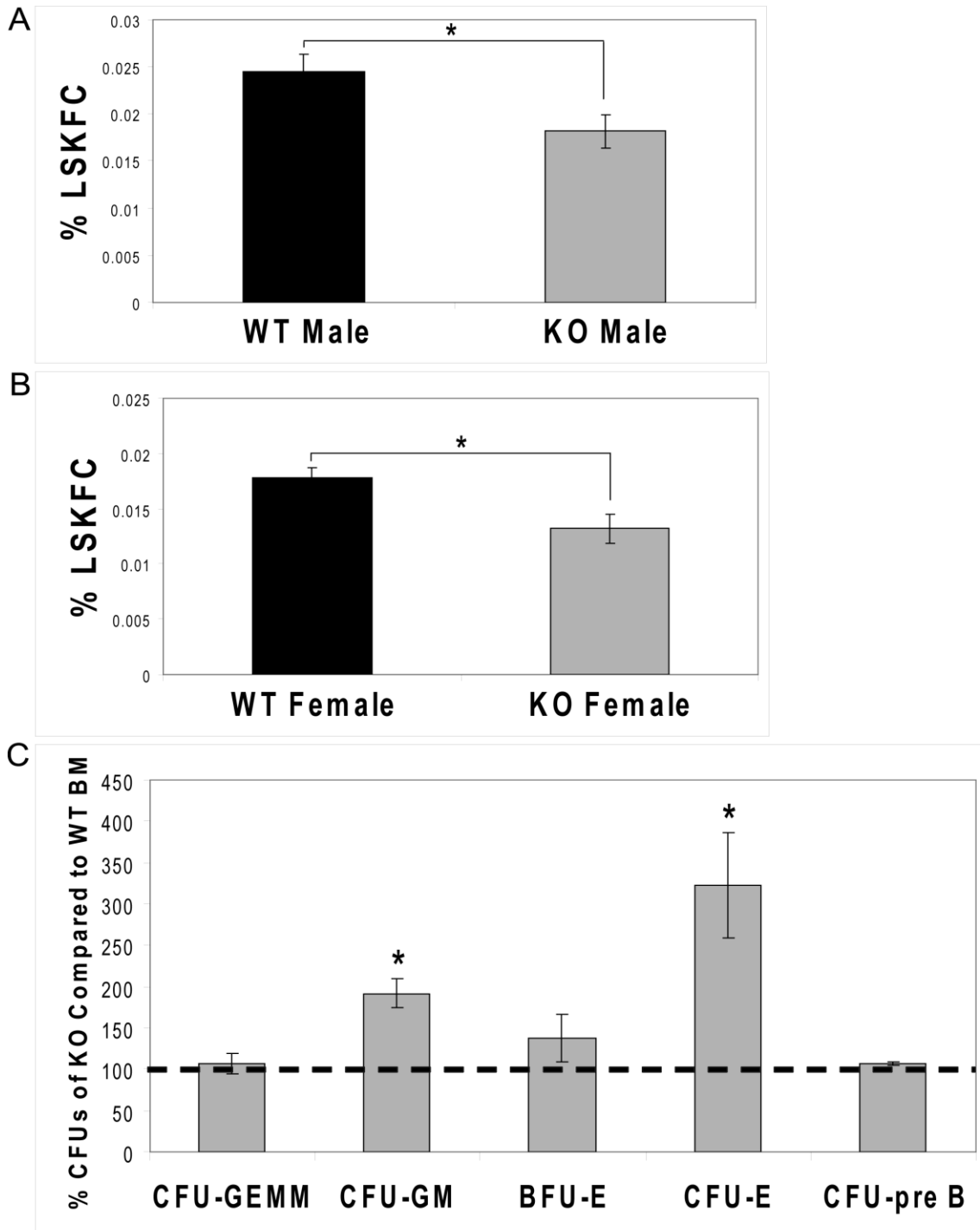
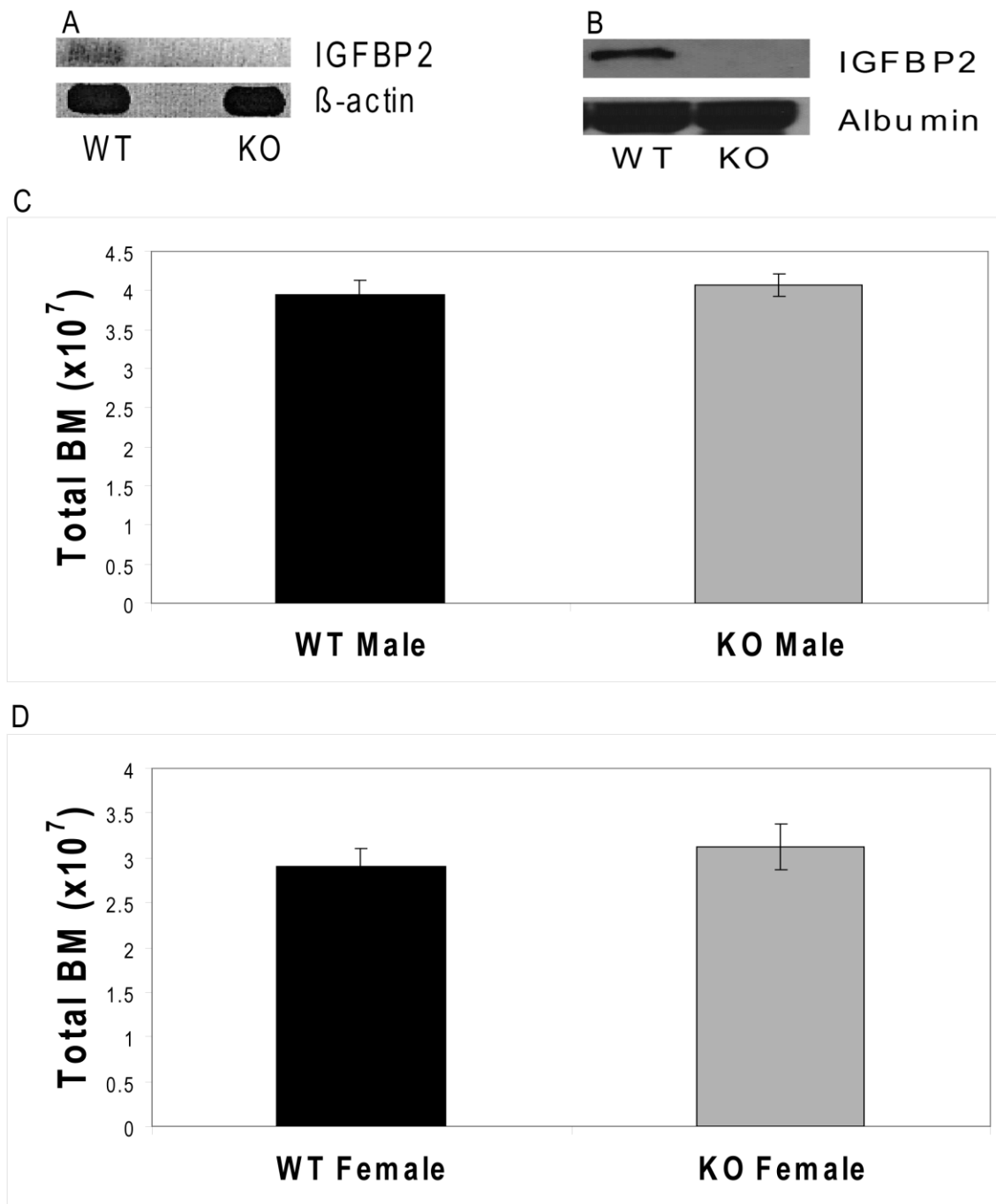


Figure 1. IGFBP2-null mice have fewer HSCs than wild-type mice. LT-HSCs were measured as $\text{Lin}^- \text{Sca-1}^+ \text{Kit}^+ \text{Flk2}^- \text{CD34}^-$ in (A) male littermates ($n = 8$) and (B) female littermates ($n = 7-8$). (C) Colony-forming units assays were performed to evaluate the hematopoietic progenitor cells in the BM as CFU-GEMMs (granulocyte, erythrocyte, monocyte, and megakaryocyte), CFU-GMs (granulocyte and macrophage), BFU-Es (erythroid burst-forming units), CFU-Es (erythroid), and CFU-pre-Bs (pre B-lymphoid) ($n = 4-5$).



Supplementary Figure 1. Characterization of the IGFBP2 null mice. (A) Total BM was isolated and lack of *IGFBP2* in IGFBP2-null mice was confirmed by RT-PCR. (B) Serum samples were harvested, and western blots were performed to detect IGFBP2 protein. Total BM cellularity was measured for (C) male littermates (n = 8) and (D) female littermates (n = 6).

IGFBP2 has little cell-autonomous effect on HSCs

We first collected different hematopoietic populations from mouse BM by flow cytometry and determined the levels of expression of IGFBP2 using real-time RT-PCR. We detected little *IGFBP2* expression in Lin⁻Sca-1⁺Kit⁺Flk2⁻CD34⁻ cells. The level of *IGFBP2* mRNA was 2-fold greater in the BM CD45⁺ hematopoietic populations, and non-hematopoietic CD45⁻ stromal cells had approximately 8-fold higher levels compared to HSCs (Fig. 2a). We then sorted various BM stromal cell populations and measured *IGFBP2* expression. In general, *IGFBP2* mRNA was expressed more abundantly in CD105⁺, CD44⁺, SSEA4⁺, CD29⁺, and Sca-1⁺ BM CD45⁻ stromal cells than in HSCs (Supplementary Fig. 2). These cells may be enriched for mesenchymal stromal cells³⁵. By contrast, CD45⁻CD31⁻ cells expressed greater amounts than CD45⁻CD31⁺ endothelial cells. These results suggest that IGFBP2 may be predominantly expressed by mesenchymal stromal cells but not endothelial cells in the mouse BM.

To test whether IGFBP2 has cell-autonomous function on HSCs, we used the CD45 congenic mouse model to perform competitive BM transplantation. We injected 500 freshly isolated CD45.2 Lin⁻Sca-1⁺Kit⁺Flk2⁻CD34⁻ donor cells from WT and IGFBP2-null mice into lethally irradiated CD45.1 recipients, along with 1x10⁵ CD45.1 total BM cells as competitors. The donors were analyzed for short-term (ST, 6 weeks) and long-term (LT, 17 weeks) repopulation after transplantation (Fig. 2b). No significant difference was observed for the ST and LT donor repopulating activities between the WT and IGFBP2-null HSCs. Both WT and null donor cells repopulated myeloid and lymphoid lineages (Fig. 2c). Taken together, our results suggest that IGFBP2 has minimal cell-autonomous effect on HSCs.

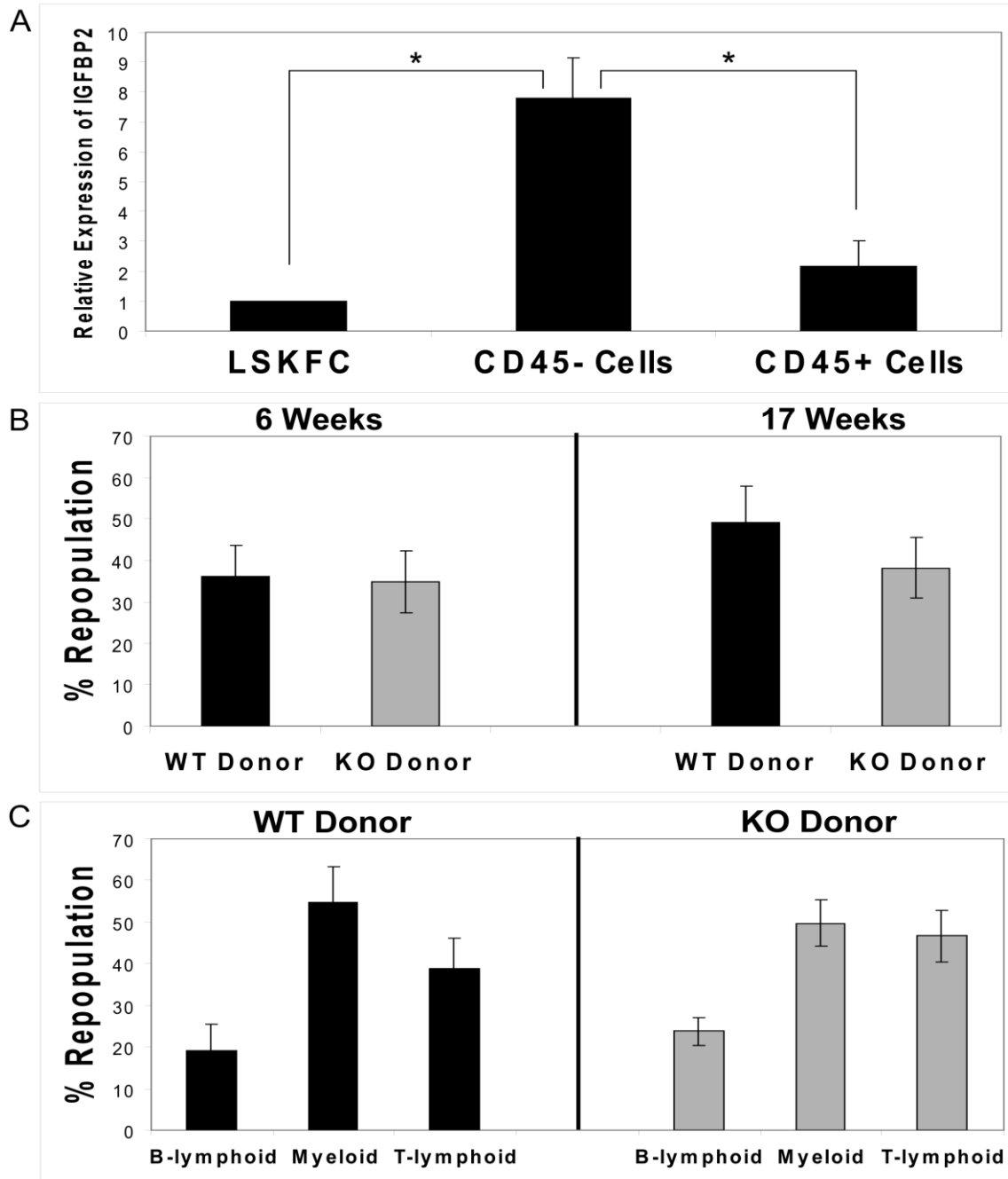
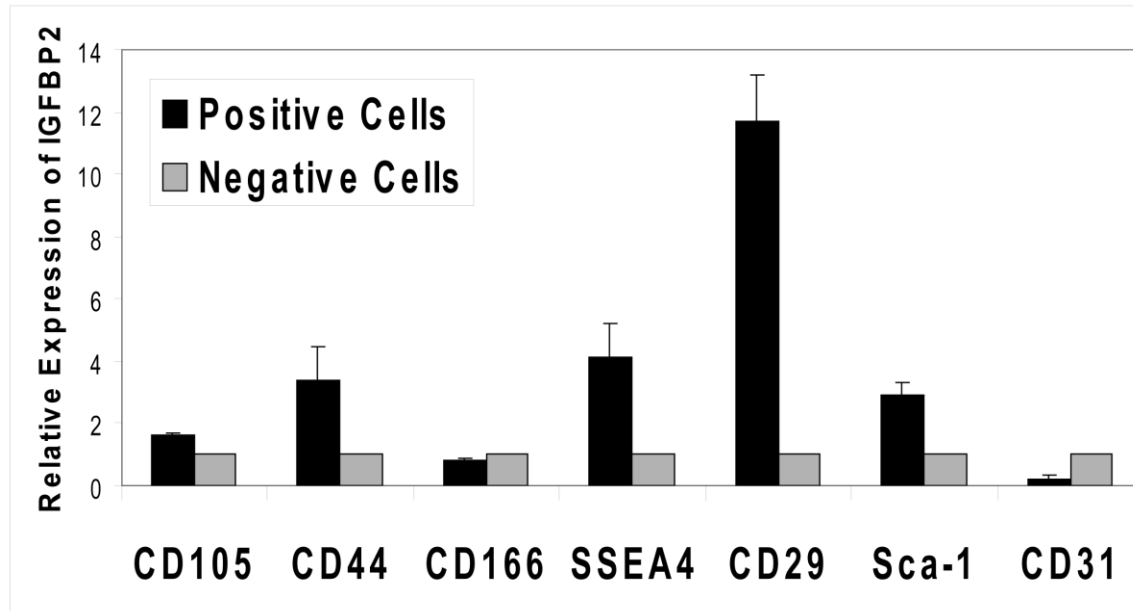


Figure 2. IGFBP2 has little cell-autonomous effect on HSCs. (A) $\text{Lin}^- \text{Sca-1}^+ \text{Kit}^+ \text{Flk2}^- \text{CD34}^-$, hematopoietic CD45^+ , and non-hematopoietic CD45^- stromal cells were freshly isolated from BM, and IGFBP2 gene expression was determined by real-time RT-PCR ($n = 4-5$). (B) Five hundred freshly isolated $\text{CD45.2} \text{Lin}^- \text{Sca-1}^+ \text{Kit}^+ \text{Flk2}^- \text{CD34}^-$ cells from WT or IGFBP2-null mice were co-transplanted with 1×10^5 CD45.1 total BM cells into CD45.1 recipients, and the ST and LT donor repopulating activities were evaluated at indicated time after transplantation ($n = 8$). (C) Different donor lineages from long-term repopulation were determined. Representative data from one of two independent experiments that gave similar results are shown.



Supplementary Figure 2. The expression pattern of IGFBP2 in BM stroma. Various BM CD45⁻ stromal cell populations were isolated, and *IGFBP2* expression was determined by real-time RT-PCR (n = 2-3).

IGFBP2 from the host environment supports HSC activity

Because IGFBP2 was expressed abundantly by the non-hematopoietic BM stromal cells (Supplementary Fig. 2), we sought to test whether IGFBP2 from the BM environment had any effect on HSC function. Here, we transplanted 5×10^5 total CD45.1 BM cells into lethally irradiated CD45.2 WT or IGFBP2-null mice without competitors. We measured percentages of donor-derived phenotypic HSCs (CD45.1⁺ Lin⁻Sca-1⁺Kit⁺Flk2⁻CD34⁻ cells) from the WT or null recipients at 4 months after transplantation, when the hematopoietic system had reached homeostasis (Supplementary Fig. 3). We found that donor-derived HSCs made up 0.014% and 0.009% of HSCs in the WT and null recipients, respectively; recapitulating the higher percentages of HSCs in untransplanted WT mice (Figs. 1a and b).

Next, we conducted a secondary competitive transplantation to measure the repopulation and self-renewal of HSCs. One million of the BM cells from the primarily repopulated WT and IGFBP2-null recipient mice were collected for secondary transplantation along with 10^5 competitor cells (Fig. 3a). We found that the repopulating activity of cells that originated from the primary null recipients was significantly decreased compared to those from the primary WT recipients. Over time, the secondary repopulation of original donor HSCs from the WT primary recipients was about 4-fold higher than that of the same donor cells from the IGFBP2-null primary recipients (Fig. 3b, see bars for 4.5 months). Original donor HSCs repopulated both myeloid and lymphoid lineages (Fig. 3c). Overall these results indicate that IGFBP2 in the BM environment supports *in vivo* expansion and self-renewal of HSCs.

To directly test whether IGFBP2-producing BM cells support HSC expansion, we co-cultured 120 CD45.2 Lin⁻Sca-1⁺Kit⁺Flk2⁻CD34⁻ cells with 360 CD45⁻ stromal cells isolated from the WT or IGFBP2-null mice. After 5 days, the co-cultured cells were used for competitive reconstitution to measure HSC activity. As shown in Figure 3d-e, at 7 and 20-weeks post-transplant, HSCs co-cultured with WT CD45⁻ stromal cells had dramatically increased repopulation efficiency relative to those co-cultured with IGFBP2-null CD45⁻ cells. This result provided functional evidence that IGFBP2 produced by BM CD45⁻ cells supports HSC activity.

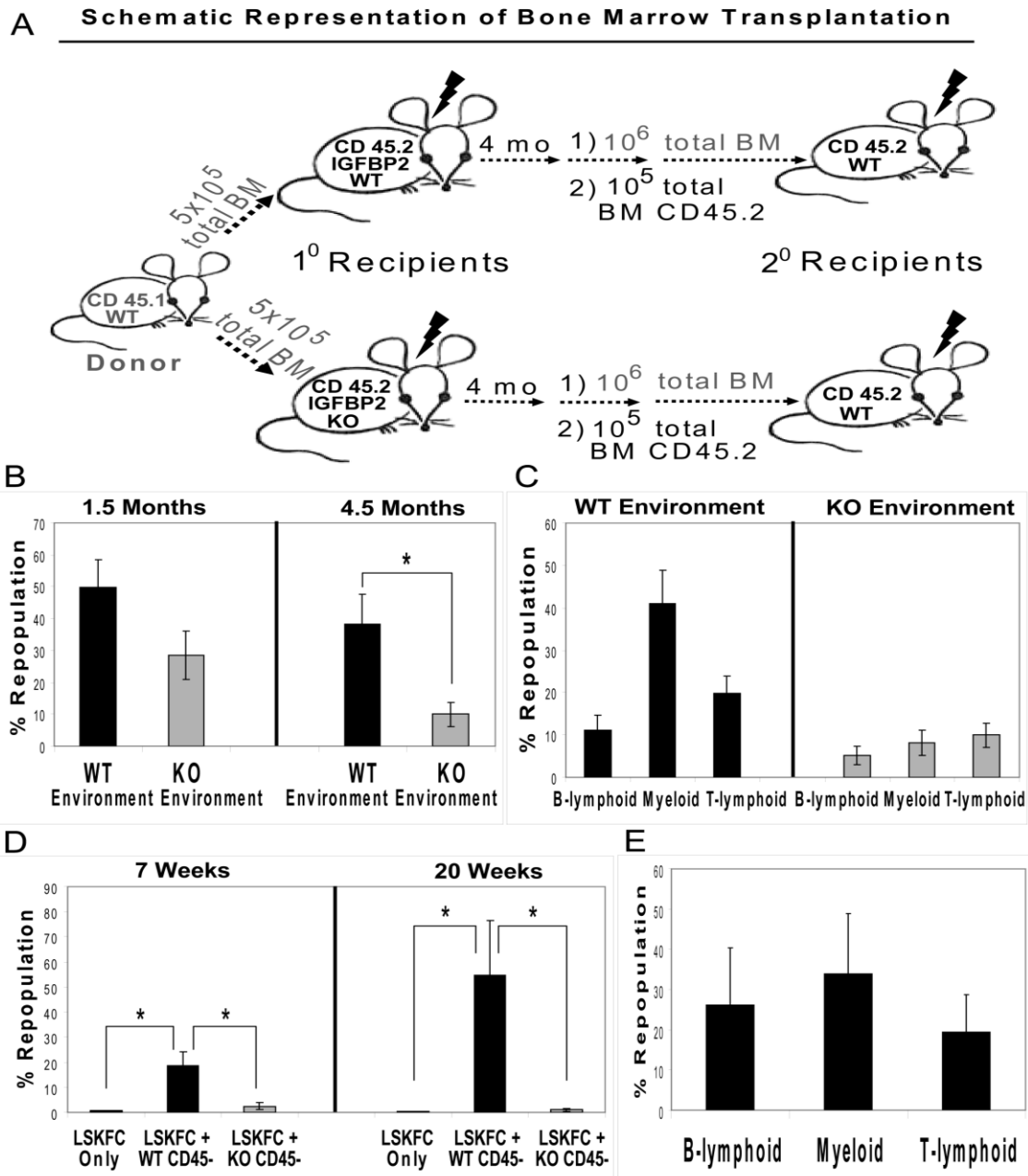
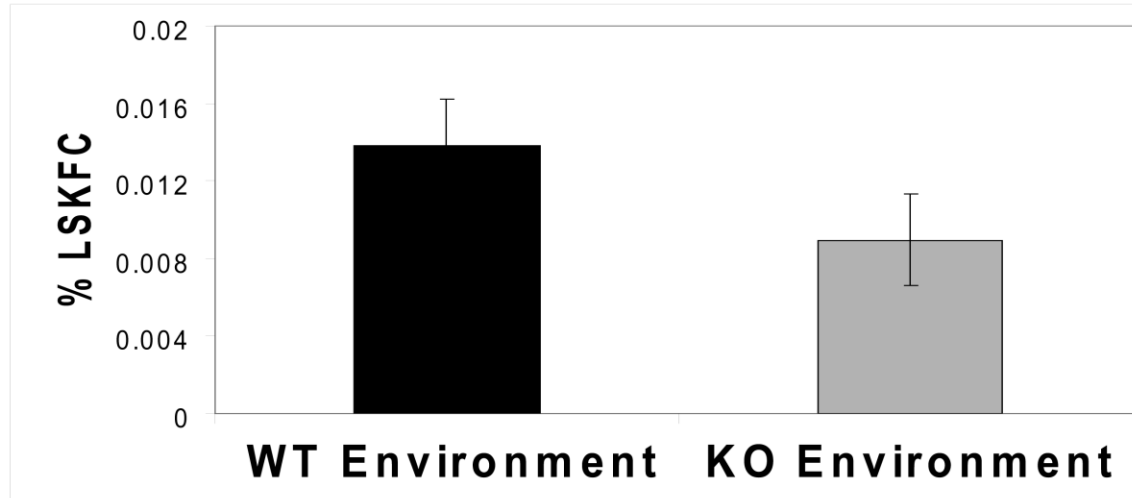


Figure 3. IGFBP2 supports the repopulation of HSCs in the BM environment. (A) A schematic representation of BM transplantation. (B) CD45.1 total BM cells (5×10^5) were transplanted into lethally irradiated CD45.2 WT or IGFBP2-null recipients for 4 months. Subsequently, 1×10^6 CD45.1 total BM cells from primary WT or IGFBP2-null recipients were co-transplanted with 1×10^5 CD45.2 total BM cells into secondary CD45.2 recipients ($n = 9$). Shown are donor repopulations at indicated time after transplantation. Data shown are representative of two independent experiments that gave similar results. (C) Different donor lineages from long-term repopulation were determined. (D) One hundred twenty CD45.2 donor $\text{Lin}^- \text{Sca-1}^+ \text{Kit}^+ \text{Flk2}^- \text{CD34}^-$ cells were co-cultured with 360 WT or IGFBP2-null CD45 $^-$ cells in STF medium containing 10% FBS for 5 days. The cultured cells were then co-transplanted with 1×10^5 CD45.1 total BM cells into CD45.1 recipients

(n = 5). Shown are donor repopulations at indicated time after transplantation. Data shown are representative of two independent experiments that gave similar results. (E) Different donor lineages of long-term repopulation from WT CD45⁺ co-cultured were determined.



Supplementary Figure 3. IGFBP2 supports the increase of the number of HSCs in the BM environment. CD45.1 total BM cells (5×10^5) were transplanted into CD45.2 WT or IGFBP2-null recipients. The donor-derived stem cells from WT or IGFBP2-null primary recipients were measured as Lin⁻Sca-1⁺Kit⁺Flk2⁻CD34⁻ cells at 4 months after transplantation (n = 3).

IGFBP2 promotes the survival and cell cycling of HSCs

To identify the mechanisms by which IGFBP2 supports HSC activity, we first measured the percentages of Lin⁻Sca-1⁺Kit⁺ cells that underwent apoptosis in WT and null mice by flow cytometry. Although there was no significant difference in early apoptosis (annexinV⁺7-AAD⁻) between WT and IGFBP2-null HSCs, IGFBP2-null HSCs showed a significant increase in late apoptosis (annexinV⁺7-AAD⁺) compared to WT counterparts (Fig. 4a).

We also compared the cell cycle status of HSCs in 7-8 week old adult WT and IGFBP2-null mice. The proportion of LT-HSCs (Lin⁻Sca-1⁺Kit⁺Flk2⁻CD34⁻) and ST-HSCs (Lin⁻Sca-1⁺Kit⁺Flk2⁺CD34⁺) in G0 was evaluated by Hoechst 33342 and pyronin

Y staining³³. No significant difference was observed between the cell cycle status of WT and null ST-HSCs (Fig. 4b). In contrast, approximately 20% of WT LT-HSCs were in G₀, a significantly lower percentage than that in IGFBP2-null mice (30%; Fig. 4c). A similar pattern was observed in 1 year old mice for ST-HSCs (Supplementary Fig. 4a), and LT-HSCs (Supplementary Fig. 4b). Moreover, we isolated donor Lin⁻Sca-1⁺Kit⁺Flk2⁻CD34⁻ cells from CD45.1 HSC-transplanted WT or IGFBP2-null recipient mice. LT-HSCs in null hosts were more quiescent than those from WT hosts (Supplementary Fig. 4c), suggesting that IGFBP2 produced by the environment increased the cycling of LT-HSCs. To further confirm that the stem cells of WT mice cycle faster than those from the IGFBP2-null mice, we analyzed BrdU incorporation into Lin⁻Sca-1⁺Kit⁺ cells. Indeed, WT cells incorporated BrdU significantly faster than IGFBP2-null cells ($41.25 \pm 1.74\%$ vs. $33.46 \pm 2.39\%$, respectively) as shown in Fig. 4d.

To examine the spontaneous mobilization of HSCs, we determined levels of Lin⁻Sca-1⁺Kit⁺ cells circulating in the peripheral blood. The level of Lin⁻Sca-1⁺Kit⁺ cells in circulation of IGFBP2-null mice was higher than that in WT mice on average (Supplementary Fig. 4d); however, the difference was not statistically significant. To examine the homing ability of HSCs in WT and IGFBP2-null mice, we labeled and injected 1×10^7 total BM cells into each recipient via retro-orbital injection. Our analysis of recipient BM, spleen, and liver indicated that HSCs had similar homing abilities in WT and IGFBP2-null mice (Supplementary Fig. 4e).

Real-time RT-PCR was performed to confirm the results of apoptosis and cell cycle analyses. To obtain manageable cell numbers and reliable results for real-time RT-PCR, we used Lin⁻Sca-1⁺Kit⁺ cells from WT and IGFBP2-null mice. Concordant with the

phenotypic analyses, our quantitative PCR showed that anti-apoptotic gene Bcl-2 was significantly decreased whereas the cell cycle inhibitors p16, p19, p21, p57, and PTEN were increased in the null Lin⁻Sca-1⁺Kit⁺ cells compared to those of WT cells (Fig. 4e).

Cumulatively, these data showed that IGFBP2 supported HSC survival and cycling in LT-HSCs but not ST-HSCs. Based on this result and our observation that IGFBP2 in the BM enhances the number and repopulation of HSCs in primary and secondary transplantation, we propose that IGFBP2 supports the self-renewal of LT-HSCs.

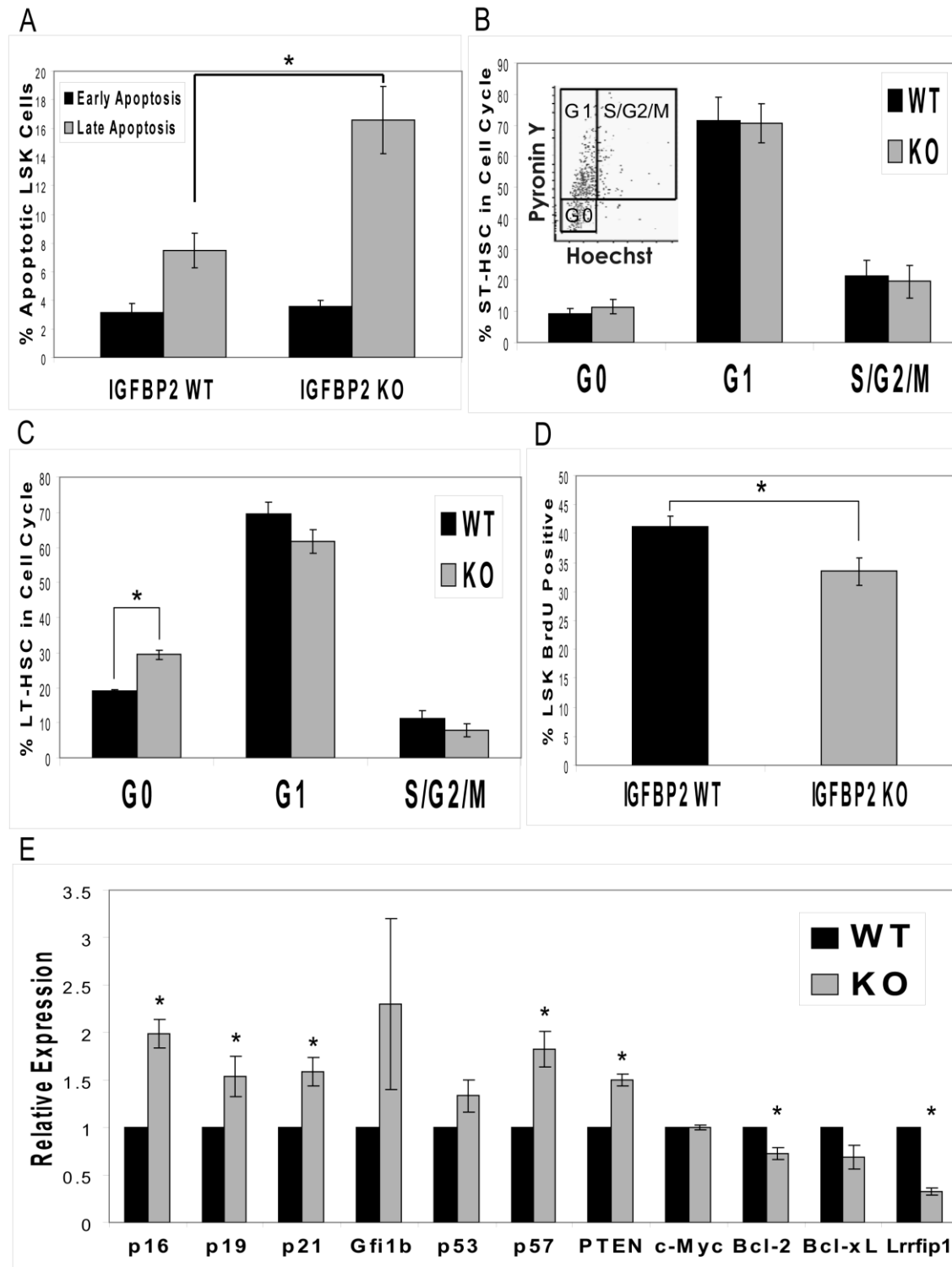
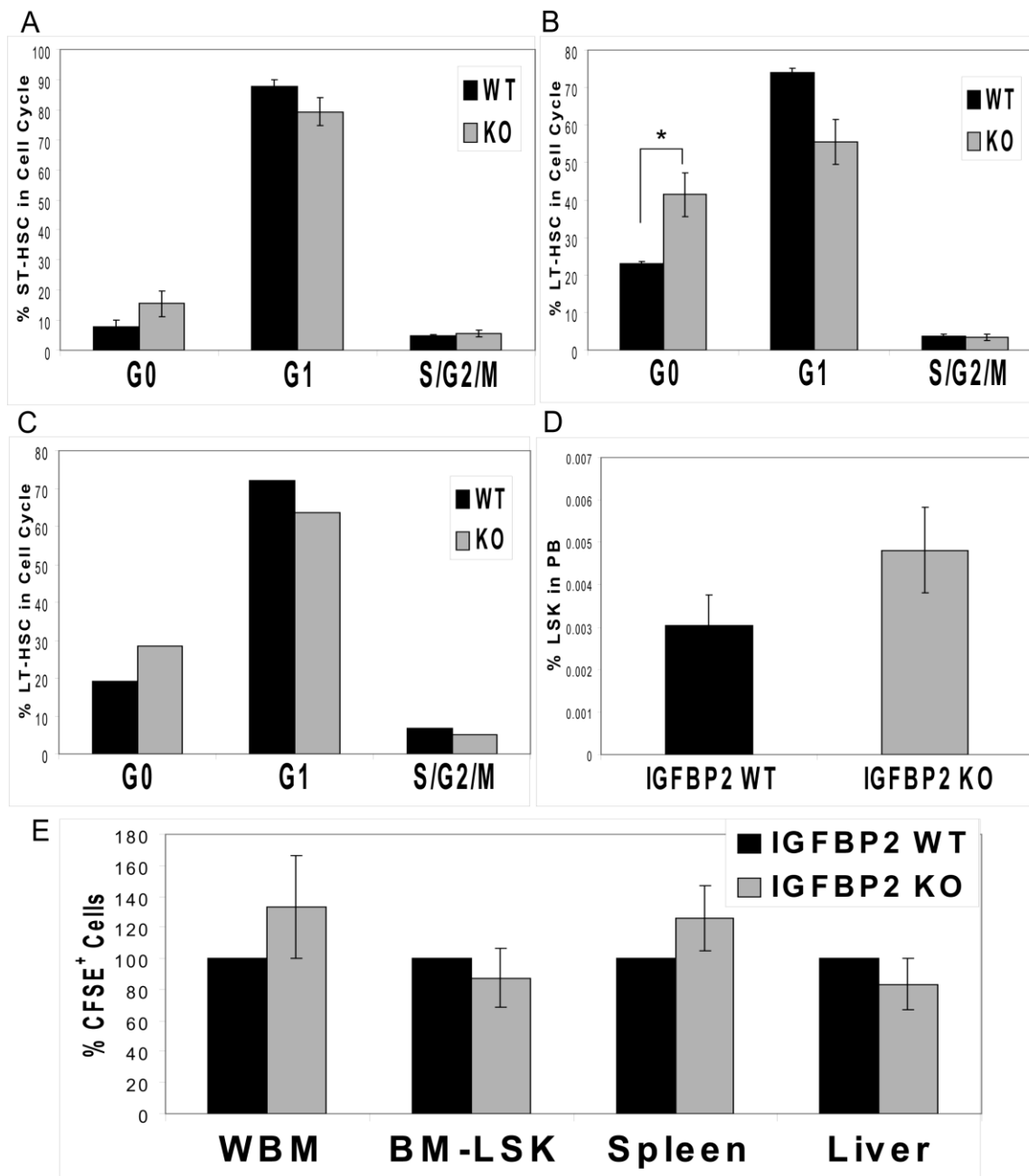


Figure 4. IGFBP2 supports the survival and cycling of HSCs in the BM. (A) Lin⁻Sca-1⁺Kit⁺ cells from BM of WT or IGFBP2-null mice were analyzed for early apoptosis (annexinV⁺7-AAD⁻) and late apoptosis (annexinV⁺7-AAD⁺) markers (n = 6). (B) Cell cycle status of Lin⁻Sca-1⁺Kit⁺Flk2⁺CD34⁺ cells and (C) Lin⁻Sca-1⁺Kit⁺Flk2⁻CD34⁻ cells was evaluated by Hoechst 33342 and pyronin Y staining (n = 6). (D) BrdU incorporation

into Lin⁻Sca-1⁺Kit⁺ cells was measured (n = 8). (E) The expression of certain growth and survival related genes in freshly isolated BM Lin⁻Sca-1⁺Kit⁺ cells was evaluated by real-time RT-PCR (n = 4-6).



Supplementary Figure 4. Characterization of cell fates of HSCs in IGFBP2-null mice. Cell cycle status of (A) BM Lin⁻Sca-1⁺Kit⁺Flk2⁺CD34⁺ cells and (B) Lin⁻Sca-1⁺Kit⁺Flk2⁻CD34⁻ cells isolated from 1 year old mice was evaluated by Hoechst 33342 and pyronin Y staining (n = 5). (C) Cell cycle status of donor-derived BM Lin⁻Sca-1⁺Kit⁺Flk2⁻CD34⁻ cells isolated from transplanted WT or IGFBP2-null mice at 4 months post-transplantation (n = 3). (D) Numbers of circulating Lin⁻Sca-1⁺Kit⁺ cells in the

peripheral blood at normal steady-state ($n = 9$) were measured. (E) The homing ability of WT cells in WT or IGFBP2-null mice was compared ($n = 5$).

The C-terminus of IGFBP2 is important for supporting HSC activity

It has been shown that integrin $\alpha 5$ binds to IGFBP2, specifically to the RGD²⁶⁷ motif. This binding can be abolished by mutating the RGD²⁶⁷ of IGFBP2 to RGE²⁶⁷ ^{14, 36}. To test whether the RGD domain mediates the function of extrinsic IGFBP2 in HSCs, we constructed two IGFBP2 mutants, one with the RGD²⁶⁷ to RGE²⁶⁷ mutation and the other with 41 amino acids deleted from the C-terminus (Fig. 5a).

We overexpressed these constructs in 293T cells. The WT or mutant IGFBP2 was secreted into the conditioned medium (Fig. 5b). A normalized amount of this conditioned medium in STF medium was used to culture HSCs for 10 days as described ⁶. The abilities of these IGFBP2 variants to support HSC growth were evaluated by transplanting the cultured cells into lethally irradiated recipient mice in a competitive reconstitution analysis. The donor repopulating activities were analyzed at 1 and 4 months after transplanted. RGE IGFBP2 supported HSCs activities equally as well as WT IGFBP2 (Fig. 5c), suggesting that the RGD domain does not mediate IGFBP2's effect on HSC expansion. In striking contrast, the truncated IGFBP2 was unable to support the expansion of ST or LT repopulating HSCs (Fig. 5c). Therefore, the C-terminal region of IGFBP2 is important for supporting HSC function.

Because the C-terminus of IGFBP2 is involved in both IGF binding ³⁷ and IGF-independent signaling ³⁸, we sought to determine whether IGFBP2's effect on HSCs depended on IGF signaling. Here, we compared the repopulation of IGF-IR-null donor cells in WT and IGFBP2-null recipients. Because IGF-IR-null is lethal at birth, we used

IGF-IR-null fetal liver cells to reconstitute mice. Using competitive reconstitution analysis, we demonstrated that the IGF-IR-null HSCs repopulating ability was similar to WT counterparts with no defects in differentiation (data not shown). Next, we transplanted 1×10^5 IGF-IR-null fetal liver cells into lethally irradiated WT or IGFBP2-null mice. We measured the donor stem cells ($\text{Lin}^- \text{Sca-1}^+ \text{Kit}^+ \text{Flk2}^- \text{CD34}^+$) from the WT or IGFBP2-null BM 4 months after transplantation, and found significantly fewer IGF-IR-null HSCs in the IGFBP2-null environment than in the WT (Supplementary Fig. 5). This decrease was similar to the difference between WT HSC repopulation in the WT and IGFBP2-null environments (compare Supplementary Fig. 3 and 5).

We then performed secondary competitive BM transplantation 4 months after primary transplantation similar to the experiment shown in Fig. 3a. The donors from the WT environment repopulated more efficiently than the donors from IGFBP2-null environment in the short-term ($47.11 \pm 9.28\%$ vs. $21.59 \pm 6.64\%$) and long-term ($16.61 \pm 3.37\%$ vs. $4.89 \pm 1.41\%$) as shown in Fig. 5d. Donors from both environments had normal differentiated lineages (Fig. 5e). Therefore, HSCs that were defective in IGF-IR signaling had decreased repopulation in IGFBP2-null recipients. This result can be explained by two possibilities: 1) IGFBP2 stimulates IGF-IR signaling, or 2) IGFBP2's regulation of HSC activity is independent of IGF-IR signaling. Because we found that, as demonstrated by numerous other studies, IGFBP2 in fact blocks the binding of IGF to IGF-IR (not shown), the first possibility does not exist. Our result thus suggests that the environmental effect of IGFBP2 on HSCs is independent of IGF-IR-mediated signaling.

A Schematic Representation For IGFBP2 Mutants

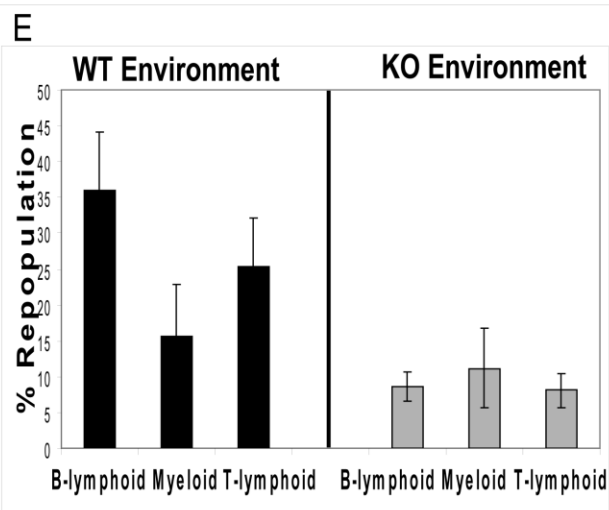
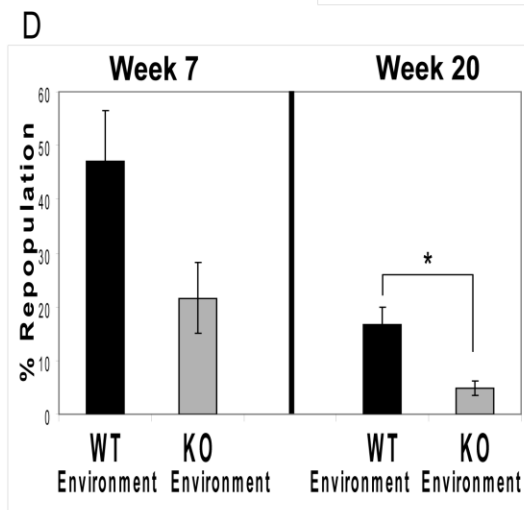
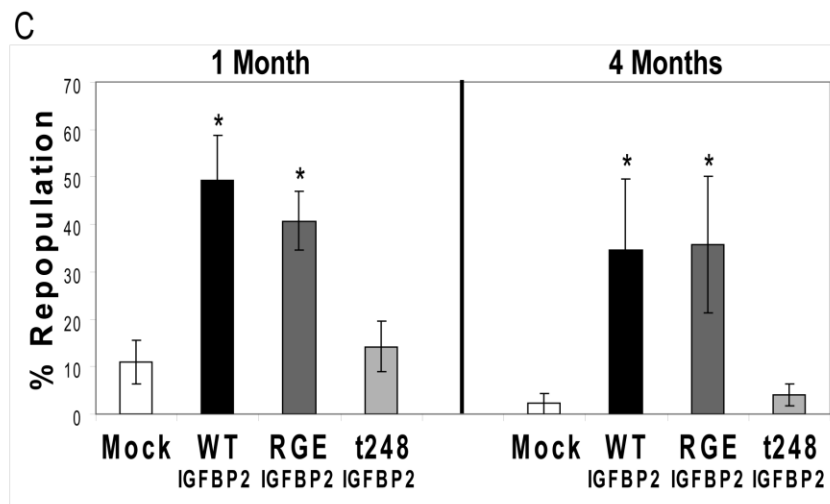
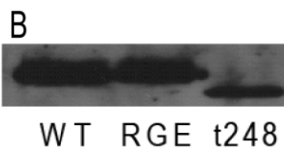
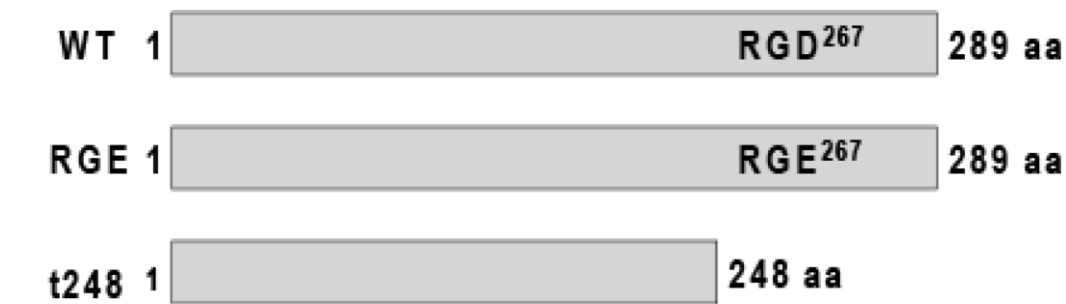
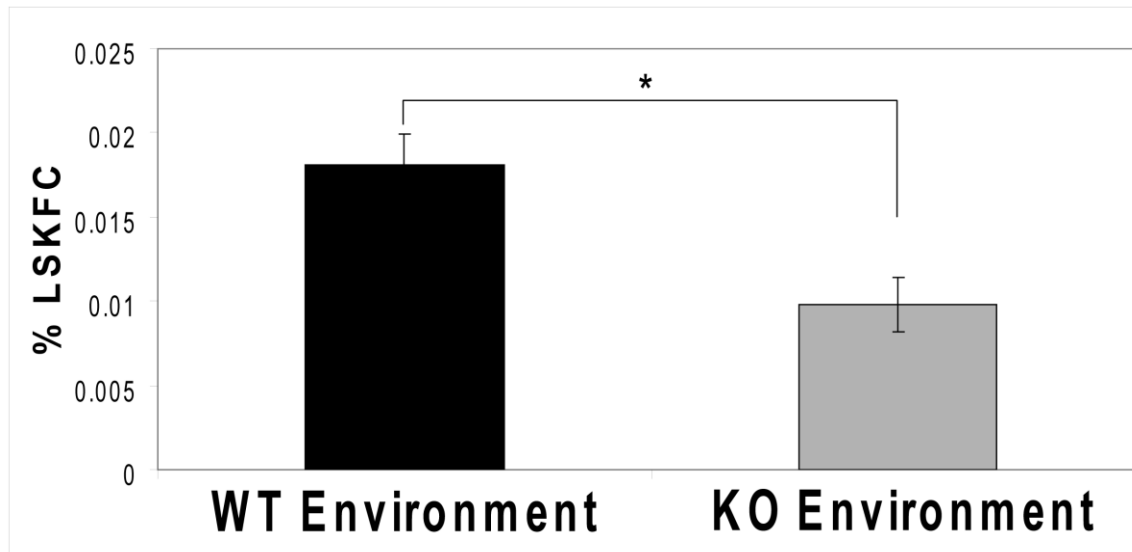


Figure 5. The C-terminus of IGFBP2 is essential for IGFBP2's HSC supportive activity. (A) Schematic representation for IGFBP2 mutants. (B) WT, RGE²⁶⁷, and t248 IGFBP2 constructs were transfected into 293T cells and the levels of secreted IGFBP2 proteins in the media at 60 hr after transfection were evaluated by western blot. (C) Normalized amounts of the WT and mutant IGFBP2 in the conditioned media (~500 ng/ml) were added to STF medium, and then 20 CD45.1 donor Lin⁻Sca-1⁺Kit⁺Flk2⁻CD34⁻

cells were cultured for 10 days. The cultured cells were co-transplanted with 1×10^5 CD45.2 total BM cells into CD45.2 recipients ($n = 6$). The data shown are representative of two independent experiments that gave similar results. **(D)** Total IGF-IR-null fetal liver cells (1×10^5) were transplanted into lethally irradiated WT or IGFBP2-null recipients. After 4 months, 1×10^6 total donor BM cells from primary WT or IGFBP2-null recipients were co-transplanted with 1×10^5 CD45.1 total BM cells into secondary CD45.1 recipients ($n = 5$). **(E)** Different donor lineages from long-term repopulation were determined. Representative data from two independent experiments that gave similar results are shown.



Supplementary Figure 5. The HSC supportive effect of IGFBP2 is independent of IGF-IR mediated signaling. Total IGF-IR-null fetal liver cells (1×10^5) were transplanted into lethally irradiated WT or IGFBP2-null recipients. The donor-derived stem cells from WT or IGFBP2-null primary recipients were measured as Lin⁻Sca-1⁺Kit⁺Flk2⁻CD34⁻ cells at 4 months after transplantation ($n = 3$).

IGFBP2 modulates Wnt signaling in HSCs

Our data suggested that integrin $\alpha 5 \beta 1$ is not important for HSC expansion. It led us to test alternatives receptor(s) for IGFBP2. Recent study showed that several IGFBPs, including IGFBP4 and IGFBP2, antagonized the canonical Wnt signaling in cardiomyocytes by binding to Frizzled 8 (Frz8) receptor and LDL receptor-related protein 6 (LRP6)²². However, the binding of IGFBP2 is weaker than IGFBP4. Fleming et al. 2008 used DKK1-transgenic mice to show that Wnt signaling in the bone marrow

niche is required for hematopoietic stem cell to maintain its quiescence³⁹. Our data showed that IGFBP2 promotes cell cycling in long-term HSCs (Fig. 4c). To determine whether IGFBP2 plays any role in modulating the Wnt signaling on HSCs, we freshly isolated Lin⁻Sca1⁺Kit⁺ cells from either wild-type or null mice. Real-time RT-PCR was performed, and gene expression of Wnt target genes was evaluated as well as cell cycle regulators (Fig. 6a). Indeed, IGFBP2 null mice significantly up-regulated Axin2, β -catenin, cyclin D1, p21, and Frz8. In particular, LRP6 is not significantly up-regulated in IGFBP2 null mice. Suggesting Frz8 plays a major role in hematopoietic stem cell homeostasis involving IGFBP2 *in vivo*.

To confirm the *in vivo* observation that IGFBP2 could modulates Wnt activities on HSCs, we isolated wild-type LSK cells and treated with Wnt3a, IGFBP2, or a combination of Wnt3a and IGFBP2 at different time points *in vitro*. HSCs treated with Wnt3a, IGFBP2, or combination of wnt3a and IGFBP2 for 6 hours do not have any significant effect (Fig. 6b). However, some target genes for Wnt pathway are increased when treated with Wnt3a for 24 to 38 hours (Fig. 6c). Interestingly, IGFBP2 alone does not have much effect on these indicated Wnt target genes. When wnt3a added together with IGFBP2, these Wnt target genes were down-regulated significantly, which is recapitulated the *in vivo* observation.

To further test whether IGFBP2 could modulate the Wnt signaling in a simplified model, we used pTOPflash plasmid to test the luciferase activity for IGFBP2 through Frz8/LRP6 that act as receptor/co-receptor for Wnt3a. Indeed, our real-time PCR results showed both Frz8 and LRP6 are expressed abundantly in the mouse bone marrow Lin⁻Kit⁺Sca1⁺ cells. Initially, we cotransfected pTOPflash plasmid with either Frz8 or LRP6

plasmid into 293T cells for 22 hours. The transfected 293T cells were then treated with Wnt3a, IGFBP2, or Wnt3a/IGFBP2 mixture for additional 24 hours. The cells were harvested, and luciferase activities were measured. IGFBP2 treatment alone could activate the luciferase activities significantly (Figs. 7a & b). We expected the luciferase level would be additive, if not synergistic, when IGFBP2 was added together with wnt3a ligand. Interestingly, the luciferase level was modestly decreased when two ligands were added together.

Next we cotransfected pTOPflash with both Frz8 and LRP6 into 293T cells, and treated with ligands as above for 24 hours. The luciferase activity pattern was similar to that of Frz8- or LRP6-transfected cells (Fig. 7c). We also treated the LRP6-, and Frz8/LRP6-transfected 293T cells with ligands for 6 and 10 hours, but IGFBP2 apparently has no effect at these early time points (Figs. 7d-f).

Zhu et al 2008 showed that IGFBP1, IGFBP2, IGFBP4, and IGFBP6 can bind to Frz8 and LRP6. The authors concluded that those IGFBPs are the inhibitors of canonical Wnt signaling pathway; however, IGFBP4 is the strongest inhibitor. Consistent with data published by Zhu et al 2008, our data showed that IGFBP2 could decrease the luciferase activities at a modest level when combined with Wnt3a. However, in our luciferase assay, the IGFBP2 alone could activate the Wnt signaling (Figs. 7a-c). This suggests that IGFBP2 may not necessarily act as an inhibitor of the Wnt signaling, but its binding to Frz8 or LRP6 may not be as tight as Wnt ligands, at least for 293T cells. Whether the result in 293T cells would indicate the situation in primary HSCs is unknown. Future investigation is warranted to clarify the role of IGFBP2 in Wnt signaling.

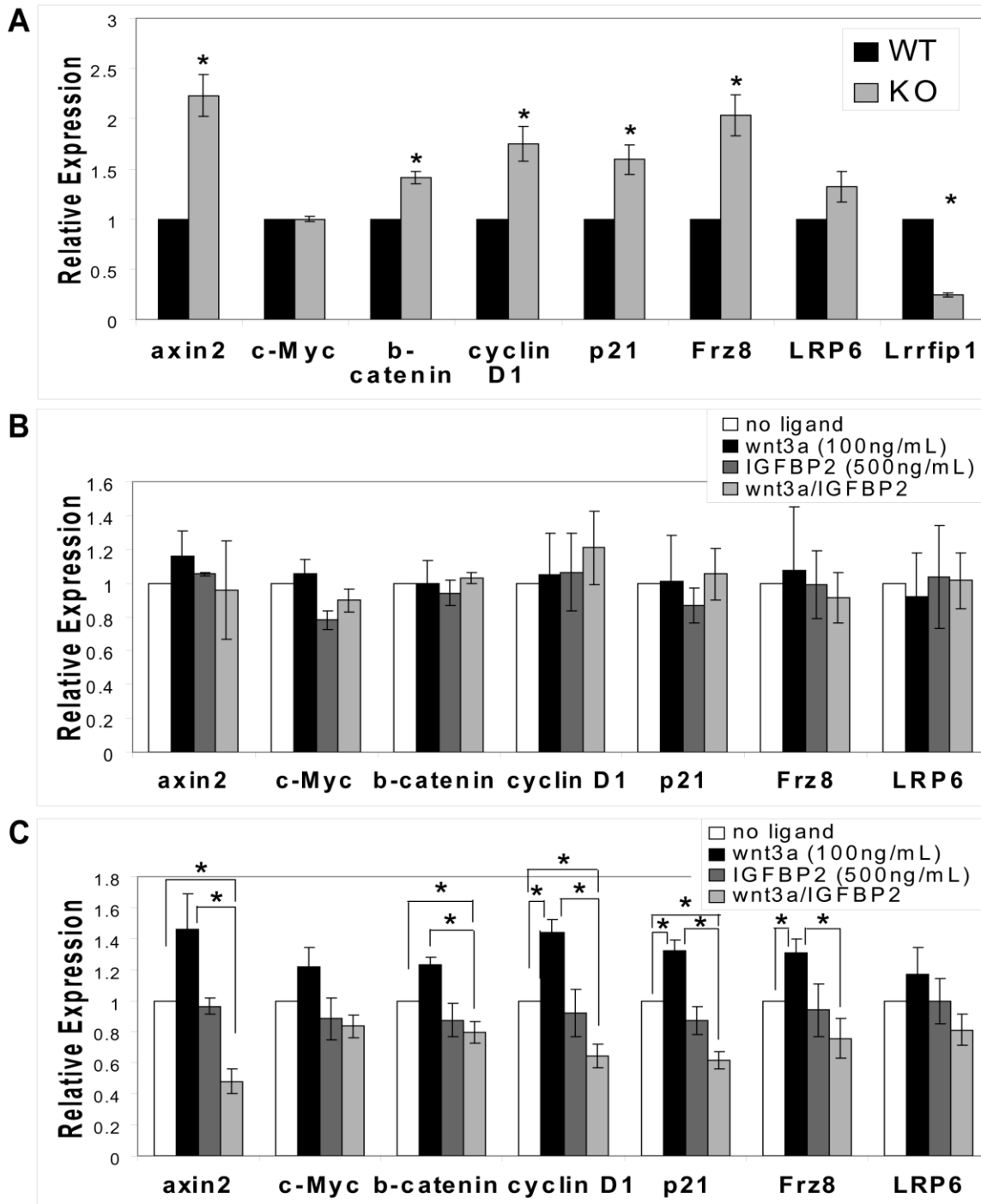
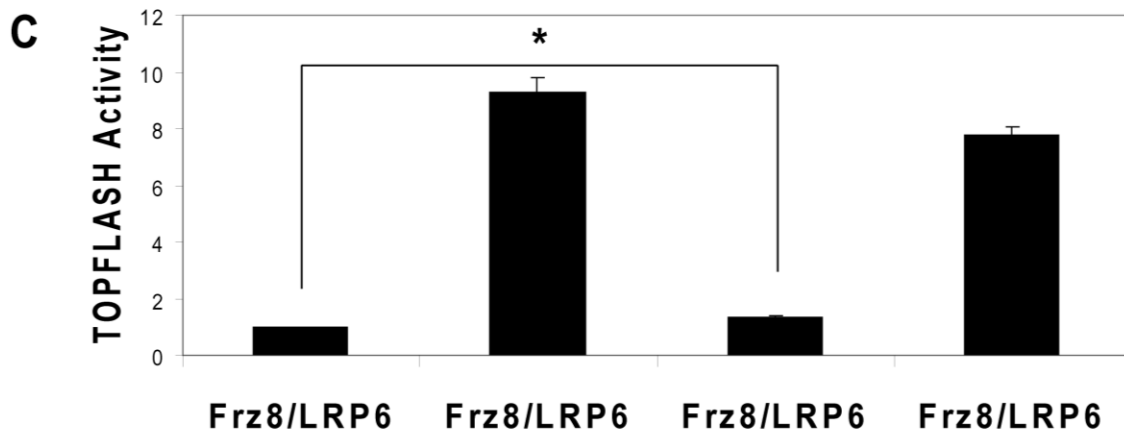
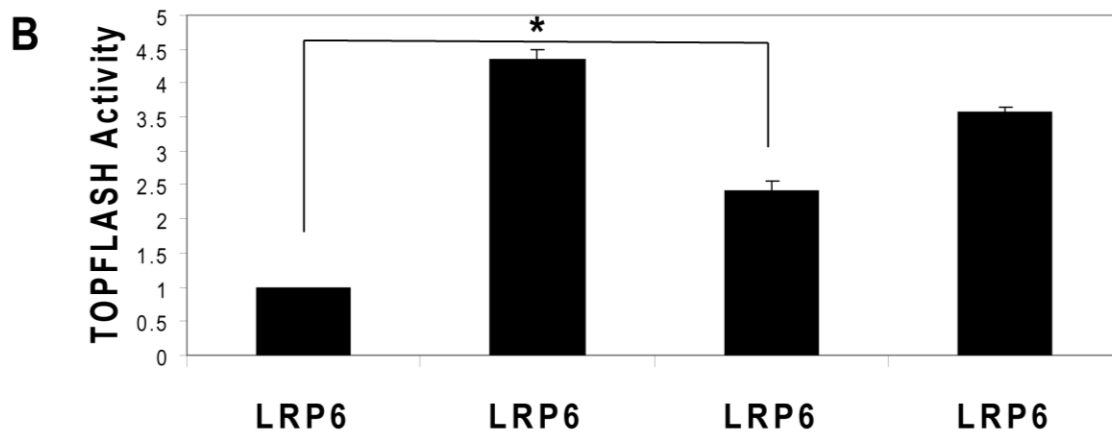
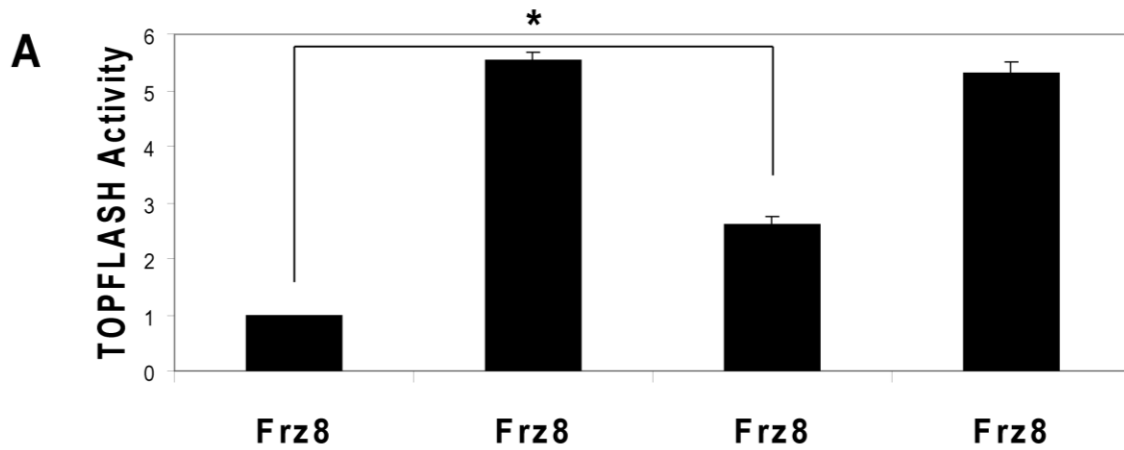


Figure 6. IGFBP2 modulates Wnt activities in hematopoietic stem cells. (A) Freshly isolated Lin⁻Sca-1⁺Kit⁺ from BM of wild-type or IGFBP2-null mice, and gene expression of Wnt targets was evaluated by real-time RT-PCR (n = 6). Wild-type LSK cells were isolated and treated with Wnt3a, IGFBP2, or combination of Wnt3a and IGFBP2 for (B) 6 hours (n = 3), or (C) 24-38 hours (n = 4). Real-time RT-PCR was performed. *, Significant different.



Wnt3a (100ng/mL)	-	+	-	+
IGFBP2 (500 ng/mL)	-	-	+	+

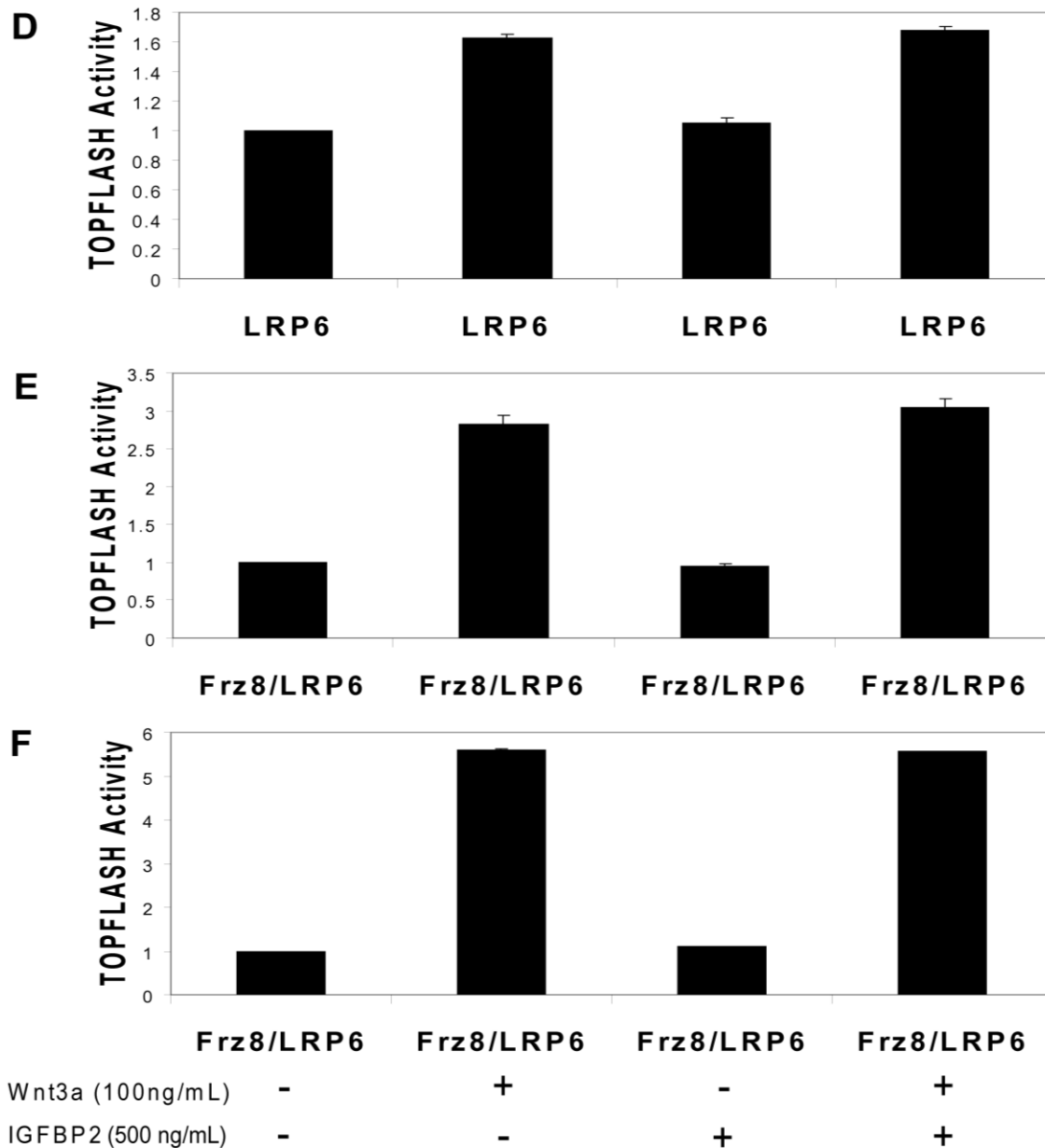


Figure 7. IGFBP2 induces the TOPFLASH activities through Frizzled 8 receptor and LDL receptor-related protein 6. Cotransfection of pTOPflash plasmid with Frz8 (A), LRP6 (B), or Frz8/LRP6 (C) plasmids in 293T cells for 22 hours, and the transfected 293T cells were treated with Wnt3a, IGFBP2, or Wnt3a/IGFBP2 mixture for additional 24 hours. (D) Cotransfection of pTOPflash plasmid with LRP6 plasmid in 293T cells for 22 hours, and the transfected cells were treated with indicated ligands for 6 hours. Cotransfection of pTOPflash plasmid with both Frz8 and LRP6 plasmids in 293T cells for 22 hours, and the transfected cells were treated with Wnt3a, IGFBP2, or Wnt3a/IGFBP2 for additional 6 hours (E), and 10 hours (F).

DISCUSSION

Previously, we showed that IGFBP2 stimulated *ex vivo* expansion of mouse and human HSCs^{6, 7}. Here, we demonstrated that, even though IGFBP2 does not have a significant cell-autonomous effect on HSCs, it supports HSC repopulation as an extracellular factor in the bone marrow *in vivo*. In principle, the homeostasis of HSCs is regulated by self-renewal, apoptosis, differentiation, and mobility. Our data showed that the decreased number and activity of HSCs in IGFBP2-null mice is due to increased apoptosis and slower cycling of the HSCs. Furthermore, we found that the C-terminus but not the RGD domain of IGFBP2 was essential to its HSC supportive activity, and that the effect of IGFBP2 on HSCs was independent of IGF-IR mediated signaling.

To our knowledge, this is the first demonstration that IGFBP2 supports survival and cycling of HSCs *in vivo*. The increased repopulation in secondary transplant suggests that increased cycling involves increased self-renewal. Indeed, IGFBP2 increased the expression of anti-apoptotic molecule Bcl-2 and suppressed the levels of multiple CDK inhibitors including p21, p19, p16, p57, and PTEN. This is consistent with the report that IGFBP2 suppresses PTEN expression⁴⁰ and supports the survival and expansion of glioma cells¹³, glioma cancer stem cells¹⁷, and epidermal progenitors⁴¹. This is also in accord with the report that CCN3/NOV, a protein containing an IGFBP domain, supports expansion of human cord blood HSCs⁴², and that IGFBP2 may be important for supporting the activity of fetal liver HSCs⁴³. Whether IGFBP2 has similar effects on differentiated blood cells is unclear. In fact we observed opposite trends in HSCs and in certain CFUs in IGFBP2-null mice, suggesting either that the effects of IGFBP2 on HSCs and differentiated blood cells are different or that the increases in certain CFUs are

caused by a compensatory effect. If the first possibility holds true, IGFBP2 may inhibit HSC differentiation, concordant with previous reports that IGFBP inhibits the differentiation of adipose progenitors^{44, 45}.

A major question in IGFBP biology is whether the effect of IGFBP is IGF-dependent, and whether the IGFBP2 acts in an extracellular or intracellular manner. We found that HSCs express little IGFBP2 so it should not play a significant cell-autonomous role. Our results suggest that the effect is extrinsic and independent of the IGF signaling receptor IGF-IR. First, IGFBP2 supported *ex vivo* expansion of HSCs in serum-free medium that did not contain IGFs⁶. Second, different deletion mutants of extrinsic recombinant IGFBP2 showed different effects. In particular, we found that the C-terminus of IGFBP2 is important for HSC function. The C-terminus of IGFBP2 is known to exist as a native fragment *in vivo* and bind to cell surface, trigger MAP activation, and stimulate cell growth³⁸. Third, IGFBP2 was capable of regulating gene expression essential for HSC survival and cycling. Lastly, IGF-IR-null donor HSCs did not differ from WT HSCs in repopulation activity in IGFBP2-null recipient mice. It has been shown that both extrinsic and intrinsic IGFBP2 binds to integrin $\alpha 5\beta 1$ ^{9, 14}; although our data suggested that integrin $\alpha 5\beta 1$ may not mediate IGFBP2's extrinsic effect on HSC function/expansion, it is still possible that IGFBP2 binds to other surface receptor(s) on HSCs. Recently, Zhu et al. 2008 showed that several IGFBPs, including IGFBP4 and IGFBP2, are inhibitors of canonical Wnt signaling in cardiomyocytes by binding to Frizzled 8 receptor and LDL receptor-related protein 6²². Fleming et al. used DKK1-transgenic mice to show that Wnt activation in the niche is required to enforce HSC quiescence and to limit their proliferation³⁹. Therefore, the regulation of Wnt target

genes by extrinsic IGFBP2 and the quiescent phenotype of IGFBP2-null HSCs suggest that IGFBP2 may also modulate Wnt signaling in HSCs. Other unidentified surface receptor(s) for IGFBP2 may also exist. Further investigation will clarify this issue.

The co-culture of HSCs and BM stroma showed that IGFBP2-null stroma had dramatically decreased ability to support HSC expansion, suggesting that IGFBP2 regulates HSCs in the local BM microenvironment. We know of the existence of at least two BM HSC niches: the endosteal niche and vascular niche ⁴⁶. Recently, it was demonstrated that Nestin-expressing mesenchymal stem cells represent a unique niche ⁴⁷. IGFBP2-null mice have male-specific defects in osteoblasts ^{25, 26}, but we found that the decreased HSC numbers and activities in IGFBP2-null mice are gender independent. Therefore the environmental effect of IGFBP2 may not come from osteoblasts in the BM. In fact, the expression of IGFBP2 in BM stroma suggests that mesenchymal stromal cells may be an important source of IGFBP2. Because IGFBP2 is overexpressed by the AKT-activated but not MAPK-activated endothelial cells and is essential for the ability to support expansion of HSCs ²⁴, and we did not detect high IGFBP2 level in BM CD45⁻CD31⁺ cells, we speculate that these CD45⁻CD31⁺ BM cells used in our analysis were not enriched for the HSC-supportive activated endothelial cells. New markers that allow identification of different functional types of endothelium will help the study in the future. Furthermore, in the BM, in addition to its direct effect to HSCs, IGFBP2 may support HSC activity indirectly. For example, IGFBP2 can inhibit the differentiation of adipocyte precursors and decrease fat accumulation ⁴⁵. Consistently, we observed IGFBP2-null mice were more obese than WT mice (data not shown). Since fat cells in the

BM negatively regulate HSC activity⁴⁸, it is possible that the increased fat in IGFBP2-null BM contributes to decreased HSC activity.

What is the relationship between quiescence and apoptosis in IGFBP2-null HSCs? While we are not certain if these two fates are independent events, there is a possibility that apoptosis causes compensatory quiescence of IGFBP2-null HSCs. For these HSCs, if apoptosis continues over time, the HSCs pool should be exhausted as the mice age. However, our data suggest that their HSC levels remained constant as the mice get to 1 year of age. Thus, we speculate that IGFBP2-null HSCs become more quiescent as a secondary effect to counteract the apoptosis. This is supported by previous reports that apoptosis led to quiescence of cells and slowed cell death⁴⁹. Either way, our results indicate that it is not necessary that more quiescent HSCs have higher repopulation rates. Similarly, *AKT1^{-/-}AKT2^{-/-}* HSCs are more quiescent but have lower repopulation efficiencies than WT HSCs⁵⁰.

In addition to its expression during embryonic development and in normal adulthood, IGFBP2 is overexpressed in many tumors and its expression appears to correlate with the grade of malignancy⁹⁻¹¹. The level of IGFBP2 is low in well-differentiated tumors but high in poorly differentiated tumors¹². In the hematopoietic system, a lower IGFBP2 level is associated with the survival of patients with acute myeloid leukemia (AML) and acute lymphoblastic leukemia (ALL)^{27, 28} and the expression of IGFBP2 is an independent factor for the prediction of relapse of AML and ALL^{27, 29-31}. Our previous data showed that the presence of IGFBP2 in the medium, together with other growth factors, resulted in significant expansion of mouse and human HSCs *ex vivo*^{6, 7}. The *in vivo* data shown here indicates that IGFBP2 promotes self-

renewal and survival in HSCs. Therefore it is reasonable to speculate that IGFBP2 also plays a role in supporting the activity of certain leukemia stem cells.

REFERENCES

1. Blank U, Karlsson G, Karlsson S. Signaling pathways governing stem-cell fate. *Blood*. 2008;111:492-503.
2. Zhang CC, Lodish HF. Cytokines regulating hematopoietic stem cell function. *Curr Opin Hematol*. 2008;15:307-311.
3. Zhang CC, Lodish HF. Insulin-like growth factor 2 expressed in a novel fetal liver cell population is a growth factor for hematopoietic stem cells. *Blood*. 2004;103:2513-2521.
4. Zhang CC, Lodish HF. Murine hematopoietic stem cells change their surface phenotype during *ex vivo* expansion. *Blood*. 2005;105:4314-4320.
5. Zhang CC, Kaba M, Ge G, et al. Angiopoietin-like proteins stimulate *ex vivo* expansion of hematopoietic stem cells. *Nat Med*. 2006;12:240-245.
6. Huynh H, Iizuka S, Kaba M, et al. Insulin-like growth factor-binding protein 2 secreted by a tumorigenic cell line supports *ex vivo* expansion of mouse hematopoietic stem cells. *Stem Cells*. 2008;26:1628-1635.
7. Zhang CC, Kaba M, Iizuka S, et al. Angiopoietin-like 5 and IGFBP2 stimulate *ex vivo* expansion of human cord blood hematopoietic stem cells as assayed by NOD/SCID transplantation. *Blood*. 2008;111:3415-3423.
8. Ranke MB, Elmlinger M. Functional role of insulin-like growth factor binding proteins. *Horm Res*. 1997;48 Suppl 4:9-15.
9. Schutt BS, Langkamp M, Rauschnabel U, et al. Integrin-mediated action of insulin-like growth factor binding protein-2 in tumor cells. *J Mol Endocrinol*. 2004;32:859-868.

10. Moore MG, Wetterau LA, Francis MJ, et al. Novel stimulatory role for insulin-like growth factor binding protein-2 in prostate cancer cells. *Int J Cancer*. 2003;105:14-19.
11. Hoeflich A, Reisinger R, Lahm H, et al. Insulin-like growth factor-binding protein 2 in tumorigenesis: protector or promoter? *Cancer Res*. 2001;61:8601-8610.
12. Akmal SN, Yun K, MacLay J, et al. Insulin-like growth factor 2 and insulin-like growth factor binding protein 2 expression in hepatoblastoma. *Hum Pathol*. 1995;26:846-851.
13. Dunlap SM, Celestino J, Wang H, et al. Insulin-like growth factor binding protein 2 promotes glioma development and progression. *Proc Natl Acad Sci U S A*. 2007;104:11736-11741.
14. Wang GK, Hu L, Fuller GN, et al. An interaction between insulin-like growth factor-binding protein 2 (IGFBP2) and integrin alpha5 is essential for IGFBP2-induced cell mobility. *J Biol Chem*. 2006;281:14085-14091.
15. Migita T, Narita T, Asaka R, et al. Role of insulin-like growth factor binding protein 2 in lung adenocarcinoma: IGF-independent antiapoptotic effect via caspase-3. *Am J Pathol*. 2010;176:1756-1766.
16. Kim DS, Cho HJ, Yang SK, et al. Insulin-like growth factor-binding protein contributes to the proliferation of less proliferative cells in forming skin equivalents. *Tissue Eng Part A*. 2009;15:1075-1080.
17. Hsieh D, Hsieh A, Stea B, et al. IGFBP2 promotes glioma tumor stem cell expansion and survival. *Biochem Biophys Res Commun*. 2010;397:367-372.

18. Chakrabarty S, Kondratick L. Insulin-like growth factor binding protein-2 stimulates proliferation and activates multiple cascades of the mitogen-activated protein kinase pathways in NIH-OVCAR3 human epithelial ovarian cancer cells. *Cancer Biol Ther.* 2006;5:189-197.
19. Bartling B, Koch A, Simm A, et al. Insulin-like growth factor binding proteins-2 and -4 enhance the migration of human CD34-/CD133+ hematopoietic stem and progenitor cells. *Int J Mol Med.* 2010;25:89-96.
20. Russo VC, Schutt BS, Andaloro E, et al. Insulin-like growth factor binding protein-2 binding to extracellular matrix plays a critical role in neuroblastoma cell proliferation, migration, and invasion. *Endocrinology.* 2005;146:4445-4455.
21. Pereira JJ, Meyer T, Docherty SE, et al. Bimolecular interaction of insulin-like growth factor (IGF) binding protein-2 with alphavbeta3 negatively modulates IGF-I-mediated migration and tumor growth. *Cancer Res.* 2004;64:977-984.
22. Zhu W, Shiojima I, Ito Y, et al. IGFBP-4 is an inhibitor of canonical Wnt signalling required for cardiogenesis. *Nature.* 2008;454:345-349.
23. Besnard V, Corroyer S, Trugnan G, et al. Distinct patterns of insulin-like growth factor binding protein (IGFBP)-2 and IGFBP-3 expression in oxidant exposed lung epithelial cells. *Biochim Biophys Acta.* 2001;1538:47-58.
24. Kobayashi H, Butler JM, O'Donnell R, et al. Angiocrine factors from Akt-activated endothelial cells balance self-renewal and differentiation of haematopoietic stem cells. *Nat Cell Biol.* 2010;12:1046-1056.

25. Wood TL, Rogler LE, Czick ME, et al. Selective alterations in organ sizes in mice with a targeted disruption of the insulin-like growth factor binding protein-2 gene. *Mol Endocrinol.* 2000;14:1472-1482.
26. DeMambro VE, Clemmons DR, Horton LG, et al. Gender-specific changes in bone turnover and skeletal architecture in igfbp-2-null mice. *Endocrinology.* 2008;149:2051-2061.
27. Vorwerk P, Mohnike K, Wex H, et al. Insulin-like growth factor binding protein-2 at diagnosis of childhood acute lymphoblastic leukemia and the prediction of relapse risk. *J Clin Endocrinol Metab.* 2005;90:3022-3027.
28. Hattori H, Matsuzaki A, Suminoe A, et al. Identification of novel genes with prognostic value in childhood leukemia using cDNA microarray and quantitative RT-PCR. *Pediatr Hematol Oncol.* 2006;23:115-127.
29. Dawczynski K, Steinbach D, Wittig S, et al. Expression of components of the IGF axis in childhood acute myelogenous leukemia. *Pediatr Blood Cancer.* 2008;50:24-28.
30. Dawczynski K, Kauf E, Zintl F. Changes of serum growth factors (IGF-I,-II and IGFBP-2,-3) prior to and after stem cell transplantation in children with acute leukemia. *Bone Marrow Transplant.* 2003;32:411-415.
31. Dawczynski K, Kauf E, Schlenvoigt D, et al. Elevated serum insulin-like growth factor binding protein-2 is associated with a high relapse risk after hematopoietic stem cell transplantation in childhood AML. *Bone Marrow Transplant.* 2006;37:589-594.

32. Holzenberger M, Dupont J, Ducos B, et al. IGF-1 receptor regulates lifespan and resistance to oxidative stress in mice. *Nature*. 2003;421:182-187.
33. Zheng J, Huynh H, Umikawa M, et al. Angiopoietin-like protein 3 supports the activity of hematopoietic stem cells in the bone marrow niche. *Blood*. 2010.
34. Simsek T, Kocabas F, Zheng J, et al. The distinct metabolic profile of hematopoietic stem cells reflects their location in a hypoxic niche. *Cell Stem Cell*. 2010;7:380-390.
35. Parekkadan B, Milwid JM. Mesenchymal stem cells as therapeutics. *Annu Rev Biomed Eng*. 2010;12:87-117.
36. Hoeflich A, Reisinger R, Vargas GA, et al. Mutation of the RGD sequence does not affect plasma membrane association and growth inhibitory effects of elevated IGFBP-2 in vivo. *FEBS Lett*. 2002;523:63-67.
37. Kibbey MM, Jameson MJ, Eaton EM, et al. Insulin-like growth factor binding protein-2: contributions of the C-terminal domain to insulin-like growth factor-1 binding. *Mol Pharmacol*. 2006;69:833-845.
38. Kiepe D, Van Der Pas A, Ciarmatori S, et al. Defined carboxy-terminal fragments of insulin-like growth factor (IGF) binding protein-2 exert similar mitogenic activity on cultured rat growth plate chondrocytes as IGF-I. *Endocrinology*. 2008;149:4901-4911.
39. Fleming HE, Janzen V, Lo Celso C, et al. Wnt signaling in the niche enforces hematopoietic stem cell quiescence and is necessary to preserve self-renewal in vivo. *Cell Stem Cell*. 2008;2:274-283.

40. Perks CM, Vernon EG, Rosendahl AH, et al. IGF-II and IGFBP-2 differentially regulate PTEN in human breast cancer cells. *Oncogene*. 2007;26:5966-5972.
41. Villani RM, Adolphe C, Palmer J, et al. Patched1 inhibits epidermal progenitor cell expansion and basal cell carcinoma formation by limiting Igfbp2 activity. *Cancer Prev Res (Phila)*. 2010;3:1222-1234.
42. Gupta R, Hong D, Iborra F, et al. NOV (CCN3) functions as a regulator of human hematopoietic stem or progenitor cells. *Science*. 2007;316:590-593.
43. Krosl J, Mamo A, Chagraoui J, et al. A mutant allele of the Swi/Snf member BAF250a determines the pool size of fetal liver hemopoietic stem cell populations. *Blood*. 2010;116:1678-1684.
44. Boney CM, Moats-Staats BM, Stiles AD, et al. Expression of insulin-like growth factor-I (IGF-I) and IGF-binding proteins during adipogenesis. *Endocrinology*. 1994;135:1863-1868.
45. Wheatcroft SB, Kearney MT, Shah AM, et al. IGF-binding protein-2 protects against the development of obesity and insulin resistance. *Diabetes*. 2007;56:285-294.
46. Oh IH, Kwon KR. Concise review: multiple niches for hematopoietic stem cell regulations. *Stem Cells*. 2010;28:1243-1249.
47. Mendez-Ferrer S, Michurina TV, Ferraro F, et al. Mesenchymal and haematopoietic stem cells form a unique bone marrow niche. *Nature*. 2010;466:829-834.
48. Naveiras O, Nardi V, Wenzel PL, et al. Bone-marrow adipocytes as negative regulators of the haematopoietic microenvironment. *Nature*. 2009;460:259-263.

49. Furuichi Y, Goi K, Inukai T, et al. Fms-like tyrosine kinase 3 ligand stimulation induces MLL-rearranged leukemia cells into quiescence resistant to antileukemic agents. *Cancer Res.* 2007;67:9852-9861.
50. Juntilla MM, Patil VD, Calamito M, et al. AKT1 and AKT2 maintain hematopoietic stem cell function by regulating reactive oxygen species. *Blood.* 2010;115:4030-4038.

Components of the Hematopoietic Compartments in Tumor Stroma and Tumor-bearing Mice

ABSTRACT

Solid tumors are composed of cancerous cells and non-cancerous stroma. A better understanding of the tumor stroma could lead to new therapeutic applications. However, the exact compositions and functions of the tumor stroma are still largely unknown. Here, using a Lewis lung carcinoma implantation mouse model, we examined the hematopoietic compartments in tumor stroma and tumor-bearing mice. Different lineages of differentiated hematopoietic cells existed in tumor stroma with the percentage of myeloid cells increasing and the percentage of lymphoid and erythroid cells decreasing over time. Interestingly, tumor stroma also contained cells that can repopulate multiple hematopoietic lineages. All hematopoietic cells in the tumor stroma originated from bone marrow. In the bone marrow and peripheral blood of tumor-bearing mice, myeloid populations increased and lymphoid and erythroid populations decreased and numbers of hematopoietic stem cells markedly increased with time. To investigate the function of hematopoietic cells in tumor stroma, we co-implanted various types of hematopoietic cells with cancer cells. We found that total hematopoietic cells in the tumor stroma promoted tumor development. Furthermore, the growth of the primary implanted Lewis lung carcinomas and their metastasis were significantly decreased in mice reconstituted with IGF type I receptor-deficient hematopoietic stem cells, indicating that IGF signaling in the hematopoietic tumor stroma supports tumor outgrowth. These results reveal that hematopoietic cells in the tumor stroma regulate tumor development and that tumor progression significantly alters the host hematopoietic compartment.

INTRODUCTION

Solid tumors are composed of cancerous and non-cancerous cells. The non-cancerous cells, including endothelial cells, hematopoietic cells, fibroblasts, myofibroblasts, pericytes, and mesenchymal stem cells, collectively form the cancer stroma or microenvironment¹⁻³. These stromal cells come from the local environment or from bone marrow (BM) via the circulation system and appear to provide important support for cancer cell growth and metastasis^{2,3}. For instance, BM-derived cells are recruited to the cancer site to stimulate outgrowth of tumors and form angiogenic and pre-metastatic niches for cancer growth⁴⁻⁶. Stromal fibroblasts and mesenchymal stem cells also play critical roles in angiogenesis and metastasis, respectively^{7,8}. However, the exact compositions and functions of the microenvironment that surround solid cancer are still largely unknown. Since a tumor cannot develop without the parallel expansion of a tumor stroma, the lack of understanding of this cancer microenvironment has severely hampered cancer research and the development of effective therapeutic approaches.

There is ample evidence that certain differentiated hematopoietic cells, including macrophages, T cells, and mast cells, are incorporated into the tumor microenvironment^{2,3}; however, a systematic investigation of the composition of the hematopoietic compartment of the tumor stroma has not been carried out. Hematopoiesis in vertebrates is a hierarchically organized developmental process in that highly specialized differentiated cells, including progenitors, precursors, and different lineages of blood cells, originate through an ordinate maturation program from the primitive hematopoietic stem cells (HSCs)⁹. Of these cells, HSCs are defined by their ability to self-renew and to differentiate into all blood cell types, whereas various progenitors possess much more

limited self-renewal capacity and differentiation potential. In adults, HSCs mainly reside in BM; a small fraction also circulate in the blood stream and can be found in extramedullary organs including spleen and liver^{9,10}. The flow cytometry-based surface phenotype analysis and various functional assays, including the BM reconstitution analysis, remain the assays of choice for the analysis of the presence and activities of various hematopoietic cell types⁹.

We sought to determine the composition and function of hematopoietic cells in tumor stroma and to determine whether tumor development affects the hematopoietic compartment of a tumor-bearing host. These studies are of fundamental importance to our understanding of the basic molecular and cellular mechanisms of tumor pathogenesis. A more complete understanding of the tumor microenvironment will make possible novel types of anti-tumor therapy.

MATERIALS AND METHODS

Cell lines, animals, and tumor implantation and measurement

Murine Lewis lung carcinoma (LL2) cells were obtained from the ATCC and cultured under standard conditions. Retroviral MSCV-GFP was introduced into LL2 cells to produce stable GFP⁺ LL2 cells. C57BL/6 CD45.2 and CD45.1 mice were purchased from the Jackson Laboratory or the National Cancer Institute. IGF-IR^{-/+} mice as previously described¹¹ were in pure C57BL/6 background. All animals were maintained at the University of Texas Southwestern Medical Center animal facility and animal experiments were performed with the approval of UT Southwestern Committee on Animal Care. Tumor cells were injected subcutaneously into mice and mice were maintained for about 3 weeks. Tumor size was measured on the flanks of live mice using calipers; volume was calculated as (length of tumor) x (width of tumor)²/2. To analyze lung metastasis, entire lungs were harvested and single cell suspensions were prepared by collagenase treatment. GFP⁺ LL2 cells originating from the distant implanted tumor were counted by flow cytometry analysis. To confirm the flow cytometry result, GFP⁺ surface foci of the harvested lung were counted under a dissecting microscope. GFP⁺ foci that were visible under 4x magnification were counted as micrometastases; GFP⁺ foci that were visible by naked eye were counted as macrometastases.

Preparation of hematopoietic cells from tumors

Mice were perfused with cold PBS and primary tumors were removed and chopped with a McIlwain Tissue Chopper (Mickle Laboratory Engineering Company).

The tissue was washed with PBS and then placed in collagenase-dispase medium (Liver Digest Medium, Invitrogen) at 37°C for 90 min as we described previously¹². Cells passed through a 70- μ m strainer were used for further flow cytometry analysis or sorting.

Flow cytometry

BM and PB cells were isolated from 5-8 week old C57BL/6 mice. Lin⁻Sca-1⁺Kit⁺ or Lin⁻Sca-1⁺Kit⁺CD34⁻Flk-2⁻ cells were isolated by staining with a biotinylated lineage cocktail (anti-CD3, anti-CD5, anti-B220, anti-Mac-1, anti-Gr-1, anti-Ter119, and anti-7-4; Stem Cell Technologies) followed by streptavidin-PE/Cy5.5, anti-Sca-1-FITC, and anti-Kit-APC, and anti-CD34-PE and anti-Flk-2-PE if necessary. To analyze hematopoietic lineages and repopulation of mouse HSCs, mouse peripheral blood cells were collected by retro-orbital bleeding, followed by lysis of red blood cells and staining with anti-CD45.2-FITC, and anti-CD45.1-PE, and anti-Thy1.2-PE (for T-lymphoid lineage), anti-B220-PE (for B-lymphoid lineage), anti-Mac-1-PE, anti-Gr-1-PE (cells co-staining with anti-Mac-1 and anti-Gr-1 were deemed to be of the myeloid lineage), or anti-Ter119-PE (for erythroid lineage) monoclonal antibodies. All antibodies were from BD Pharmingen. The “percent reconstitution” shown in figures was based on the staining results of anti-CD45.2 and anti-CD45.1. In all cases flow cytometry analysis of hematopoietic lineages was also performed to confirm multilineage reconstitution.

Hematopoietic colony assays

CD45⁺ cells from LL2 tumor stroma or normal BM cells were resuspended in IMDM with 2% FBS and were then seeded into methylcellulose medium M3334

(StemCell Technologies) for CFU-E, M3434 (StemCell Technologies) for CFU-GM, or M3630 (StemCell Technologies) for CFU-Pre-B assays, according to the manufacturer's protocols and as described previously¹³.

HSC cell cycle analysis

The cell cycle analysis with Hoechst and pyronin Y staining was performed as follows. The Lin⁻Sca-1⁺Kit⁺Flk2⁻CD34⁻ cells were collected in Hank's buffered salt solution medium containing 10% FBS, 1 g/liter glucose, and 20 mM Hepes (pH 7.2). Cells were washed, Hoechst 33342 (20 µg/ml, Invitrogen) was added, and cells were incubated at 37 °C for 45 min after which pyronin Y (1 µg/ml, Sigma) was added. Cells were incubated for another 15 min at 37 °C, washed, and resuspended in cold PBS. Samples were immediately analyzed by flow cytometry (BD Biosciences, FACSAria).

Competitive reconstitution analysis

The indicated numbers of mouse CD45.2 or CD45.1 donor cells were mixed with 1 or 2 x 10⁵ freshly isolated CD45.1 or CD45.2 competitor BM cells, and the mixture were injected intravenously *via* the retro-orbital route into each of a group of 6-9 week old CD45.1 or CD45.2 mice previously irradiated with a total dose of 10 Gy. For secondary transplantation, CD45.1⁺ cells were collected from primary recipients and 10⁶ cells were injected with 10⁵ CD45.2 competitors into lethally irradiated secondary recipient mice. To measure reconstitution of transplanted mice, PB was collected at the indicated times post-transplant and the presence of CD45.1⁺ and CD45.2⁺ cells in lymphoid and myeloid compartments were measured as described¹³⁻¹⁶. Calculation of

CRUs in limiting dilution experiments was conducted using L-Calc software (StemCell Technologies) ¹⁷.

Statistical analysis

Data are expressed as mean \pm SEM. Tumor growth curves for different experimental groups were compared using the Generalized Estimating Equations (GEE) method with AR(1) correlation structure. Tumor sizes among different experimental groups were also compared at each time points using t-test. SAS 9.1.3 was used for the analysis. Data were considered statistically significant if $p < 0.05$.

RESULTS

Various hematopoietic populations exist in tumor stroma

Using the Lewis lung carcinoma (LL2) implantation mouse model, we characterized the hematopoietic compartment in the tumor stroma. Figures 1A-C and Table 1 show the results of staining for hematopoietic cell surface antigens in dissociated tumor masses arising after the subcutaneous injection of 10^6 LL2 cells into C57BL/6 CD45.1 host mice at various time points post-implantation. The composition of hematopoietic cells in tumor stroma differed from that from host peripheral blood (PB) or BM (Table 1), indicating that there exists a unique hematopoietic compartment in tumor stroma. The percentage of hematopoietic cells in the LL2 tumor stroma modestly increased from 20% at day 12 to 25% at day 19 after tumor implantation (Fig. 1A). The relative composition of myeloid cells (Mac-1⁺ and Gr-1⁺) increased whereas that of lymphoid cells (T cells as Thy1.2⁺ and B cells as B220⁺) and erythroid cells (Ter119⁺) in this compartment decreased over time (Fig. 1A).

We also measured the existence of hematopoietic progenitors and phenotypic HSCs in the tumor stroma. The number of progenitors for granulocytes and monocytes (CFU-GM) was low, with 3.5 per 1,000,000 tumor cells at day 19 post-implantation (Table 1). Interestingly, in the LL2 tumor stroma, we found phenotypic HSCs, measured as CD45⁺Lin⁻Sca-1⁺Kit⁺ cells (Fig. 1B). The flow cytometry analyses indicate that there were few Lin⁻Kit⁺ cells in the tumor stroma, concordant with a previous report⁴. The average frequency of these phenotypic HSCs increased over time from 0.0004% at day 12, to 0.0016% at day 15, and to 0.006% at day 19 (Fig. 1C). In particular, the frequency

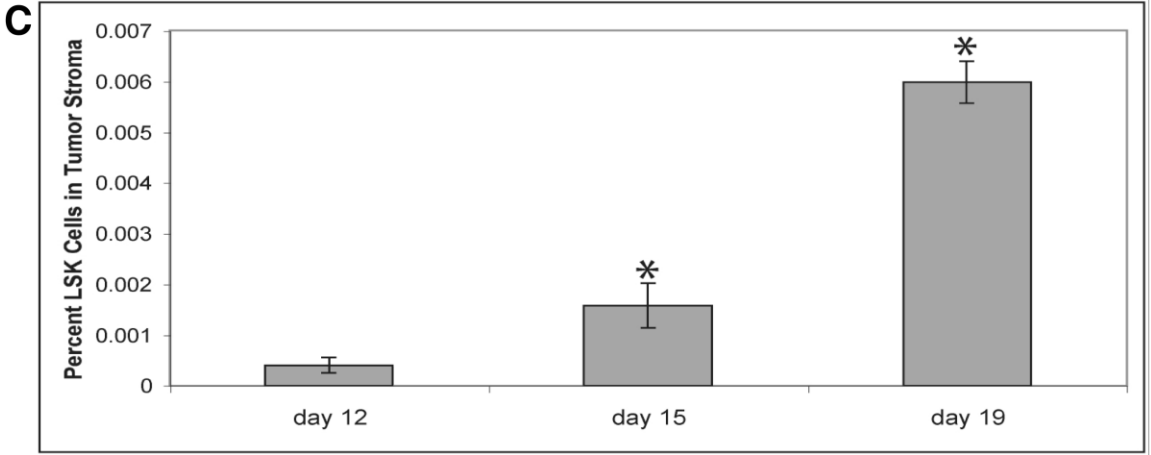
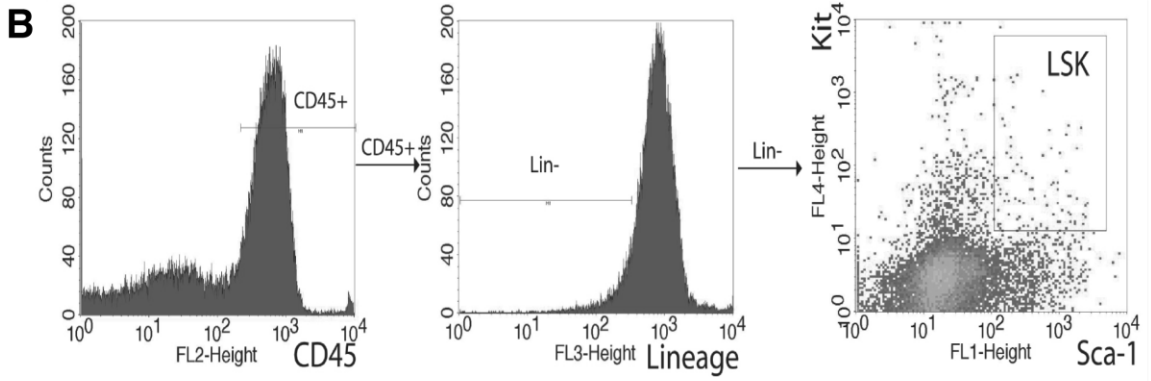
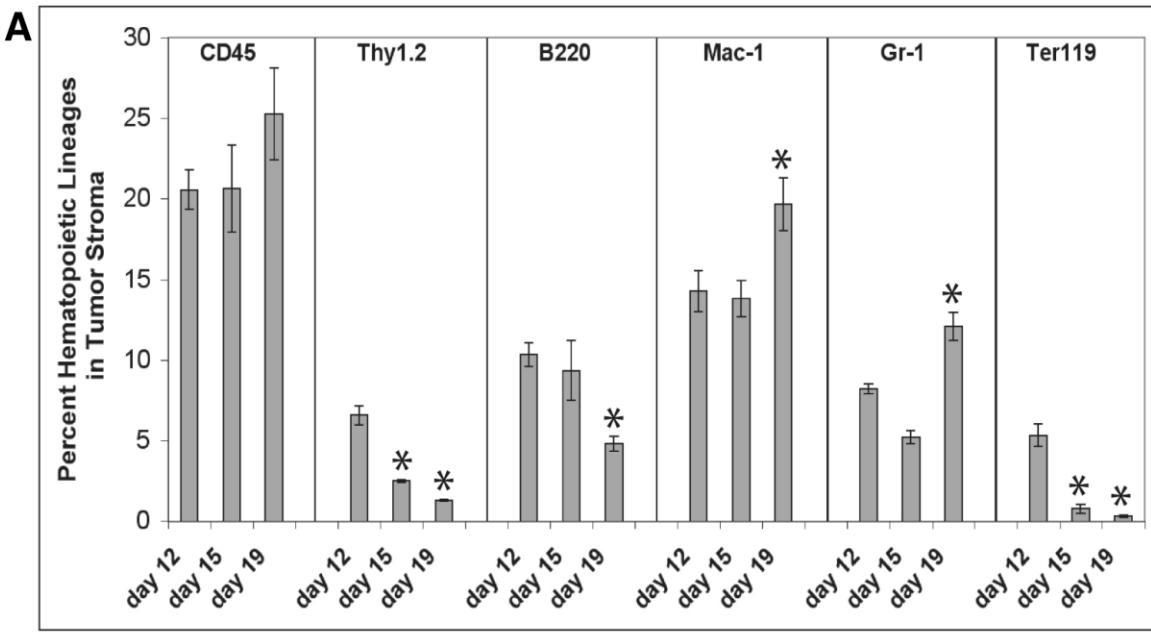
of phenotypic HSCs detected in the tumor stroma (0.006 ± 0.001 %) at day 19 was 1/13 or 1/33 of that in BM of normal mice or tumor-bearing mice respectively (0.08 ± 0.05 and 0.20 ± 0.02 % respectively) (Table 1).

Since the surface phenotype of HSCs in extramedullary organs can be different from that of BM HSCs¹⁰, we used BM reconstitution analysis, the “gold standard” for measuring HSC repopulating activity, to determine whether functional HSCs existed in the tumor stroma. An extremely stringent 18-month competitive reconstitution analysis and a secondary transplantation showed that the tumor stroma contained long-term repopulating HSCs (Fig. 1D). These cells were capable of repopulating both lymphoid and myeloid lineages in long-term reconstitution analysis (Fig. 1E), attesting that these are functional HSCs. Using the limiting dilution analysis¹⁶, we found that the frequency of these tumor stromal HSCs was 1 in 1.8×10^6 cells (Fig. 1F). The frequency of these functional multipotent cells in the LL2 tumor stroma was about 1/60 of that in the BM of normal C57BL/6 mouse, which is about 1 in 30,000¹⁵.

To determine whether the hematopoietic cells in tumor stroma originated from the BM or from the local environment, we transplanted CD45.1 C57BL/6 donor BM cells into lethally irradiated CD45.2 C57BL/6 mice. At 4 months post-transplant, the recipient BM was completely repopulated by the donor CD45.1 cells, whereas peripheral tissues contained mostly CD45.1 cells with certain CD45.2 cells as reported¹⁰. We implanted LL2 tumor cells subcutaneously into these mice. Three weeks later, we isolated tumors and used flow cytometry to characterize the hematopoietic cells in stroma. We found that all of the tumor stromal CD45⁺ cells were CD45.1⁺ (Fig. 1G). Accordant with previous studies⁴, we concluded that hematopoietic cells in the LL2 stroma are derived from BM.

Table 1. Repopulating hematopoietic stem cells and differentiated hematopoietic cells exist in LL2 tumor stroma (n = 5). Data from tumor mice were obtained from dissociated tumor masses arising after the subcutaneous injection of 10^6 LL2 cells into C57BL/6 CD45.1 host mice at day 19 post-implantation.

1	2	4	5	6	7	8	9	10
	CD45 ⁺ %	Thy1.2 ⁺ %	B220 ⁺ %	Mac-1 ⁺ %	Gr-1 ⁺ %	Ter119 ⁺ %	CFU-GM (per 1 million cells)	CD45 ⁺ Lin ⁻ Sca-1 ⁺ Kit ⁺ %
Tumor stroma	25.3 ± 2.8	1.3 ± 0.1	4.8 ± 0.4	19.7 ± 1.6	12.1 ± 0.9	0.3 ± 0.1	3.5 ± 0.5	0.006 ± 0.001
Tumor peripheral blood	98.7 ± 2.4	11.7 ± 1.9	13.1 ± 2.2	74.5 ± 3.7	66.4 ± 4.5	15.0 ± 5.6	N/D	0.009 ± 0.002
Tumor bone marrow	77.0 ± 2.0	0.9 ± 0.2	5.5 ± 2.5	70.5 ± 3.8	61.1 ± 4.7	19.4 ± 4.2	2962 ± 82	0.2 ± 0.02
Normal peripheral blood	99.3 ± 2.2	30.7 ± 9.7	39.5 ± 2.7	26.5 ± 12.2	19.3 ± 10.7	28.9 ± 3.6	N/D	0.0009 ± 0.0005
Normal bone marrow	69.7 ± 2.9	2.8 ± 0.2	20.7 ± 1.3	44.0 ± 4.4	41.5 ± 4.9	32.5 ± 2.5	1425 ± 32	0.08 ± 0.05
Normal muscle	1.6 ± 0.2	0.8 ± 0.1	0.1 ± 0.01	0.2 ± 0.01	0.5 ± 0.04	0.1 ± 0.01	0 ± 0	0.0 ± 0.0



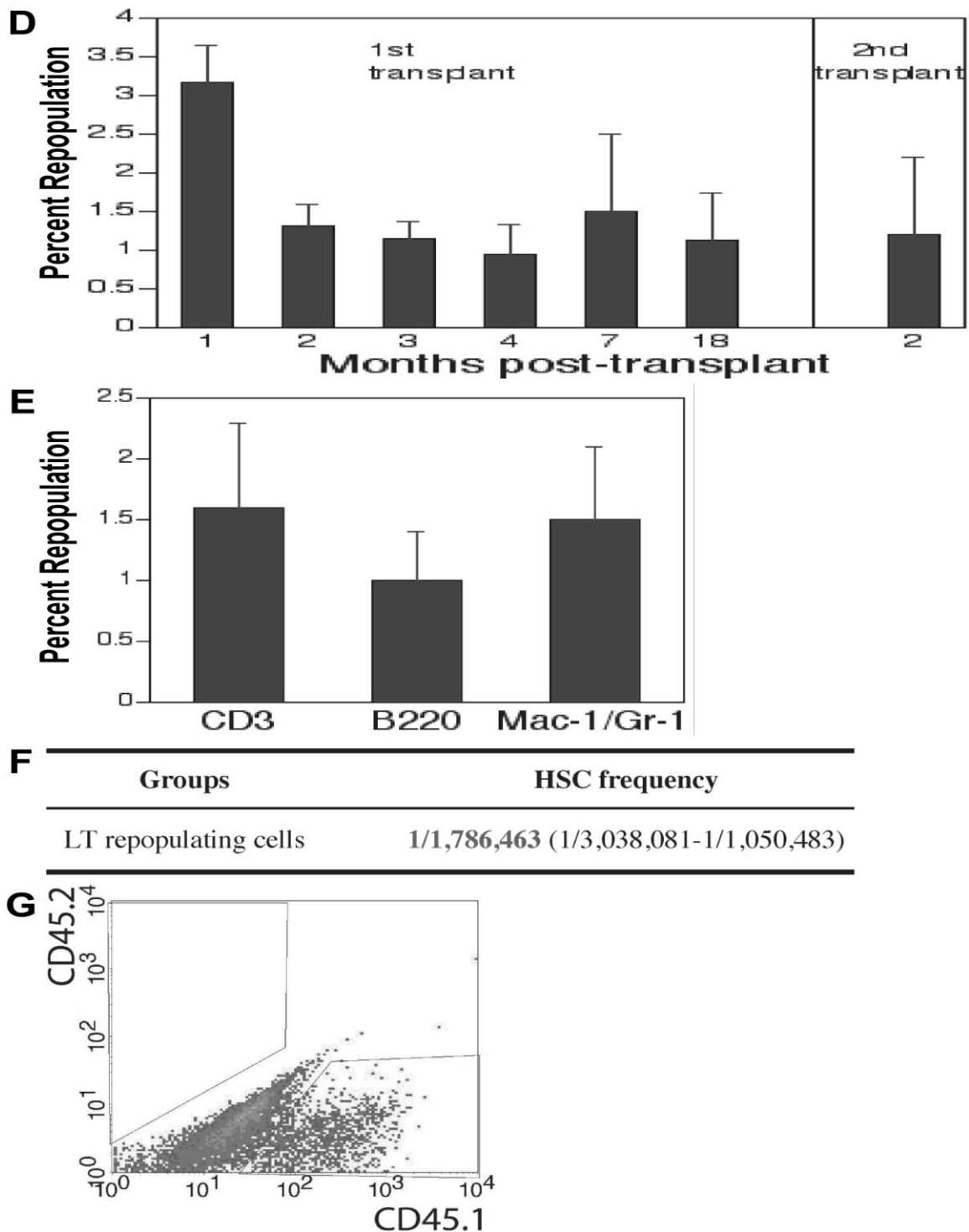


Figure 1. Analysis of the hematopoietic compartment of LL2 tumor stroma. Fig. 1A-C show the results of flow cytometry staining for hematopoietic cell surface antigens in dissociated tumor masses arising after the subcutaneous injection of 10^6 LL2 cells into C57BL/6 CD45.1 host mice at indicated days post-implantation. (A) Flow cytometry analysis of hematopoietic cells and their major lineages in LL2 tumor stroma at day 12, 15, and 19 after implantation as total hematopoietic cells (CD45), T cells (Thy1.2), B cells (B220), myeloid cells (Mac-1 and Gr-1), and erythroid cells (Ter119⁺) (n = 5). *

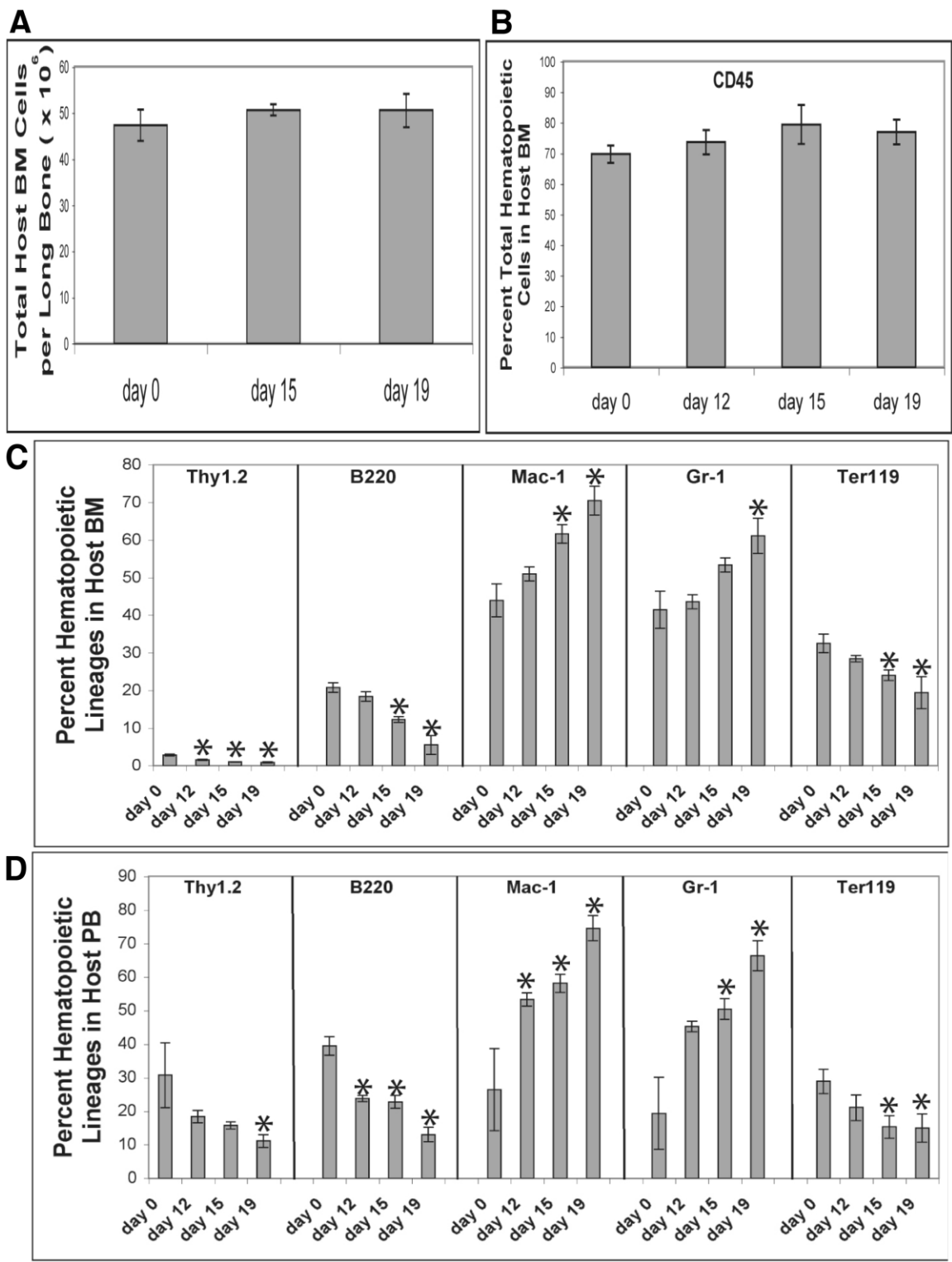
significantly different from day 12 values. **(B)** Representative flow cytometry plots showing that CD45⁺Lin⁻Sca-1⁺Kit⁺ (LSK) cells exist in LL2 tumor stroma. **(C)** Frequencies of CD45⁺Lin⁻Sca-1⁺Kit⁺ cells in LL2 tumor stroma at day 12, 15, and 19 after implantation (n = 5). * significantly different from day 12 values. **(D)** HSCs in the LL2 tumor stroma have long-term repopulation ability and repopulate secondary recipients. Lethally irradiated CD45.2 congenic mice were injected with 1 x 10⁵ CD45.2 bone marrow competitor cells and 1 x 10⁶ CD45.1 cells, isolated from the LL2 tumor mass. Shown are the repopulation activities of hematopoietic populations derived from the cancer stroma in long-term reconstitution (n = 6) and secondary reconstitution experiments (n = 5). **(E)** Donor repopulation in T lineage (CD3), B lineage (B220), and myeloid lineage (Mac-1/Gr-1) in peripheral blood in the experiment described in panel D at 18 months post-transplant (n = 6). **(F)** Frequency of repopulating HSCs in LL2 tumor stroma calculated by limiting dilution analysis. L-Calc software was used to calculate the HSC frequency, n = 23. **(G)** Hematopoietic cells in tumor stroma came from host BM. 1,000,000 CD45.1 donor BM cells were transplanted into lethally irradiated CD45.2 C57BL/6 mice. At 4 months post-transplant, the recipient BM was completely repopulated by the donor CD45.1 cells. 10⁵ LL2 tumor cells were then subcutaneously implanted into these mice. Three weeks later, flow cytometry was used to characterize the hematopoietic cells in tumor stroma. A representative flow cytometry plot shows 100% of the tumor stromal CD45⁺ cells were CD45.1⁺.

HSC numbers dramatically increase in tumor-bearing mice

Next we sought to determine whether the host hematopoietic compartment was affected by tumor growth. Total cellularity and total hematopoietic cell counts of tumor-bearing mice did not significantly change over time (Fig. 2A-B). However, in both BM and PB of tumor-bearing mice we observed significantly increased percentages of myeloid (Mac-1⁺ and Gr-1⁺) cells but decreased lymphoid (Thy1.2⁺ and B220⁺) and erythroid (Ter119⁺) cells as a function of time post-implantation (Fig. 2C-D). We analyzed the frequencies and numbers of hematopoietic progenitors and phenotypic HSCs in the tumor-bearing mice and healthy controls. CFU-GM increased more than 2-fold whereas CFU-E and CFU-Pre-B decreased at least 50% in tumor-bearing mice compared to normal mice (Fig. 2E), concordant with the total increase of myeloid cells and decrease of lymphoid and erythroid cells. The BM and PB enriched phenotypic HSCs

as Lin⁻Sca-1⁺Kit⁺CD34⁻Flk-2⁻ or Lin⁻Sca-1⁺Kit⁺ cells increased over time. Numbers of BM HSCs increased about 3-fold and PB HSCs increased 7-fold at day 19 relative to numbers on day 12 (Fig. 2F-G). This suggests that the presence of a tumor induces *in vivo* expansion of HSCs and progenitors in the BM, which leads to increased HSCs and progenitors in the circulation. Consistent with this result, the tumor-bearing mice display splenomegaly, with 2-fold increase of spleen size and weight compared to healthy controls (data not shown).

Because numbers of HSCs in the tumor-bearing mice significantly increased, we tested whether the cell cycle of HSCs in the host BM changed. As shown in Figure 2H, there was no significant changes in fractions of cells in given cell cycle stages in HSCs in the BM of tumor-bearing mice at day 21 compared to normal mice, suggesting that the tumor did not significantly alter the quiescence of host BM HSCs.



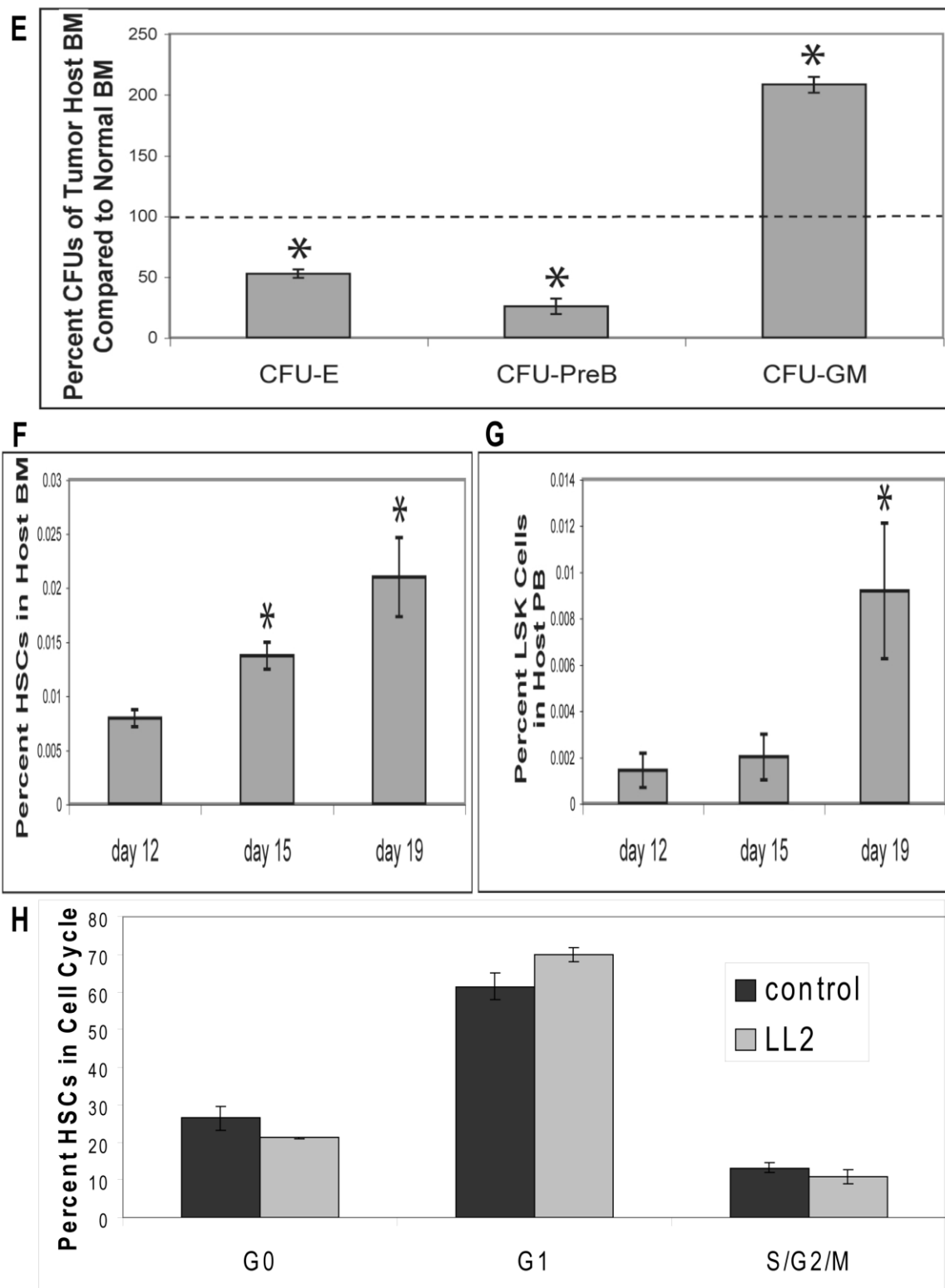


Figure 2. Analysis of the hematopoietic compartment of the LL2 tumor-bearing mice. (A-G) Total BM cells (A), total hematopoietic cells in BM (B), hematopoietic lineages in BM (C), hematopoietic lineages in PB (D), hematopoietic progenitors in BM (E), CD45⁺Lin⁻Sca-1⁺Kit⁺Fli2⁻CD34⁻ cells in BM (F), and CD45⁺Lin⁻Sca-1⁺Kit⁺ cells in

PB (**G**) at indicated days in C57BL/6 CD45.1 host mice before and after the subcutaneous injection of 10^5 LL2 cells were analyzed by flow cytometry or colony assays (n = 5). * significantly different from day 0 or normal values (for panel **B-E**), or from day 12 values (for panel **F-G**). (**H**) The cell cycle status of BM HSCs in tumor-bearing mice at day 21 post-implantation does not significantly differ from that of counterparts in normal mice. HSCs as Lin⁻Sca-1⁺Kit⁺Flk2⁻CD34⁻ cells were stained with Hoechst 33342 and pyronin Y, and analyzed for cell cycle stage (n = 5).

Co-implanted hematopoietic cells from tumor stroma promote tumor development

We developed an assay to test the ability of hematopoietic cells to collaborate functionally with tumor cells to affect the tumor development. In this assay, we use FACS to isolate different populations of hematopoietic cells and mix them with a fixed number of LL2 cancer cells prior to injection into the C57BL/6 mice. The kinetics of tumor growth was determined to evaluate the tumor-promoting ability of the co-implanted hematopoietic cells. In the experiment summarized in Figure 3A, we co-implanted 1×10^5 LL2 cells with 1×10^4 CD45.1 total BM cells or with enriched normal BM HSCs as Lin⁻Sca-1⁺Kit⁺ cells subcutaneously into C57BL/5 CD45.2 host mice. During the 3-week period of analysis, the tumor size was measured. These data show that both total BM cells and the enriched HSC population positively regulated tumor growth. It is noteworthy that the co-implantation of total BM cells with LL2 cells led to similar level of tumor size as the same number of transplanted LSK cells. Clearly, differentiated hematopoietic cells did promote tumor progression. This suggests that additional HSCs in the tumor local environment do not necessarily further promote tumor growth.

To determine the effect of hematopoietic cells in tumor stroma, we isolated CD45⁺ cells from LL2 tumors or host PB and co-injected them with GFP⁺LL2 tumor cells into secondary mice. We found that, although PB CD45⁺ cells stimulated LL2 tumor

growth compared to LL2 cells alone, CD45⁺ cells isolated from previously existing tumor stroma had significantly increased ability to enhance LL2 tumor growth than these PB CD45⁺ cells (Fig. 3B). These tumor stromal hematopoietic cells also supported metastasis to the lung better; however, the metastasis level was not statistically significant (Fig. 3C). This result suggests that 1) hematopoietic cells in tumor stroma enhance tumor growth, 2) hematopoietic cells from tumor stroma are different from those from PB in promoting tumor growth, not unexpectedly as the compositions of these two sources of cells are different (Table 1), 3) tumor stroma has certain “educating” effect on hematopoietic cells that leads to tumor development.

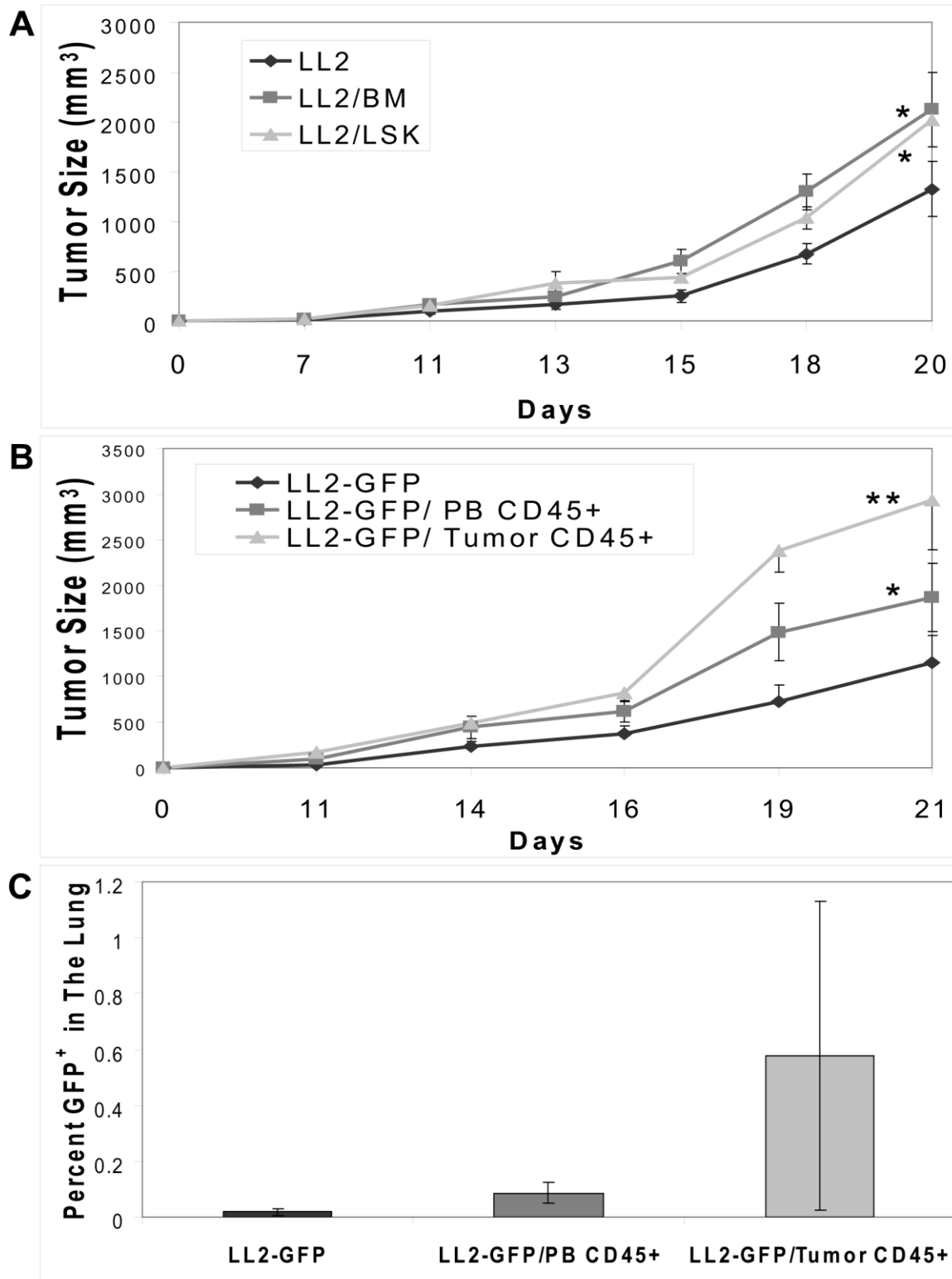


Figure 3. Tumor stromal hematopoietic cells stimulate LL2 tumor development. (A) Co-implanted HSCs or total BM cells stimulate the growth of primary LL2 tumor. 100,000 GFP-marked LL2 cells were co-implanted with with 1×10^4 CD45.1 total BM cells or enriched normal bone marrow HSCs (as Lin⁻Sca-1⁺Kit⁺ cells) subcutaneously

into C57BL/5 CD45.2 host mice ($n = 8$). During the 3-week period of analysis, the size of the primary tumor was measured. **(B-C)** Tumor stromal hematopoietic cells stimulate tumor growth and metastasis. 10,000 tumor stromal CD45⁺ cells or PB cells from tumor-bearing mice were collected by FACS and co-implant with 10⁵ LL2 cells into healthy mice ($n = 5$). The percentages of GFP⁺ tumor cells that migrated from primary tumor to the lung were determined by flow cytometry **(C)**. Shown are the sizes of the primary tumors. * significantly different from LL2-GFP value, ** significantly different from LL2-GFP and LL2/PB CD45⁺ values, $p < 0.05$.

IGF-IR expressed on cells from hematopoietic stroma is important for tumor development and metastasis

IGF type I receptor (IGF-IR) is the signaling receptor for insulin-like growth factor 1 and 2 (IGF-1 and IGF-2). The IGF pathway has been reported to play important roles in the development of a range of malignancies, including both non-small cell lung cancer and small cell lung cancer (see review¹⁸). For example, elevated plasma levels of IGF-1 and single nucleotide polymorphisms within the IGF axis are associated with an increased risk of lung cancer¹⁸. The activation of IGF-IR facilitates malignant transformation and the majority of IGF-2 transgenic mice develop lung cancer by 18 months of age¹⁸. It is noteworthy that these studies were focused on the activity of IGF-IR that is expressed on cancer cells. We sought to test whether IGF-IR expressed by the hematopoietic stroma plays any role in the development of the LL2 tumors.

We previously showed that IGF-IR is expressed on the surface of all HSCs¹⁴. Although IGF-IR^{-/-} mice die after birth^{11, 19}, we were able to collect IGF-IR^{-/-} HSCs from the fetal liver. Then we reconstituted recipient mice with IGF-IR^{-/-} fetal liver HSCs. Four months later, the recipients were fully repopulated by the donor IGF-IR^{-/-} HSCs, and we implanted LL2 cancer cells into these mice. The IGF-IR^{-/-} HSCs had no apparent defect in engrafting the recipient mice (Fig. 4A), nor did they have a noticeable skew in lineage

differentiation compared to HSCs from wild-type mice (Fig. 4B). Nevertheless, LL2 tumors grew significantly more slowly in these IGF-IR^{-/-} HSC reconstituted mice than in mice engrafted with wild-type HSCs (Fig. 4C, $p < 0.05$). Interestingly, the LL2 tumors implanted in the IGF-IR^{-/-} reconstituted mice also had dramatically decreased metastasis to the lung (Fig. 4D). This experiment suggests that the lack of IGF signaling in the hematopoietic compartment of tumor stroma, but rather than the defect in differentiation of tumor stromal hematopoietic cells, hampers the solid tumor development.

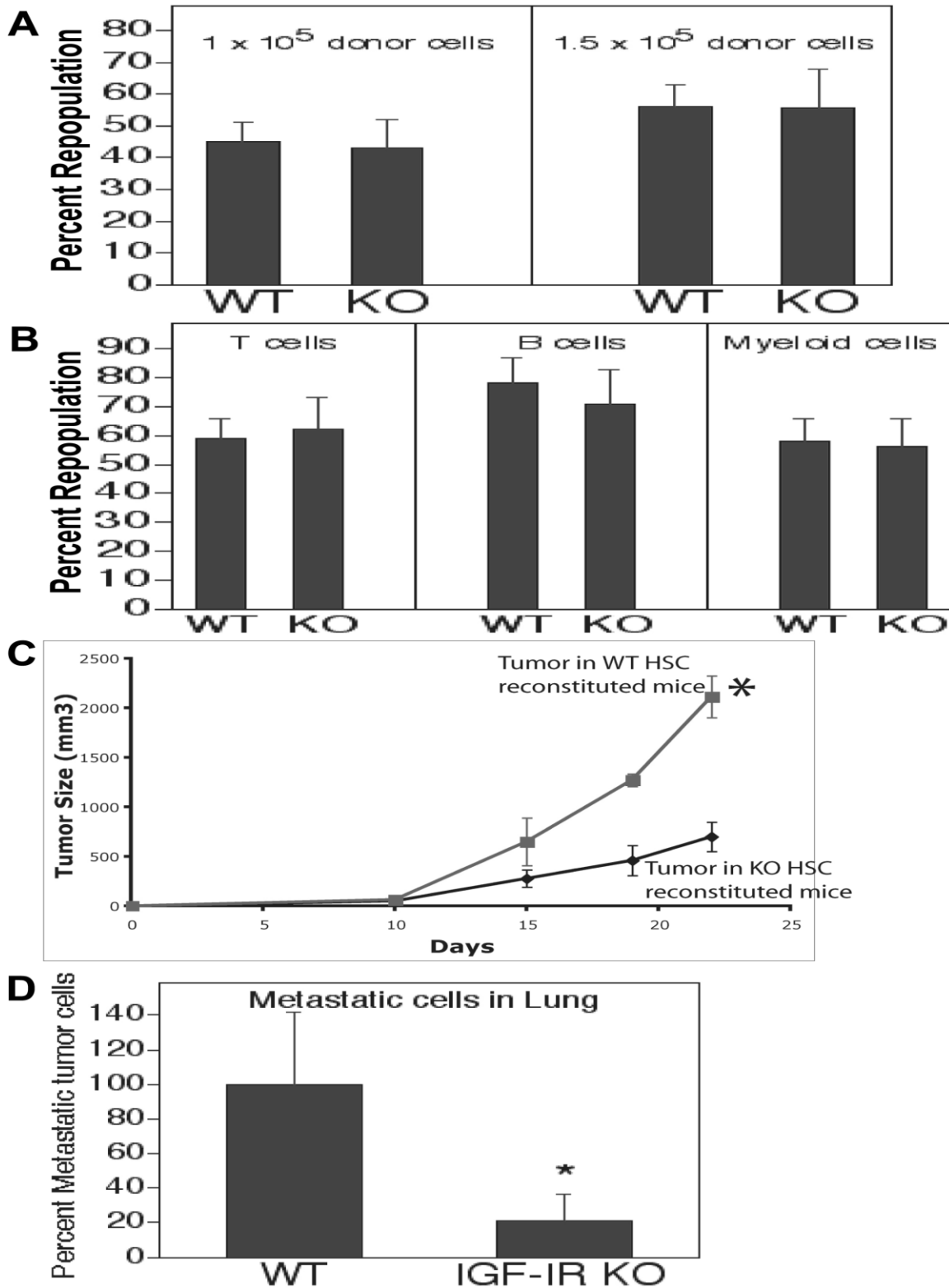


Figure 4. Mice with the IGF-IR^{-/-} tumor stromal HSCs had slower tumor development in the LL2 implantation model than mice reconstituted with wild-type HSCs. (A) E15.5 IGF-IR^{-/-} fetal liver HSCs had similar engraftment as WT HSCs in recipient mice in a competitive repopulation analysis at 4 months post-transplant (n = 7).

(B) IGF-IR^{-/-} HSCs had similar differentiation into T, B, and myeloid lineages as WT HSCs at 4 month post-transplant (n = 7). **(C)** Mice with the IGF-IR^{-/-} tumor stromal HSCs had slower tumor growth in the LL2 implantation model. Shown is a representative result of three independent experiments of tumor growth measured after 1 x 10⁵ LL2 cells were implanted subcutaneously into IGF-IR^{-/-} or WT HSCs reconstituted mice at 4 month post-transplant (n = 5). * significantly different, p < 0.05. **(D)** Mice with the IGF-IR^{-/-} tumor stromal HSCs had dramatically decreased GFP⁺ LL2 tumor cell metastasis in lung compared to those reconstituted with WT HSCs. Results shown were from pooled data from three experiments (in each experiment n = 3-5). * significantly different, p < 0.05.

DISCUSSION

Since cancer pathogenesis involves a concerted interplay between the tumor and the microenvironment, it is desirable to elucidate the roles of tumor stroma in tumor development. In this study, we sought to determine the composition and potential function of hematopoietic cells in the stroma of solid tumors and in tumor-bearing mice. To this end, we used an LL2 implantation tumor model. Cells of the LL2 line are advantageous because they produce tumors in syngeneic C57BL/6 mice; these mice are also ideal for quantitating HSCs by reconstitution analysis based on congenic CD45.1 and CD45.2 markers. Because these cells are syngeneic with their hosts, their tumorigenicity can proceed in the presence of a fully competent host immune system. This is especially important in a study of the hematopoietic compartment of the tumor stroma and the tumor-bearing host. Moreover, LL2 cells, when injected subcutaneously, can form lung metastases. This makes it possible to compare the effects of different stromal components on regulation of potential tumor cell migration.

Here we provide evidence that functional hematopoietic progenitors and HSCs exist in tumor stroma. Although the very low frequency of HSCs in tumor stroma makes them impossible to observe by immunohistochemistry, we were able to detect these cells using flow cytometry analysis and the “gold standard” BM reconstitution assay. It is apparent that these tumor stromal HSCs are not contaminants from PB: this was demonstrated by the different frequencies of various hematopoietic populations in tumor stroma and PB and the isolation of hematopoietic cells from perfused tumors. Nevertheless, these tumor stromal hematopoietic cells do originate from BM and may be recruited to tumor sites through inflammatory signals. Our result is supported by the

emerging evidence showing that HSCs or progenitors can themselves home to sites of inflammation to rapidly produce cells that are essential for the immune response²⁰. We previously demonstrated that tumor cells can secrete proteins to support *ex vivo* expansion of HSCs¹⁷; therefore it is reasonable to assume a similar scenario happens in tumor mass *in vivo*, so that HSCs may be supported by tumor stromal environment. Although we showed the existence of functional HSCs in tumor stroma, we do not yet know if the phenotype of HSCs in tumor stroma is exactly the same as that of BM HSCs, as HSCs may change their surface phenotype in extramedullary tissue such as in the liver¹⁰. Further investigation coupling FACS-based cell fractionation with BM reconstitution analysis will be needed to clarify this issue.

Concordant with the idea that tumors release certain endocrine signals that change the representation of stem cells or progenitors in other tissues or organs⁴, we also showed that the tumor-bearing mice had 3-fold and 7-fold increases in of BM and PB HSCs, respectively, relative to numbers on the day of LL2 implantation. It is hypothesized that hormone signals reach BM, thus BM HSCs increase. Then the increased proliferation of BM HSCs exceeds the capacity of HSC microenvironment leading to HSC mobilization and increases in numbers of PB HSCs. Consistently, during tumor development, the percentage of faster proliferating myeloid cells (including myeloid progenitors) increased and that of slower growing lymphoid cells decreased over time in host BM and PB. We demonstrated that these BM derived hematopoietic cells are eventually recruited to tumor and become the source of hematopoietic cells in tumor stroma.

The better understanding of the alteration of the hematopoietic compartment in host and tumor stroma during tumor progression may lead to new strategies for cancer

treatment. For instance, the effective retention of BM HSCs in their BM niche or block of the migration of BM-derived hematopoietic cells in cancer patients negatively affect the cancer development. Moreover, one of the key features of hematopoietic cells is their ability to migrate and access to various tissues and organs. We hypothesize that this ability may contribute to the formation of clusters of hematopoietic cells that have been “educated” by the primary tumor that serve as pre-metastatic niches. It thus will be interesting to study the relationship between hematopoietic cells in the primary cancer and the stroma of the metastatic cancer. It will also be critical to determine the hematopoietic compositions of human tumor stroma.

Is the existence of non-cancerous cells in tumor stroma a consequence or a cause of tumor development? So far numerous lines of prior evidence already indicate that stromal cells play important roles in tumor progression. Endothelial cells recruited to the tumor mass support neovascularization. BM-derived cells have been shown to support tumor outgrowth and form pre-metastatic niches⁴⁻⁶. Stromal fibroblasts and mesenchymal stem cells also play important roles in angiogenesis and metastasis, respectively^{7,8}. Our studies provide further evidence that supports the concept that tumor stromal hematopoietic cells regulate the tumor growth and metastasis. We found that the co-implantation of normal HSCs with cancer cells in a mouse tumor model promoted tumor growth. Since total BM cells had similar ability to stimulate co-implanted tumor growth as LSK cells, HSCs may not directly affect tumor growth; instead, it may be hematopoietic cells that differentiate in the tumor microenvironment that play a role in growth and metastasis. When we co-implanted individual lineage cells such as CD3⁺ (T cells), B220⁺ (B cells), Mac-1⁺ (monocytes), Gr-1⁺ (granulocytes), or Ter119⁺ cells (red

blood cells) with LL2 cells, we found their tumor-promoting effects were not as potent as LSK cells or total BM cells (data not shown). This suggests that the full lineage spectrum that is derived from HSCs locally may have the strongest activity in tumor promotion. Consistent with this view, we showed that previously “educated” tumor stromal total hematopoietic cells had greater ability to support tumor growth and metastasis than circulating hematopoietic cells.

The IGF ligands IGF-1 and IGF-2 bind to their common signaling receptor IGF-IR and initiate a variety of signaling events. It is known that IGF-IR regulates cell growth, survival, adhesion, and motility¹⁸. Our previous work demonstrated that all normal HSCs express the receptor for IGF-2 and that IGF-2 stimulates *ex vivo* expansion of these normal HSCs¹⁴. In the present study, we found that tumor stromal HSCs are originally derived from BM. We also showed that tumor growth and metastasis in IGF-IR^{-/-} reconstituted mice were significantly hampered. This led to the conclusion that, in addition to its direct role in cancer survival and growth, IGF signaling in tumor stroma is also important for solid cancer development. Our results do not contradict but rather complement the conventional view that IGF signaling is important for cancer development.

REFERENCES

1. Li H, Fan X, Houghton J. Tumor microenvironment: The role of the tumor stroma in cancer. *J Cell Biochem.* 2007;101:805-815.
2. McAllister SS, Weinberg RA. Tumor-host interactions: a far-reaching relationship. *J Clin Oncol.* 2010;28:4022-4028.
3. Kaplan RN, Psaila B, Lyden D. Niche-to-niche migration of bone-marrow-derived cells. *Trends Mol Med.* 2007;13:72-81.
4. McAllister SS, Gifford AM, Greiner AL, et al. Systemic endocrine instigation of indolent tumor growth requires osteopontin. *Cell.* 2008;133:994-1005.
5. Heissig B, Hattori K, Dias S, et al. Recruitment of stem and progenitor cells from the bone marrow niche requires MMP-9 mediated release of kit-ligand. *Cell.* 2002;109:625-637.
6. Kaplan RN, Riba RD, Zacharoulis S, et al. VEGFR1-positive haematopoietic bone marrow progenitors initiate the pre-metastatic niche. *Nature.* 2005;438:820-827.
7. Orimo A, Gupta PB, SgROI DC, et al. Stromal fibroblasts present in invasive human breast carcinomas promote tumor growth and angiogenesis through elevated SDF-1/CXCL12 secretion. *Cell.* 2005;121:335-348.
8. Karnoub AE, Dash AB, Vo AP, et al. Mesenchymal stem cells within tumour stroma promote breast cancer metastasis. *Nature.* 2007;449:557-563.
9. Bryder D, Rossi DJ, Weissman IL. Hematopoietic stem cells: the paradigmatic tissue-specific stem cell. *Am J Pathol.* 2006;169:338-346.

10. Kotton DN, Fabian AJ, Mulligan RC. A novel stem-cell population in adult liver with potent hematopoietic-reconstitution activity. *Blood*. 2005;106:1574-1580.
11. Holzenberger M, Dupont J, Ducos B, et al. IGF-1 receptor regulates lifespan and resistance to oxidative stress in mice. *Nature*. 2003;421:182-187.
12. Liao MJ, Zhang CC, Zhou B, et al. Enrichment of a population of mammary gland cells that form mammospheres and have in vivo repopulating activity. *Cancer Res*. 2007;67:8131-8138.
13. Zhang CC, Steele AD, Lindquist S, et al. Prion protein is expressed on long-term repopulating hematopoietic stem cells and is important for their self-renewal. *Proc Natl Acad Sci U S A*. 2006;103:2184-2189.
14. Zhang CC, Lodish HF. Insulin-like growth factor 2 expressed in a novel fetal liver cell population is a growth factor for hematopoietic stem cells. *Blood*. 2004;103:2513-2521.
15. Zhang CC, Lodish HF. Murine hematopoietic stem cells change their surface phenotype during ex vivo expansion. *Blood*. 2005;105:4314-4320.
16. Zhang CC, Kaba M, Ge G, et al. Angiopoietin-like proteins stimulate ex vivo expansion of hematopoietic stem cells. *Nat Med*. 2006;12:240-245.
17. Huynh H, Llizuka S, Kaba M, et al. IGFBP2 secreted by a tumorigenic cell line supports ex vivo expansion of mouse hematopoietic stem cells. *Stem Cells*. 2008;26:1628-1635.
18. Dziadziuszko R, Camidge DR, Hirsch FR. The insulin-like growth factor pathway in lung cancer. *J Thorac Oncol*. 2008;3:815-818.

19. Liu JP, Baker J, Perkins AS, et al. Mice carrying null mutations of the genes encoding insulin-like growth factor I (Igf-1) and type 1 IGF receptor (Igf1r). *Cell*. 1993;75:59-72.
20. Jaiswal S, Weissman IL. Hematopoietic stem and progenitor cells and the inflammatory response. *Ann N Y Acad Sci*. 2009;1174:118-121.

ACKNOWLEDGEMENTS

I would like to thank the past and present members of the Zhang Laboratory, and the members of the Department of Developmental Biology for their technical assistances.

I would like to thank Karen Kazemzadeh and Harmony Hilton of the Immunology Graduate Program for their administrative assistances. In particular, I would like to thank Nancy McKinney and Dr. Melanie Cobb their tremendous supports and advocacies.

I would like to thank my dissertation committee, Dr. Philip Thorpe, Dr. Rolf Brekken, and Dr. Felix Yarovinsky, for their helps and guidance to complete this dissertation. I also would like to thank Dr. Lily Huang for serving on my dissertation defense.